Electronic Supplementary Material (ESI) for Chemical Science.

Supporting information

Accelerated Robotic Discovery of Type II Porous Liquids

Rachel J. Kearsey,[a] Ben M. Alston, [a] Michael E. Briggs, [a] Rebecca L. Greenaway*[a] and Andrew I. Cooper*[a]

[a] Department of Chemistry and Materials Innovation Factory, University of Liverpool, Liverpool, L69 7ZD, UK

Email: aicooper@liverpool.ac.uk, rebecca.greenaway@liverpool.ac.uk

Table of Contents

1. General synthetic and analytical methods

Materials: 1,3,5-Triformylbenzene was purchased from Manchester Organics (UK). Other chemicals were purchased from Fluorochem UK, TCI UK or Sigma-Aldrich. Solvents were reagent or HPLC grade purchased from Fischer Scientific. All materials were used as received unless stated otherwise.

Synthesis: All reactions were stirred magnetically using Teflon-coated stirrer bars. Where heating was required, the reactions were warmed using a stirrer hotplate with heating blocks, with the stated temperature being measured externally to the reaction flask with an attached probe. Removal of solvents was done using a rotary evaporator.

High-throughput synthesis and solubility screening: High-throughput automated synthesis was carried out using a Chemspeed Accelerator SLT-100 automated synthesis platform, and the high-throughput solubility testing was performed on a ChemSpeed Swing platform. Organic solvents were removed using a Combidancer evaporator.

IR Spectra: Infra-red (IR) spectra were recorded on a Bruker Tensor 27 FT-IR using ATR measurements for oils and solids as neat samples, or using transmission mode on a 96-well silica wafer deposited as a thin film as part of the high-throughput analysis.

NMR Spectra: ^{1}H Nuclear magnetic resonance (NMR) were recorded using an internal deuterium lock for the residual protons in $CDCl_3$ (δ = 7.26 ppm), D_2O (δ = 4.79 ppm), or CD_2Cl_2 (δ = 5.32 ppm) at ambient probe temperature on either a Bruker Avance 400 (400 MHz) or Bruker DRX500 (500 MHz) spectrometer. NMR studies of porous liquids were conducted using an in-house calibrated capillary of TMS in d_2-DCM (made using 100 µL sample from 10 µL TMS in 0.5 mL d_2-DCM).

Data are presented as follows: chemical shift, integration, peak multiplicity (s = singlet, d = doublet, t = triplet, q = quartet, quint = quintet, m = multiplet, br = broad), coupling constants (*J* / Hz), and assignment. Chemical shifts are expressed in ppm on a δ scale relative to δ_{TMS} (0 ppm), δ_{D2O} (4.79 ppm), δ_{CD2Cl2} (5.32 ppm), or δ_{CDCl3} (7.26 ppm). Assignments were determined either on the basis of unambiguous chemical shift or coupling patterns, or by analogy to fully interpreted spectra for structurally related compounds.

^{13}C NMR Spectra were recorded using an internal deuterium lock using $CDCl_3$ (δ = 77.16 ppm) at ambient probe temperatures on the following instruments: Bruker Avance 400 (101 MHz) or Bruker DRX500 (126 MHz).

HPLC Spectra: HPLC analysis was carried out using a Dionex UltiMate 3000 with a diode array UV detector using a Thermo-Scientific Syncronis C8 column, 150 x 4.6 mm, 3 µm (SN 10136940, Lot 12459). The mobile phase was isocratic MeOH at a flow rate of 1 mL/min for a 10-30 min run time, and the column temperature was set to 30 °C. The injection volume was 10 µL and the sample concentration was approximately 1 mg/mL. Detection for UV analysis was conducted at 254 nm.

HRMS spectra: High resolution mass spectrometry (HRMS) was carried out using an Agilent Technologies 6530B accurate-mass QTOF Dual ESI mass spectrometer (capillary voltage 4000 V, fragmentor 225 V) in positive-ion detection mode. The mobile phase was MeOH + 0.1% formic acid at a flow rate of 0.25 mL/min.

PXRD: Laboratory powder X-ray diffraction data were collected in transmission mode on samples held on a black opaque 96-shallow well microplate (ProxiPlate-96 Black) on a Panalytical X'Pert PRO MPD equipped with a high-throughput screening (HTS) XYZ stage, X-ray focusing mirror and PIXcel detector, using Ni-filtered Cu Kα radiation. Data were measured over the range 5–30° in ~0.013° steps over 15 minutes.

Gas uptake and evolution studies: All uptakes in the porous liquid samples were measured using gases purchased from BOC of the following grades: methane (N4.5) and xenon (N5.0), in 10 mL GC headspace vials (22 mm x 45 mmm screw top, ThermoScientific). All samples had gas addition and measurements conducted between 23-25 °C in a temperature-controlled laboratory.

The gas flow rate was measured and controlled using a Gilmont calibrated flowmeter (tube size 0, Gilmont EW-03201-22) with a stainless steel (SS) float and 0-100 scale. The flow rate for each gas was calculated using the correlated flow table for air from the supplier, and the general correction equations. These equations approximate the gas flow compared to air by using each gas density (g/mL) at standard conditions (taken from the NIST Chemistry WebBook[1] and Gilmont calibrated at 1 atm, 294 K), with corrections for temperature and pressure. Each gas was maintained at a ~50-60 mL/min flow rate by setting the regulator output pressure to 0.5 bar and fine-controlling the flow with a needle valve to the calculated scale readings (see table below).

The gas evolved from the porous liquids was collected and measured by water displacement in an inverted Rotaflo stopcock 25 mL burette (0.1 mL graduations) in a crystallisation dish of water. The GC vial containing the sample was connected to the burette using a needle/tubing cannula.

General correction equations:

Gas flow from air flow:

$$q_G^o = q_A^o \sqrt{\frac{\rho_{Air}^o}{\rho_G^o}}$$

Correction for temperature and pressure:

$$q_G' = q_G^o \sqrt{\frac{p}{p^\circ} \cdot \frac{T^\circ}{T}}$$

Standard conditions: $p^\circ = 1$ atm $T^\circ = 21$ °C/294 K

q_A^o = standard air flow reading from meter (mL/min)
q_G^o = standard gas flow (mL/min)
ρ_{Air}^o = density of air at standard conditions (g/mL)
ρ_G^o = density of gas at standard conditions
q_G' = gas flow at p and T with volume corrected to measurement at standard conditions (mL/min)
p = absolute pressure of gas inlet (atm)
T = absolute temperature

Calculated gas flow from air flow and Gilmont flowmeter reading:

Gas	Density of gas (g/mL) at standard conditions (1 atm, 21 °C/294 K) from NIST WebBook[1]	Gilmont Scale Reading (SS Float)	Calibrated Air Flow q_A^o at standard conditions (mL/min)	Corrected Gas Flow q_G^o from Air Flow q_A^o at standard conditions (mL/min)
Air	ρ°_{Air} = 0.00120	39-43	49.69–58.40	N/A
Xe	ρ°_G = 0.00546	60–66	105.2–124.7	49.31–58.46
CH_4	ρ°_G = 0.00066	32–36	36.50–43.76	49.21–59.00

Viscosity measurements: Viscosity measurements were carried out using a calibrated RheoSense µVISC viscometer (0.01–100 or 10-2000 cP) with a temperature controller (18–50 °C). Measurements were repeated a minimum of three times with the average viscosity reported along with a standard deviation.

2. Synthesis and characterisation of diamine precursors

1,2-Diamino-2-methylpropane (Amine **A**), ethylenediamine (Amine **B**), (*R*)-propane-1,2-diamine (Amine **C**), 1,2-diaminocyclohexane (Amine **D**), (1*S*,2*S*)-(+)-1,2-diaminocyclohexane (Amine **E**), (1*S*,2*S*)-(−)-1,2-diphenylethylenediamine (Amine **F**), and 1,2-diaminopropane (Amine **K**), were purchased from TCI UK, Sigma Aldrich, or Fluorochem UK. Amines **G**-**J** were synthesised according to the steps below.

2.1. Synthesis of diimines

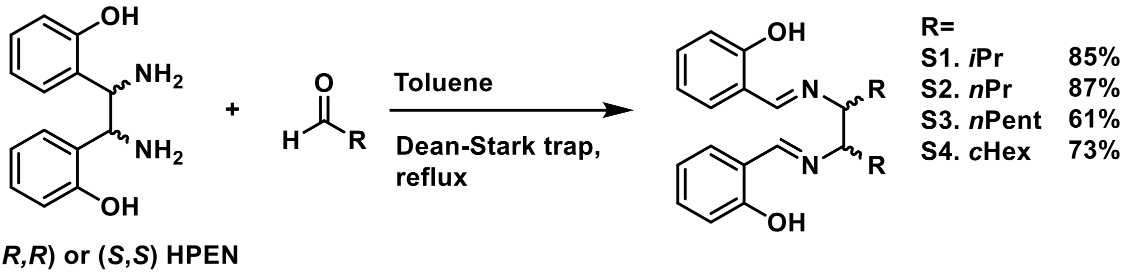

General procedure: A modification of the procedure by Kim *et al.* was used for these reactions.[2] Aldehyde (2.5 eq.) was added to a solution of either (*R*,*R*) or (*S*,*S*)-1,2-bis-(2-hydroxyphenyl)-1,2-diaminoethane (HPEN) (1.0 eq) in toluene, and the resulting solution refluxed at 120 °C for 72 hours fitted with a pre-filled Dean-Stark trap. The resulting mixture was allowed to cool to room temperature and the solvent was removed under reduced pressure. The reaction product was then purified by either: (1) the addition of methanol and the resulting precipitate collected by filtration; (2) the crude product was dissolved in the minimum amount of DCM possible, followed by the addition of hexane to precipitate the product which was collected by filtration.

2,2'-((1*E*,1'*E*)-(((3*R*,4*R*)-2,5-Dimethylhexane-3,4-diyl)bis(azaneylylidene))bis(methaneylylidene))-diphenol (S1)

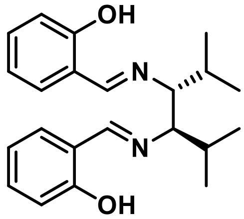

Prepared according to the general procedure using (*S*,*S*)-HPEN (10.00 g, 40.9 mmol) and isobutyraldehyde (7.38 g, 102.3 mmol) in toluene (135 mL). Purified using method (1) to give **S1** (12.20 g, 34.6 mmol, 85%) as a yellow powder.

^{1}H NMR (400 MHz, CDCl$_3$): δ 13.54 (2H, br s, O**H**), 8.16 (2H, s, imine C**H**), 7.27–7.21 (2H, m, Ar**H**), 7.13 (2H, dd, *J* = 7.7, 1.6 Hz, Ar**H**), 6.93 (2H, d, *J* = 8.0 Hz, Ar**H**), 6.78 (2H, t, *J* = 8.0 Hz, Ar**H**), 3.22 (2H, s, NC**H**), 2.17–2.03 (2H, m, C**H**), 0.97 (6H, d, *J* = 6.8 Hz, CH$_3$), 0.89 (6H, d, *J* = 6.8 Hz, C**H**$_3$); **^{13}C NMR** (101 MHz, CDCl$_3$): δ 165.43 (Imine C**H**), 161.13 (ArC**H**), 132.02 (ArC**H**), 131.23 (ArC**H**), 118.25 (ArC**H**), 118.22 (ArC**H**), 116.78 (ArC**H**), 75.98 (NC**H**), 28.23 (C**H**), 20.32 (CH$_3$), 17.16 (C**H**$_3$); **HRMS** (CI+) calculated for $C_{22}H_{28}N_2O_2$ 352.2151; found [M+H]$^+$ 353.2235. Data in accordance with literature values.[2,3]

2,2'-((1*E*,1'*E*)-(((4*S*,5*S*)-Octane-4,5-diyl)bis(azaneylylidene))bis(methaneylylidene))diphenol (S2)

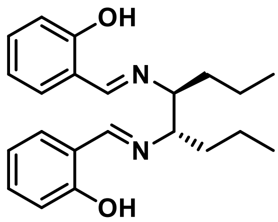

Prepared according to the general procedure using (*R*,*R*)-HPEN (4.00 g, 16.4 mmol) and butyraldehyde (2.94 g, 40.9 mmol) in toluene (100 mL). Purified using method (2) to give **S2** (5.03 g, 14.3 mmol, 87%) as a yellow powder.

^{1}H NMR (400 MHz, $CDCl_3$): δ 13.39 (2H, br s, O**H**), 8.25 (2H, s, Imine **H**), 7.27 (2H, t, *J* = 8.0 Hz, Ar**H**), 7.20 (2H, dd, *J* = 7.5, 1.6 Hz, Ar**H**), 6.96 (2H, d, *J* = 8.0 Hz, Ar**H**), 6.83 (2H, t, *J* = 7.5 Hz, Ar**H**), 3.32 – 3.27 (2H, m, NC**H**), 1.67–1.63 (4H, m, C**H**$_2$), 1.31–1.24 (4H, m, C**H**$_2$), 0.95 (9H, t, *J* = 7.3 Hz, C**H**$_3$); **^{13}C NMR** (101 MHz, $CDCl_3$): δ 165.00 (Imine C**H**), 161.42 (ArC**H**), 132.35 (ArC**H**), 131.48 (ArC**H**), 118.60 (ArC**H**), 118.60 (ArC**H**), 117.20 (ArC**H**), 73.63 (NC**H**), 34.81 (C**H**$_2$), 19.54 (C**H**$_2$), 13.99 (C**H**$_3$); HRMS (CI+) calculated for $C_{22}H_{28}N_2O_2$ 352.2151; found $[M+H]^+$ 353.2242.

2,2'-((1*E*,1'*E*)-(((*6S,7S*)-Dodecane-6,7-diyl)bis(azaneylylidene))bis(methaneylylidene))diphenol (S3)

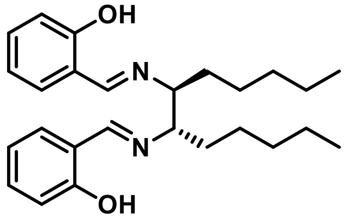

Prepared according to the general procedure using (*R,R*)-HPEN (4.28 g, 17.5 mmol) and hexanal (4.38 g, 43.8 mmol) in toluene (100 mL). Purified using method (1) to give **S3** (4.40 g, 10.8 mmol, 61%) as a yellow powder.

^{1}H NMR (400 MHz, $CDCl_3$): δ 13.45 (2H, s, O**H**), 8.25 (2H, s, Imine **H**), 7.31–7.25 (2H, m, Ar**H**), 7.21 (2H, dd, *J* = 7.7, 1.6 Hz, Ar**H**), 6.97 (2H, d, *J* = 7.9 Hz, Ar**H**), 6.84 (2H, td, *J* = 7.5, 1.6 Hz, Ar**H**), 3.29–3.26 (2H, m, NC**H**), 1.69–1.59 (4H, m, C**H**$_2$), 1.27 (12H, br s, C**H**$_2$), 0.85 (6H, t, *J* = 6.5 Hz, C**H**$_3$); **^{13}C NMR** (101 MHz, $CDCl_3$): δ 165.31 (Imine **C**H), 161.75 ArC**H**), 132.66 (Ar**C**H), 131.81 (Ar**C**H), 119.00 (ArC**H**), 118.91 (Ar**C**H), 117.53 (Ar**C**H), 74.17 (N**C**H), 32.89 (**C**H$_2$), 32.09 (**C**H$_2$), 26.38 (**C**H$_2$), 22.99 (**C**H$_2$), 14.48 (**C**H$_3$); **HRMS** (CI+) calculated for $C_{26}H_{36}N_2O_2$ 408.2777; found $[M+H]^+$ 409.2897. Data in accordance with literature values.[4]

2,2'-((1*E*,1'*E*)-(((1*R*,2*R*)-1,2-dicyclohexylethane-1,2-diyl)bis(azaneylylidene))bis(methaneylylidene)) diphenol (S4)

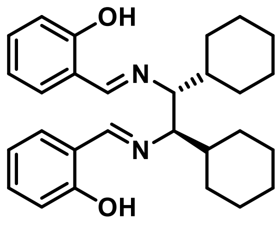

Prepared according to the general procedure using (*S,S*)-HPEN (4.35 g, 17.8 mmol) and cyclohexanecarboxaldehyde (4.98 g, 44.5 mmol) in toluene (100 mL). Purified using method (1) to give **S4** (5.61 g, 13.0 mmol, 73%) as a yellow powder.

^{1}H NMR (400 MHz, $CDCl_3$): δ 13.62 (2H, s, O**H**), 8.11 (2H, s, Imine **H**), 7.27–7.22 (2H, m, Ar**H**), 7.12 (2H, dd, *J* = 7.7, 1.6 Hz, Ar**H**), 6.93 (2H, d, *J* = 8.0 Hz, Ar**H**), 6.84 (2H, td, *J* = 7.5, 1.6 Hz, Ar**H**), 3.26 (2H, s, NC**H**), 1.76 - 1.55 (12H, m, C**H** and CH$_2$), 1.21–0.96 (10H, m, **CH**$_2$); **^{13}C NMR** (101 MHz, $CDCl_3$): δ 165.11 (Imine **C**H), 161.20 (ArCH), 131.96 (Ar**C**H), 131.18 (ArCH), 118.19 (Ar**C**H), 118.21 (Ar**C**H), 116.80 (Ar**C**H), 74.85 (N**C**H), 38.01 (**C**H), 30.70 (**C**H$_2$) 27.84 (**C**H$_2$), 26.12 (**C**H$_2$), 26.06 (**C**H$_2$), 25.97 (**C**H$_2$); **HRMS** (CI+) calculated for $C_{28}H_{36}N_2O_2$ 432.2777; found $[M+H]^+$ 433.2861. Data in accordance with literature values.[2,3]

2.2. Synthesis of diamines

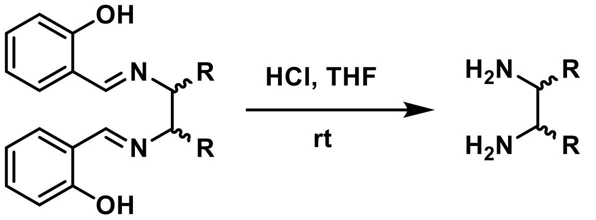

R=
Amine G, *i*Pr 79%
Amine H, *n*Pr 79%
Amine I, *n*Pent 89%
Amine J, *c*Hex 93%

General Procedure: A modification of the procedure by James *et al.* and Kim *et al*. was used in these reactions.[2,4] A solution of hydrochloric acid (37%, aqueous) in THF was added to a solution of the diimine (formed in Section 2.1.) in THF, and the reaction mixture stirred at room temperature for 48 hours. The diamine was then isolated by either: (1) the resulting precipitated hydrochloride salt in the crude reaction mixture was collected by filtration; (2) diethyl ether (100 mL) was added to the reaction mixture and the organic layer extracted with H_2O (3 x 50 mL), then the aqueous phase was basified with aqueous NaOH (1M), extracted with chloroform (3 x 50 mL), dried (Na_2SO_4), and the solvent removed under reduced pressure to afford the diamine.

(3*R*,4*R*)-2,5-Dimethylhexane-3,4-diamine dihydrochloride (Amine G)

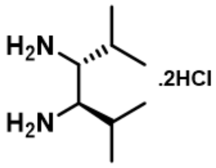

Prepared according to the general procedure using **S1** (3.93 g, 10.3 mmol) in THF (50 mL), and a solution of HCl (3 mL, 37%) in THF (50 mL). **Amine G** was purified using method (1) and collected as a colourless powder (1.77 g, 8.2 mmol, 79%).

^{1}H NMR (400 MHz, D_2O): δ 3.48 (2H, d, *J* = 8.0 Hz, C**H**), 2.19 (2H, m, C**H**), 1.10 (12H, t, *J* = 6.6 Hz, C**H₃**); **^{13}C NMR** (101 MHz, D_2O): δ 56.67 (N**C**H) 27.26 (**C**H) 18.55 (**C**H_3) 17.13 (**C**H_3); **HRMS** (CI+) calculated for $C_8H_{20}N_2$ 144.1626; found $[M+H]^+$ 145.1660. Data in accordance with literature values.[2,3]

(*4S,5S*)-Octane-4,5-diamine (Amine H)

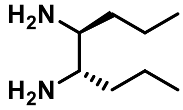

Prepared according to the general procedure using **S2** (5.03 g, 14.3 mmol) in THF (50 mL), and a solution of HCl (4 mL, 37%) in THF (50 mL). **Amine H** was purified using method (2) and collected as an orange oil (1.62 g, 11.2 mmol, 78%).

IR (ν_{max}/cm^{-1}): 2943, 2892, 2692, 1569, 1538, 1476, 1435, 1235, 1170, 1123, 1085, 1001; **^{1}H NMR** (400 MHz, $CDCl_3$): δ 2.62 (2H, s, C**H**), 1.23 (8H, s, C**H₂**), 0.84 (6H, s, C**H₃**); **^{13}C NMR** (101 MHz, $CDCl_3$): δ 55.04 (**C**H), 37.24 (**C**H_2), 20.89 (**C**H_2), 14.32 (**C**H_3); **HRMS** (ES+) calculated for $C_8H_{20}N_2$ 144.1626; found $[M+H]^+$ 145.1699.

(*6S,7S*)-Dodecane-6,7-diamine (Amine I)

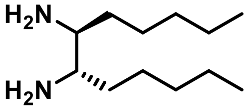

Prepared according to the general procedure using **S3** (4.23 g, 10.0 mmol) in THF (50 mL), and a solution of HCl (3.1 mL, 37%) in THF (50 mL). **Amine I** was purified using method (2) and collected as an orange oil (1.79 g, 8.9 mmol, 89%).

^{1}H NMR (400 MHz, $CDCl_3$): δ 2.54 (2H, br s, C**H**), 1.29 (16H, m, C**H$_2$**), 0.88 (6H, m, C**H$_3$**); **^{13}C NMR** (101 MHz, $CDCl_3$): δ 55.04 (**C**H), 34.72 (**C**H$_2$), 31.85 (**C**H$_2$), 26.07 (**C**H$_2$), 22.89 (**C**H$_2$), 13.87 (**C**H$_3$); **HRMS** (ES+) calculated for $C_{12}H_{28}N_2$ 200.2252; found $[M+H]^+$ 201.2327. Data in accordance with literature values.[4]

(*1R,2R*)-1,2-Dicyclohexylethane-1,2-diamine dihydrochloride (Amine J)

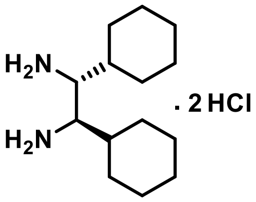

Prepared according to the general procedure using **S4** (5.60 g, 12.9 mmol) in THF (60 mL), and a solution of HCl (3.0 mL, 37%) in THF (60 mL). **Amine J** was purified using method (1) and collected as a colourless powder (3.57 g, 12.0 mmol, 93%).

^{1}H NMR (400 MHz, D_2O): δ 3.46 (2H, d, *J* = 8.0 Hz, NC**H**), 1.78–1.61 (12H, m, cyclohexane **H**), 1.23–1.06 (10H, m, cyclohexane **H**); **^{13}C NMR** (101 MHz, D_2O): δ 57.59 (N**C**H), 38.59 (**C**H), 31.59 (**C**H$_2$), 30.49 (**C**H$_2$), 27.58 (**C**H$_2$), 27.40 (**C**H$_2$), 27.37 (**C**H$_2$); **HRMS** (ES+) calculated for $C_{14}H_{28}N_2$ 224.2252; found $[M+H]^+$ 225.2330. Data in accordance with literature values.[2,3]

2.3. NMR spectra of novel precursors

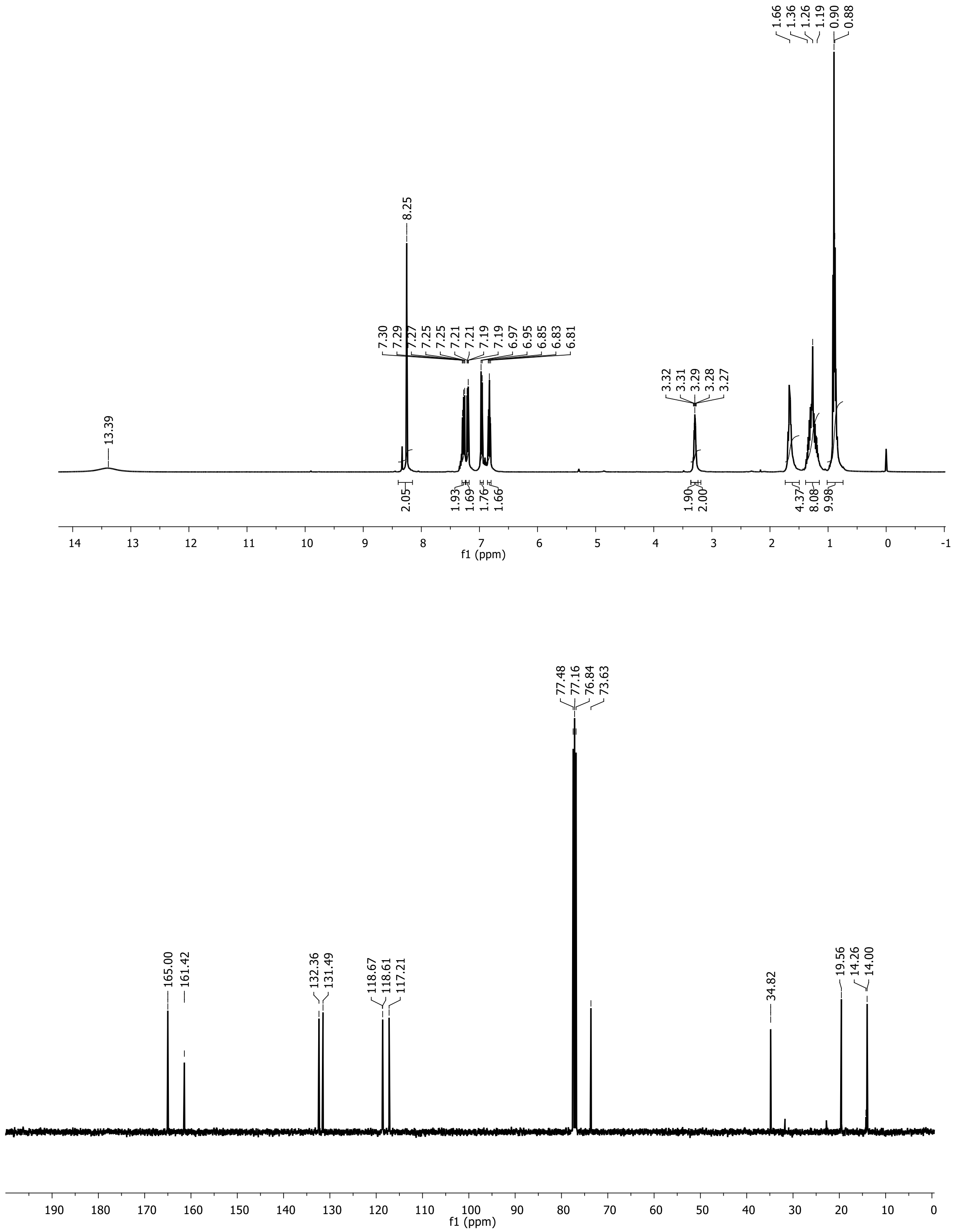

Fig. S1: ^{1}H NMR (CDCl$_3$; upper) and ^{13}C NMR (CDCl$_3$; lower) spectra of 2,2'-((1*E*,1'*E*)-(((4*S*,5*S*)-octane-4,5-diyl)bis(azaneylylidene))-bis(methaneylylidene))diphenol, **S2**

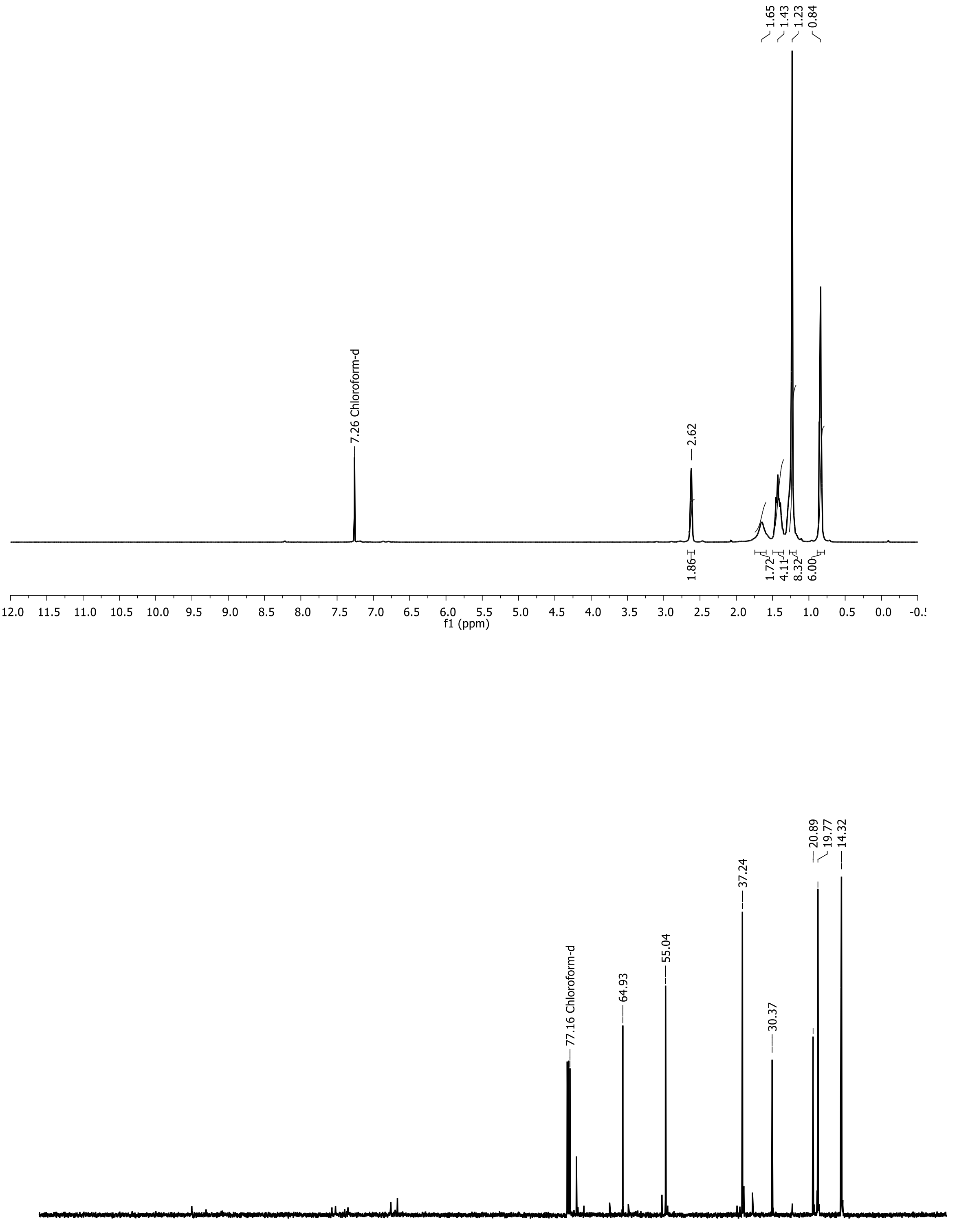

Fig. S2: ^{1}H NMR (CDCl$_3$; upper) and ^{13}C NMR (CDCl$_3$; lower) spectra of (4*S*,5*S*)-octane-4,5-diamine, Amine **H**

3. High-throughput synthesis screen

3.1. Concentration study

Usually, high dilution is used during the synthesis of organic cages formed by imine condensations because there is a risk of polymer or oligomer formation. However, there is a limit to the maximum volume of solvent that can be used in a single reactor on the synthesis platform, and with a large amount of material required for the solubility screen, it was desirable to obtain the highest quantity of scrambled cage possible in each. Therefore, we first investigated if the previously reported reaction concentration used for scrambled cage synthesis could be increased.[6]

In order to determine the maximum concentration that could be used, a trial scrambled **3^3:13^3** cage synthesis was carried out to determine the yield at up to three times the original concentration (Fig. S3).

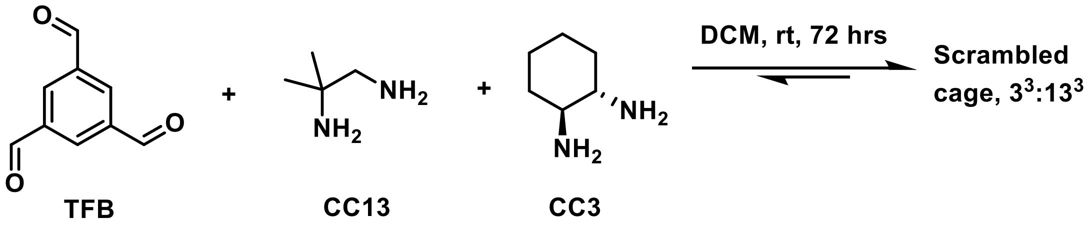

Fig. S3: General reaction scheme for the synthesis of scrambled cage **3^3:13^3**

Overall, the yield was not greatly affected by polymer formation at the higher concentration (Table S1), and the ^{1}H NMR spectra confirmed the formation of cage in reasonable purity (Fig. S4). Therefore, the high-throughput screen was carried out at three times the original concentration where there was sufficient starting material available.

Table S1: Conditions for the trial **3^3:13^3** scrambled cage synthesis using 1,2-diamino-2-methylpropane (Amine **A**) and (1*S*,2*S*)-(+)-1,2-diaminocyclohexane (Amine **E**) with 1,3,5-triformylbenzene (TFB) in DCM (60mL). Briefly, a solution of Amine **A** (3.0 eq.) in DCM (15 mL), and a solution of Amine **E** (3.0 eq.) in DCM (15 mL), were added to TFB (4 eq.) in DCM (30mL), and the resulting solution was stirred at room temperature for 72 hours. The solvent was then removed under reduced pressure, and the crude product re-dissolved in DCM and filtered to remove any insoluble precipitate. The solvent was removed in vacuo, before the solid was subsequently washed with ethyl acetate and the purified product collected by filtration.

	Mass of TFB (mg)	Mass of Amine A (mg)	Mass of Amine E (mg)	Volume of DCM (mL)	Mass recovery (g)	Yield (%)
Original concentration[6]	166.0	88.0	67.7	60	0.25	24
3 times as concentrated	498.0	263.0	203.0	60	0.57	54

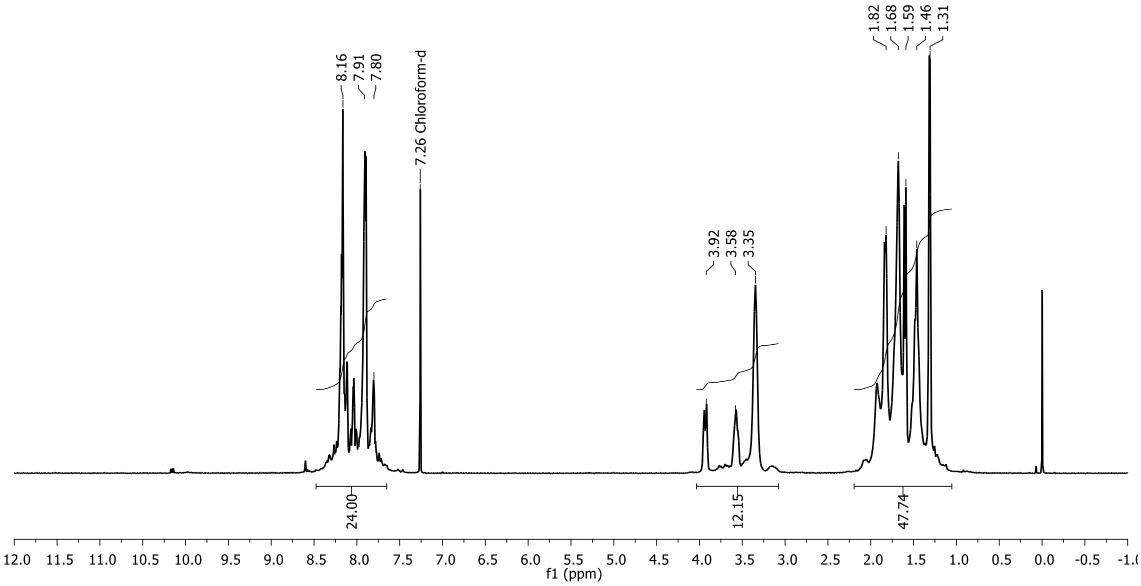

Fig. S4: ^{1}H NMR spectrum (CDCl$_3$) of scrambled **3^3:13^3** cage from the reaction carried out at three times the concentration previously reported

3.2. High-throughput scrambled cage synthesis and purification

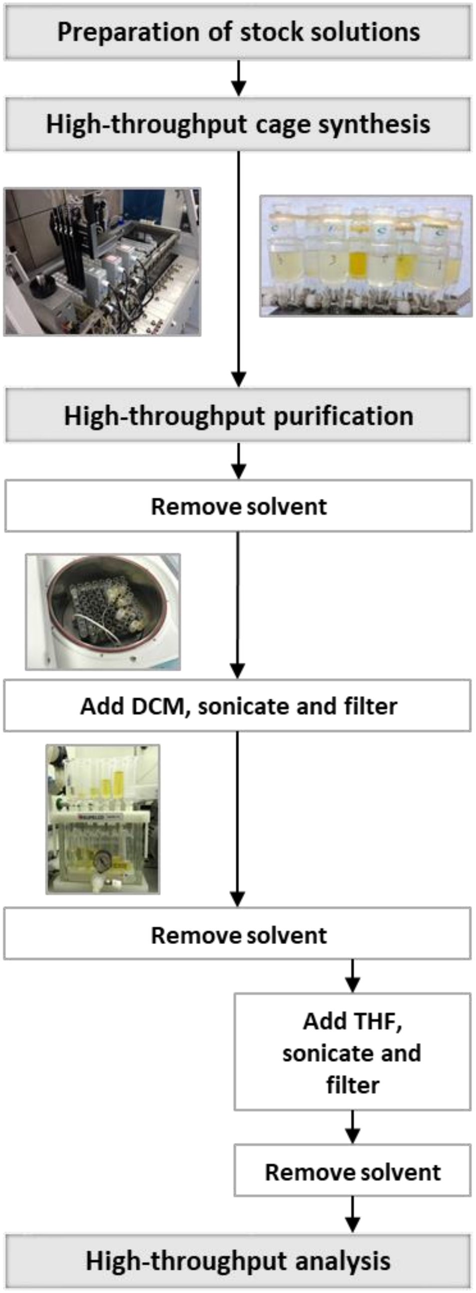

Fig. S5: General scheme showing the overall high-throughput workflow used to synthesise and purify a series of scrambled cages

General high-throughput synthetic screening procedure: All precursors (TFB and Amines **A**-**K**, Fig. S6) were dissolved in chloroform to make stock solutions (20-30 mg/mL) for use in the high-throughput screen (Table S2). Where the diamine was used as a hydrochloride salt, triethylamine (3.3 eq.) was added to the stock solution. Over 4 runs on a Chemspeed Accelerator SLT-100 platform (Fig. S7), the required volume of the TFB stock solution, followed by the required volume of each amine stock solution, was added to jacketed reactors (16 reactors with 75 mL total volume per run, 60 combinations and 2 control reactions) *via* liquid dispensing, followed by additional chloroform to make each total volume up to 60 mL (Table S3). The resulting solutions were vortexed at 800 rpm at room temperature for 72 hours, before the reaction mixtures were removed from the reactors and dispensed into vials (3 x 20 ml for each reactor) for subsequent isolation and purification.

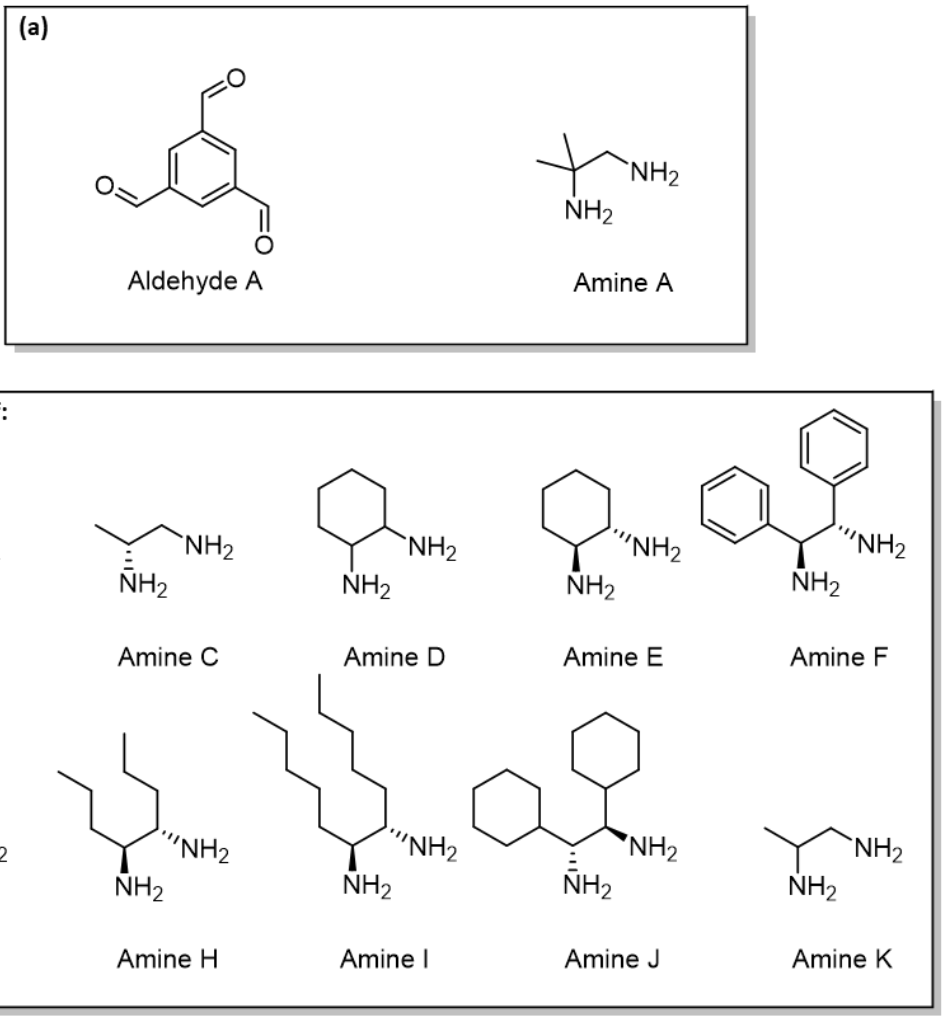

Fig. S6: The range of precursors used in the high-throughput synthetic screen targeting scrambled cage combinations: (a) Structures of the precursors used to form **CC13** which was scrambled with different diamine partners; (b) Structures of the scrambling diamine partners used in this study.

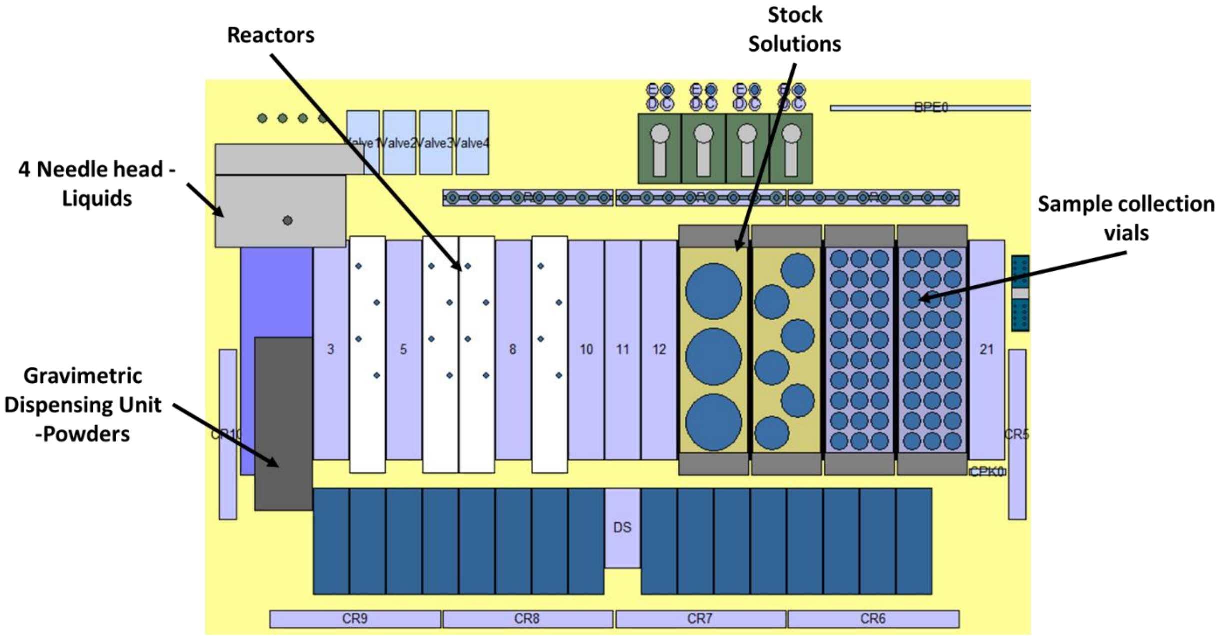

Figure S7: Graphical representation of Chemspeed Accelerator SLT-100 deck layout used for the synthesis of scrambled cages

Table S2: Summary of stock solutions in chloroform prepared for the high-throughput synthetic screen

Stock solution number	Reactant	MW (g/mol)	Stock solution concentration (mg/mL)	Stock solution concentration (mmol/ mL)	Total volume of stock solution required (mL)	Total volume of stock solution made (mL)	Mass of reactant required for stock solution (g)	NEt_3 required per reaction (mmol/ mL, 3.3 eq)	Total volume of NEt_3 added to stock solution (mL)
1	TFB	162.14	20	0.12	1341.61	1650.00	33.00	-	-
2	Amine **A**	88.15	20	0.23	408.86	500.00	10.00	-	-
3	Amine **B**	60.1	20	0.33	48.65	50.00	1.00	-	-
4*	Amine **C**	147.04	20	0.14	119.03	130.00	2.60	0.45	8.13
5	Amine **D**	114.19	20	0.18	92.44	95.00	1.90	-	-
6	Amine **E**	114.19	20	0.18	92.44	95.00	1.90	-	-
7	Amine **F**	212.3	30	0.14	120.96	125.00	3.75	-	-
8*	Amine **G**	217.18	30	0.14	106.20	95.00	2.85	0.46	5.08
9	Amine **H**	144.26	30	0.21	28.41	30.00	0.90	-	-
10	Amine **I**	200.37	30	0.15	49.23	40.00	1.20	-	-
11*	Amine **J**	297.31	30	0.10	53.46	55.00	1.65	0.33	5.11
12	Amine **K**	74.13	20	0.27	60.01	65.00	1.30	-	-

*Diamine hydrochloride salts used, therefore triethylamine was added to the stock solutions prior to use

Table S3: Summary of precursor stock solution volumes used for each reaction in the HT screen

Reaction number	Scrambled cage	TFB volume (mL)	Amount of TFB (mmol)	Amount of amine A (mmol)	Amine A volume (mL)	Amine ratio (A:X)	Scrambling amine (Amine X)	Amount of Amine X (mmol)	Amine X volume (mL)	Additional volume of chloroform added (mL) (Total volume = 60 mL)
1	A^6:B^0	25.00	3.08	4.62	20.39	6:0	**B**	0.00	0.00	14.61
2	A^5:B^1	25.00	3.08	3.85	16.99	5:1	**B**	0.77	2.32	15.69
3	A^4:B^2	25.00	3.08	3.08	13.59	4:2	**B**	1.54	4.63	16.78
4	A^3:B^3	25.00	3.08	2.31	10.19	3:3	**B**	2.31	6.95	17.86
5	A^2:B^4	25.00	3.08	1.54	6.80	2:4	**B**	3.08	9.27	18.94
6	A^1:B^5	25.00	3.08	0.77	3.40	1:5	**B**	3.85	11.58	20.02
7	A^0:B^6	25.00	3.08	0.00	0.00	0:6	**B**	4.63	13.90	21.10
8	A^5:C^1	25.00	3.08	3.85	16.99	5:1	**C**	0.77	5.67	12.34
9	A^4C^2	25.00	3.08	3.08	13.59	4:2	**C**	1.54	11.34	10.07
10	A^3:C^3	25.00	3.08	2.31	10.19	3:3	**C**	2.31	17.00	7.80
11	A^2:C^4	25.00	3.08	1.54	6.80	2:4	**C**	3.08	22.67	5.53
12	A^1:C^5	25.00	3.08	0.77	3.40	1:5	**C**	3.85	28.34	3.26
13	A^0:C^6	25.00	3.08	0.00	0.00	0:6	**C**	4.63	34.01	0.99
14	A^5D^1	25.00	3.08	3.85	16.99	5:1	**D**	0.77	4.40	13.61
15	A^4:D^2	25.00	3.08	3.08	13.59	4:2	**D**	1.54	8.80	12.61
16	A^3:D^3	25.00	3.08	2.31	10.19	3:3	**D**	2.31	13.21	11.60
17*	A^3:E^3	25.00	3.08	2.31	10.19	3:3	**E**	2.31	13.21	11.60
18	A^4:G^2	16.66	2.06	2.06	9.06	4:2	**G**	1.03	7.44	26.84
19	A^3:G^3	16.66	2.06	1.54	6.79	3:3	**G**	1.54	11.16	25.39
20	A^2:G^4	16.66	2.06	1.03	4.53	2:4	**G**	2.06	14.88	23.93
21	A^1:G^5	16.66	2.06	0.51	2.26	1:5	**G**	2.57	18.60	22.48
22	A^0:G^6	16.66	2.06	0.00	0.00	0:6	**G**	3.08	22.32	21.02
23	A^5:H^1	16.66	2.06	2.57	11.32	5:1	**H**	0.51	2.47	29.55
24	A^4:H^2	16.66	2.06	2.06	9.06	4:2	**H**	1.03	4.94	29.34
25	A^3:H^3	16.66	2.06	1.54	6.79	3:3	**H**	1.54	7.41	29.14
26	A^2:H^4	16.66	2.06	1.02	4.53	2:4	**H**	2.06	9.88	28.93
27	A^1:H^5	16.66	2.06	0.51	2.26	1:5	**H**	2.57	12.35	28.72
28	A^0:H^6	16.66	2.06	0.00	0.00	0:6	**H**	3.08	14.82	28.52
29	A^5:I^1	8.33	1.03	1.28	5.66	5:1	**I**	0.26	1.72	44.29
30	A^4:I^2	8.33	1.03	1.03	4.53	2:4	**I**	0.51	3.43	43.71
31	A^3:I^3	8.33	1.03	0.77	3.40	3:3	**I**	0.77	5.15	43.13
32	A^2:I^4	8.33	1.03	0.51	2.26	2:4	**I**	1.03	6.86	42.54
33	A^1:I^5	8.33	1.03	0.26	1.13	1:5	**I**	1.28	8.58	41.96
34	A^0:I^6	8.33	1.03	0.00	0.00	0:6	**I**	1.54	10.29	41.38
35	A^5J^1	16.66	2.06	2.57	11.32	5:1	**J**	0.51	5.09	26.93
36	A^4:J^2	16.66	2.06	2.06	9.06	4:2	**J**	1.02	10.18	24.10
37	A^3:J^3	16.66	2.06	1.54	6.79	3:3	**J**	1.54	15.27	21.27
38	A^2:J^4	16.66	2.06	1.02	4.53	2:4	**J**	2.06	20.37	18.45
39	A^1:J^5	16.66	2.06	0.51	2.26	1:5	**J**	2.57	25.46	15.62
40	A^0:J^6	16.66	2.06	0.00	0.00	0:6	**J**	3.08	30.55	12.79
41	A^5:K^1	25.00	3.08	3.85	16.99	5:1	**K**	0.77	2.86	15.15
42	A^4:K^2	25.00	3.08	3.08	13.59	4:2	**K**	1.54	5.71	15.69
43	A^3K^3	25.00	3.08	2.31	10.19	3:3	**K**	2.31	8.57	16.23
44	A^2:K^4	25.00	3.08	1.54	6.80	2:4	**K**	3.08	11.43	16.77
45	A^1:K^5	25.00	3.08	0.77	3.40	1:5	**K**	3.85	14.29	17.31
46	A^0:K^6	25.00	3.08	0.00	0.00	0:6	**K**	4.63	17.14	17.86
47*	A^3:E^3	25.00	3.08	2.31	10.19	3:3	**E**	2.31	13.21	11.60
48	A^2:D^4	25.00	3.08	1.54	6.80	2:4	**D**	3.08	17.61	10.60
49	A^1:D^5	25.00	3.08	0.77	3.40	1:5	**D**	3.85	22.01	9.59
50	A^0:D^6	25.00	3.08	0.00	0.00	0:6	**D**	4.63	26.41	8.59
51	A^5:E^1	25.00	3.08	3.85	16.99	5:1	**E**	0.77	4.40	13.61
52	A^4:E^2	25.00	3.08	3.08	13.59	4:2	**E**	1.54	8.80	12.61
53	A^3:E^3	25.00	3.08	2.31	10.19	3:3	**E**	2.31	13.21	11.60
54	A^2:E^4	25.00	3.08	1.54	6.80	2:4	**E**	3.08	17.61	10.60
55	A^1:E^5	25.00	3.08	0.77	3.40	1:5	**E**	3.85	22.01	9.59
56	A^0:E^6	25.00	3.08	0.00	0.00	0:6	**E**	4.63	26.41	8.59
57	A^5:F^1	25.00	3.08	1.28	5.66	5:1	**F**	0.26	1.82	44.19
58	A^4:F^2	8.33	1.03	1.02	4.53	4:2	**F**	0.51	3.64	43.51
59	A^3:F^3	8.33	1.03	0.77	3.40	3:3	**F**	0.77	5.45	42.82
60	A^2:F^4	8.33	1.03	0.51	2.26	2:4	**F**	1.03	7.27	42.13
61	A^1:F^5	8.33	1.03	0.26	1.13	1:5	**F**	1.28	9.09	41.45
62	A^0:F^6	8.33	1.03	0.00	0.00	0:6	**F**	1.54	10.91	40.76

*denotes a control reaction

General isolation and purification procedure: The solvent from each reaction was removed under reduced pressure using a Combidancer high-throughput evaporator. To each of the isolated solids was added DCM (10 mL), and the mixtures filtered in parallel through empty, fritted SPE cartridges to remove any insoluble precipitate. The solvent was again removed using the Combidancer and the procedure repeated with THF for those reactions containing triethylamine to remove the formed triethylamine hydrochloride salt. The purified cages were then dried overnight in a vacuum oven at 90 °C prior to characterisation.

3.3. High-throughput characterisation

The isolated solid samples from each of the scrambled cage reactions with each diamine were analysed using ^{1}H NMR spectroscopy, high-resolution mass spectrometry (HRMS) and HPLC to determine if they were successful. Powder-X-ray diffraction (PXRD) was also carried out to determine the crystallinity of the samples. For an overall summary of the successful hits see Table S4, and for a summary of the characterisation data for all the reactions see Table S5.

Table S4: Summary of the hits from the scrambled cage high-throughput synthetic screen: a successful reaction, represented by ✓, had significant evidence in the analytical data to suggest the successful formation of scrambled cage, whereas reactions represented by ✗ were considered unsuccessful because they had little or no evidence of desired product

Amine	Ratios Amine A: Amine X					
	5:1	4:2	3:3	2:4	1:5	0:6
B	✓	✓	✓	✓	✓	✓
C	✓	✓	✓	✓	✓	✓
D	✗	✗	✗	✗	✗	✗
E	✓	✗	✗	✗	✗	✗
F	✓	✗	✗	✗	✗	✗
G	✓	✓	✓	✓	✓	✓
H	✓	✓	✓	✓	✗	✗
I	✓	✓	✓	✗	✗	✗
J	✓	✓	✓	✗	✗	✗
K	✓	✓	✓	✓	✓	✓

Table S5: Summary of the characterisation data for the attempted scrambled cage reactions carried out in the high-throughput synthetic screen

Scrambled cage	**Mass recovered (g)**	**Expected mass (g)**	**Yield based on mass recovery (%)***	**Solid appearance**	**HRMS**		**HPLC**		**^{1}H NMR ($CDCl_3$)**			
					Mass ions	Species	Scrambling visible?	Comment	Scrambled cage present?	Residual TFB?	Residual amine?	Other species visible?
A^6:B^0	0.66	0.74	89	Colourless powder	961.6134	$[M+H]^+$	✓	-	✓	✓	✓	✗
A^5:B^1	0.65	0.72	90	Colourless powder	961.6130 933.5817 905.5501 877.5175 849.4856	$[M+H]^+$	✓	-	✓	✗	✗	✓
A^4:B^2	0.56	0.70	80	Colourless powder	961.6131 933.5816 905.5504 877.5188 849.4866 821.4546 793.4227	$[M+H]^+$	✓	-	✓	✓	✗	✗
A^3:B^3	0.52	0.68	77	Colourless powder	961.6090 933.5808 905.5501 877.5188 849.4873 821.4551 793.4232	$[M+H]^+$	✓	-	✓	✗	✗	✗
A^2:B^4	0.31	0.65	47	Colourless powder	905.5467 877.5176 849.4871 821.4558 793.4238	$[M+H]^+$	✓	-	✓	✗	✗	✓
A^1:B^5	0.23	0.63	36	Colourless powder	849.486 8.21.456 793.4243	$[M+H]^+$	✓	-	✓	✗	✓	✗
A^0:B^6	0.26	0.61	43	Colourless powder	793.4242	$[M+H]^+$	✓	-	✓	✗	✗	✗
A^5:C^1	0.13	0.73	18	Colourless powder	961.6126 947.5965 933.5802 919.5636	$[M+H]^+$	✓	impurities (aldehyde and small oligomers)	✓	✓	✗	✗
A^4:C^2	0.22	0.72	31	Colourless powder	961.6107 947.5955 933.5799 919.5639 905.5477	$[M+H]^+$	✓	impurities (aldehyde and small oligomers)	✓	✓	✗	✗
A^3:C^3	0.24	0.71	34	Hard orange glass	961.6100 947.5955 933.5805 919.5648 905.5489 891.5326	$[M+H]^+$	✓	impurities (aldehyde and small oligomers)	✓	✓	✗	✗
A^2:C^4	0.18	0.70	26	Colourless powder	947.5941 933.5793 919.5642 905.5487 891.5329 877.5164	$[M+H]^+$	✓	impurities (aldehyde and small oligomers	✓	✓	✗	✗
A^1:C^5	0.44	0.69	64	Hard orange glass	919.5635 905.5486 891.5334 8.775175	$[M+H]^+$	✓	impurities (aldehyde and small oligomers	✓	✓	✗	✗

A^{0}:C^{6}	0.36	0.68	53	Colourless powder	877.5159	[M+H]$^{+}$	✓	impurities (aldehyde and small oligomers	✓	✓	✗	✓
A^{5}:D^{1}	0.38	0.76	50	Glassy orange solid	961.6145 987.6309	[M+H]$^{+}$	✓	Possible scrambling but lots of impurities	✗	✓	✓	✓
A^{4}:D^{2}	0.28	0.78	36	Glassy orange solid	935.5482 961.6114 987.6285 1013.6436	[M+H]$^{+}$	✓	Possible scrambling but lots of impurities	✓	✓	✗	✗
A^{3}:D^{3}	0.48	0.80	60	Glassy orange solid	935.5463 961.5913 987.6240 1013.6424 1040.6607	[M+H]$^{+}$	✓	Possible scrambling but lots of impurities	✓	✓	✗	✗
A^{2}:D^{4}	0.61	0.82	74	Colourless powder	1013.6351 1039.6561 1065.6685 1091.6842	[M+H]$^{+}$	✗		✗	✗	✓	✗
A^{1}:D^{5}	0.16	0.84	19	Colourless powder	✗	-	✗		✗	✓	✓	✓
A^{0}:D^{6}	0.16	0.86	19	Colourless powder	1117.6998	[M+H]$^{+}$	✗		✗	✓	✓	✓
A^{5}:E^{1}	0.19	0.76	25	Colourless powder	506.5302 523.3271 545.4881	[M+2H]$^{2+}$	✓		✓	✗	✓	✗
A^{4}:E^{2}	0.80	0.78	102	Colourless powder	481.2957 513.2970 523.33254 535.2703	[M+2H]$^{2+}$	✓		✓	✗	✓	✗
A^{3}:E^{3}	0.25	0.80	31	Colourless powder	481.2900 494.3168 507.3263 520.3342 533.3422 546.3492	[M+2H]$^{2+}$	✓		✓	✗	✓	✗
A^{2}:E^{4}	0.21	0.82	26	Colourless powder	523.3354	[M+2H]$^{2+}$	✓		✓	✗	✗	✗
A^{1}:E^{5}	0.15	0.84	18	Colourless powder	481.2638 523.3246 559.3670	[M+2H]$^{2+}$	✓		✓	✗	✗	✗
A^{0}:E^{6}	0.20	0.86	23	Colourless powder	✗	-	✓		✓	✗	✗	✗
A^{5}:F^{1}	0.19	0.84	23	Colourless powder	✗	-	✓		✓	✓	✗	✗
A^{4}:F^{2}	0.13	0.93	14	Colourless powder	✗	-	✗		✗			
A^{3}:F^{3}	0.03	1.03	3	Colourless powder	✗	-	✗		✗	✓	✓	✓
A^{2}:F^{4}	0.08	1.12	7	Colourless powder	✗	-	✗		✗	✓	✓	✓
A^{1}:F^{5}	-	1.22	0	Colourless powder	✗	-	✗		✗			
A^{0}:F^{6}	0.02	1.32	2	Colourless powder	✗	-	✗		✗	✓	✓	✓
A^{5}:G^{1}	0.15	0.78	19	Colourless powder	-	-	✓	Possible scrambling but some impurities	✓	✓	✓	Solvent

A^{4}:G^{2}	0.25	0.83	30	Waxy orange solid	961.6140 1017.6764 1073.7346	[M+H]$^{+}$	✓	Possible scrambling but lots of impurities	✓	✓	✗	✗
A^{3}:G^{3}	0.32	0.87	37	Waxy orange solid	961.6111 1017.6741 1073.7367 1129.7971 1185.8594	[M+H]$^{+}$	✓	Possible scrambling but lots of impurities	✓	✓	✗	Solvent
A^{2}:G^{4}	0.47	0.91	51	Waxy orange solid	961.6150 1017.6762 1073.7369 1129.7974 1185.8613 1242.9251 1297.9911	[M+H]$^{+}$	✓	Possible scrambling but lots of impurities	✓	✓	✗	Solvent
A^{1}:G^{5}	0.49	0.96	51	Waxy orange solid	1073.350 1129.7988 1186.8643 1242.9261 1297.9853	[M+H]$^{+}$	✓	Possible scrambling but lots of impurities	✓	✓	✗	✓
A^{0}:G^{6}	0.55	1.00	55	Waxy orange solid	1297.9885	[M+H]$^{+}$	✗		✓	✓	✗	✓
A^{5}:H^{1}	0.28	0.78	36	Waxy orange solid	961.6140 1017.6764 1073.7346	[M+H]$^{+}$	✓	Possible scrambling but lots of impurities	✓	✓	✗	✗
A^{4}:H^{2}	0.50	0.83	60	Glassy orange solid	961.6132 1017.6760 1073.7364	[M+H]$^{+}$	✓	Possible scrambling but lots of impurities	✓	✓	✗	✗
A^{3}:H^{3}	0.38	0.87	44	Glassy orange solid	961.6081 1017.6730 1073.7306	[M+H]$^{+}$	✓	Possible scrambling but lots of impurities	✓	✓	✗	✗
A^{2}:H^{4}	0.26	0.91	28	Glassy orange solid	✗		✗		✓	✓	✗	✗
A^{1}:H^{5}	0.27	0.96	28	Glassy orange solid	✗		✗		✓	✓	✗	✗
A^{0}:H^{6}	0.33	1.00	33	Glassy orange solid	✗		✗		✓	✓	✗	✓
A^{5}:I^{1}	0.18	0.28	65	Waxy orange solid	961.6140 1073.7378	[M+H]$^{+}$	✓	Possible scrambling but lots of impurities	✓	✓	✗	✗
A^{4}:I^{2}	0.23	0.30	76	Waxy orange solid	961.6129 1073.7378	[M+H]$^{+}$	✓	Possible scrambling but lots of impurities	✓	✓	✗	✗
A^{3}:I^{3}	0.14	0.33	42	Colourless Powder	961.6107 1073.7357 1185.8580 1298.9890	[M+H]$^{+}$	✓	Possible scrambling but lots of impurities	✓	✗	✗	✗
A^{2}:I^{4}	-	0.36	0	-	✗	-	✓	Possible scrambling but lots of impurities	v. weak	✗	✓	✓

A^1:I^5	0.27	0.39	69	Glassy orange solid	✗	-	✓	Possible scrambling but lots of impurities	✓	✓	✗	✓
A^0:I^6	0.30	0.42	71	Glassy orange solid	✗	-	✗		✓	✓	✗	✓
A^5:J^1	0.35	0.28	124**	Waxy orange solid	961.6116 1097.7364 1233.8606	$[M+H]^+$	✓	Possible scrambling but lots of impurities	✓	✓	✓	✓
A^4:J^2	0.34	0.32	107**	Waxy orange solid	961.6118 1097.7372 1233.8612	$[M+H]^+$	✓	Possible scrambling but lots of impurities	✓	✓	✗	✗
A^3:J^3	0.48	0.35	136**	Waxy orange solid	961.61.06 1097.7355 1233.8608 1370.9898	$[M+H]^+$	✓	Possible scrambling but lots of impurities	✓	✓	✗	✗
A^2:J^4	0.49	0.39	127**	Waxy orange solid	961.6138 1097.7369 1233.8618 1370.9908 1507.1141	$[M+H]^+$	✓	Possible scrambling but lots of impurities	✓	✓	✗	✗
A^1:J^5	0.56	0.42	133**	Waxy orange solid	961.6170 1097.7408 1233.8582 1370.9882	$[M+H]^+$	✓	Possible scrambling but lots of impurities	✓	✓	✗	✗
A^0:J^6	0.43	0.46	94	Waxy orange solid	✗	-	✗		✓	✓	✗	✗
A^5:K^1	0.50	0.84	59	Hard brown solid	961.6135 947.5977 933.5822 919.5652	$[M+H]^+$	✓		✓	✗	✗	✗
A^4:K^2	0.46	0.83	55	Hard brown solid	961.6120 947.5979 933.5821 919.5665 905.5502 891.5331	$[M+H]^+$	✓		✓	✗	✗	✗
A^3:K^3	0.52	0.82	63	Foamy orange solid	933.5759 919.5606 905.5447 891.5291 877.5135	$[M+H]^+$	✓		✓	✗	✓	✗
A^2:K^4	0.29	0.81	36	Glassy orange solid	919.5606 905.5447 891.5291 877.5135	$[M+H]^+$	✓		✓	✗	✓	✗
A^1:K^5	0.30	0.80	38	Colourless powder	905.5443 891.5296 877.5139	$[M+H]^+$	✓		✓	✗	✓	✗
A^0:K^6	0.25	0.79	32	Colourless powder	877.5142	$[M+H]^+$	✓		✓	✗	✗	✗

*Mass TFB + Mass amines - mass water produced = maximum theoretical amount of isolated product, and reported yield based on comparison of mass recovery with this value

** Impurities present

3.4. Full high-throughput characterisation data

In Fig. S8-S17, full datasets are included for all 60 combinations - the characterisation data (^{1}H NMR, HPLC, HRMS, PXRD) for the different scrambled ratios relating to each specific diamine (**B-K**) were stacked to allow comparison between the variations as the feed ratio changed. Not all datasets are complete for various reasons; including lack of material or poor solubility of product. Decisions on what scrambled cage combinations to use in the subsequent solubility screen were made based on available data. Subsequently, full characterisation was carried out on scaled up and purified scrambled cages that were found to be highly soluble in the high-throughput solvent screen (see Supplementary Information Section 6).

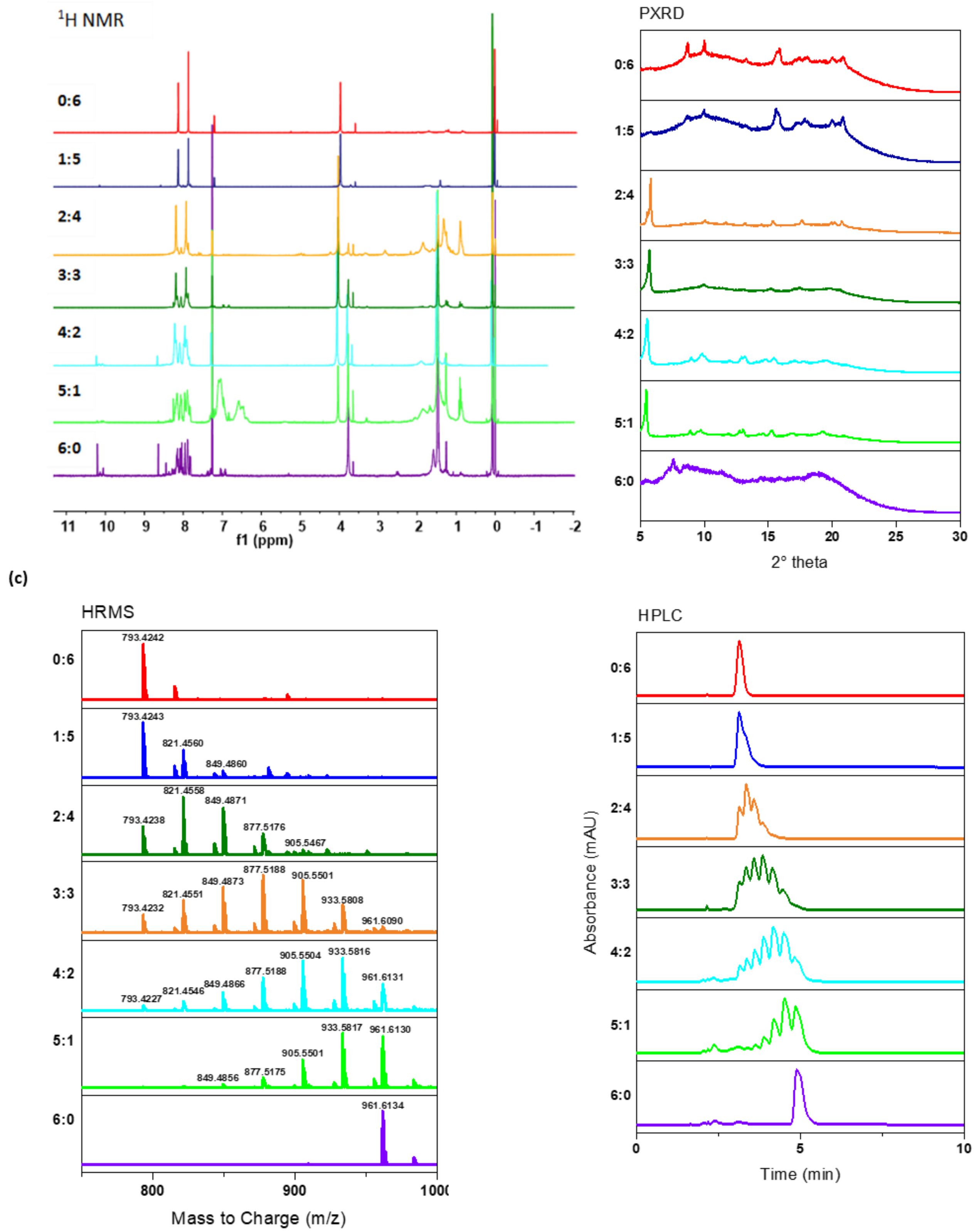

Fig. S8: Experimental data for the scrambled $\mathbf{A}^{n}$:$\mathbf{B}^{6-n}$ cage family: (a) Stacked ^{1}H NMR spectra in $CDCl_3$; (b) Stacked PXRD patterns showing the formation of mainly amorphous material; (c) Stacked mass spectra with expected masses observed for $\mathbf{A}^6\mathbf{B}^0$, $\mathbf{A}^5\mathbf{B}^1$, $\mathbf{A}^4\mathbf{B}^2$, $\mathbf{A}^3\mathbf{B}^3$, $\mathbf{A}^2\mathbf{B}^4$, $\mathbf{A}^1\mathbf{B}^5$, and $\mathbf{A}^0\mathbf{B}^6$ at 960.6003, 932.5690, 904.5377, 876.5064, 848.4751, 820.4438 and 792.4125; (d) Stacked HPLC spectra showing the formation of scrambled cages.

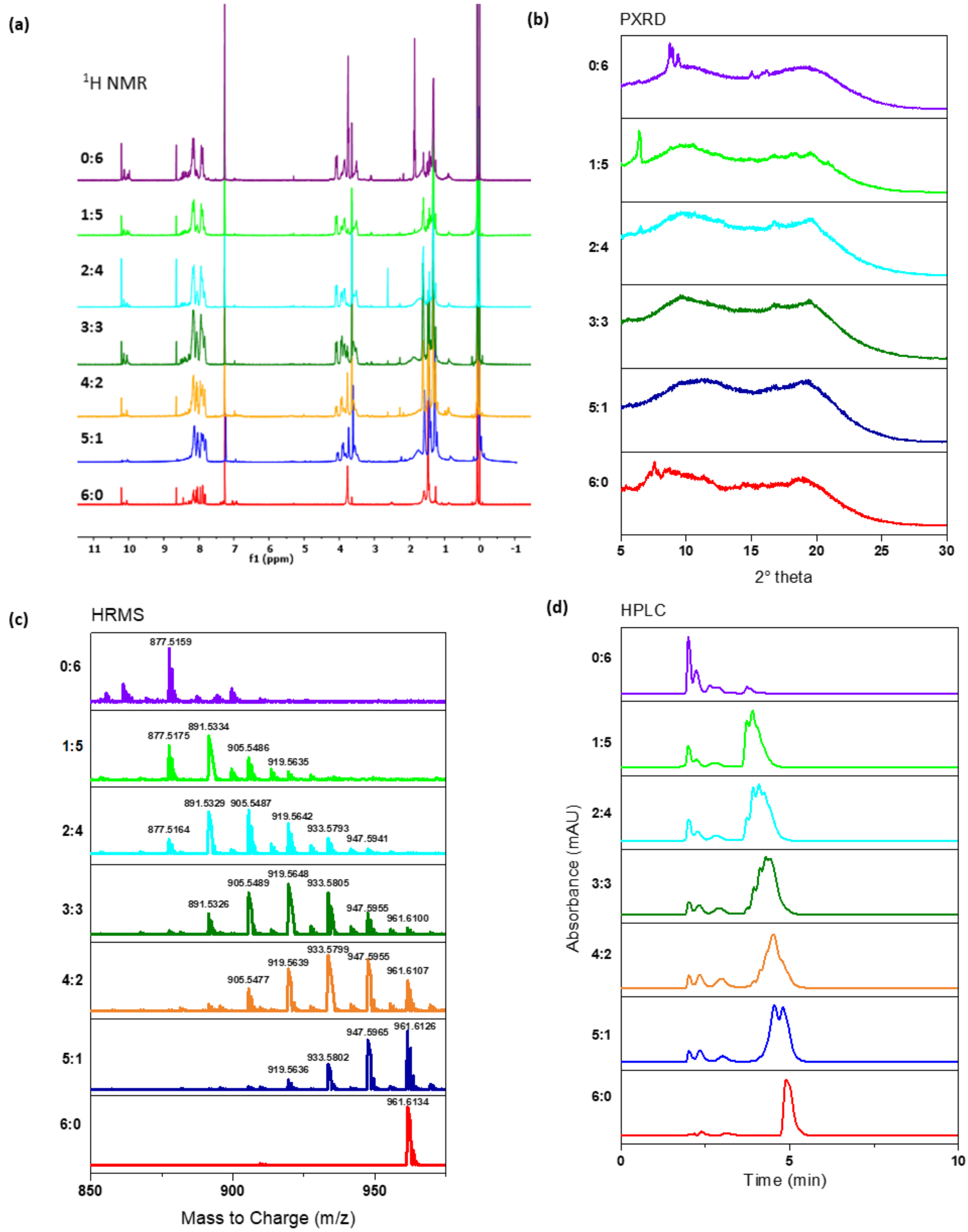

Fig. S9: Experimental data for the scrambled **A^n:C^{6-n}** cage family: (a) Stacked ^{1}H NMR spectra in CDCl$_3$; (b) Stacked PXRD patterns showing the formation of mainly amorphous material; (c) Stacked mass spectra with expected masses observed for **A^{6}C^0**, **A^{5}C^1**, **A^{4}C^2**, **A^{3}C^3**, **A^{2}C^4**, **A^{1}C^5**, and **A^{0}C^6** at 960.6003, 946.5846, 932.569, 918.5533, 904.5377, 890.522 and 876.5064; (d) Stacked HPLC spectra.

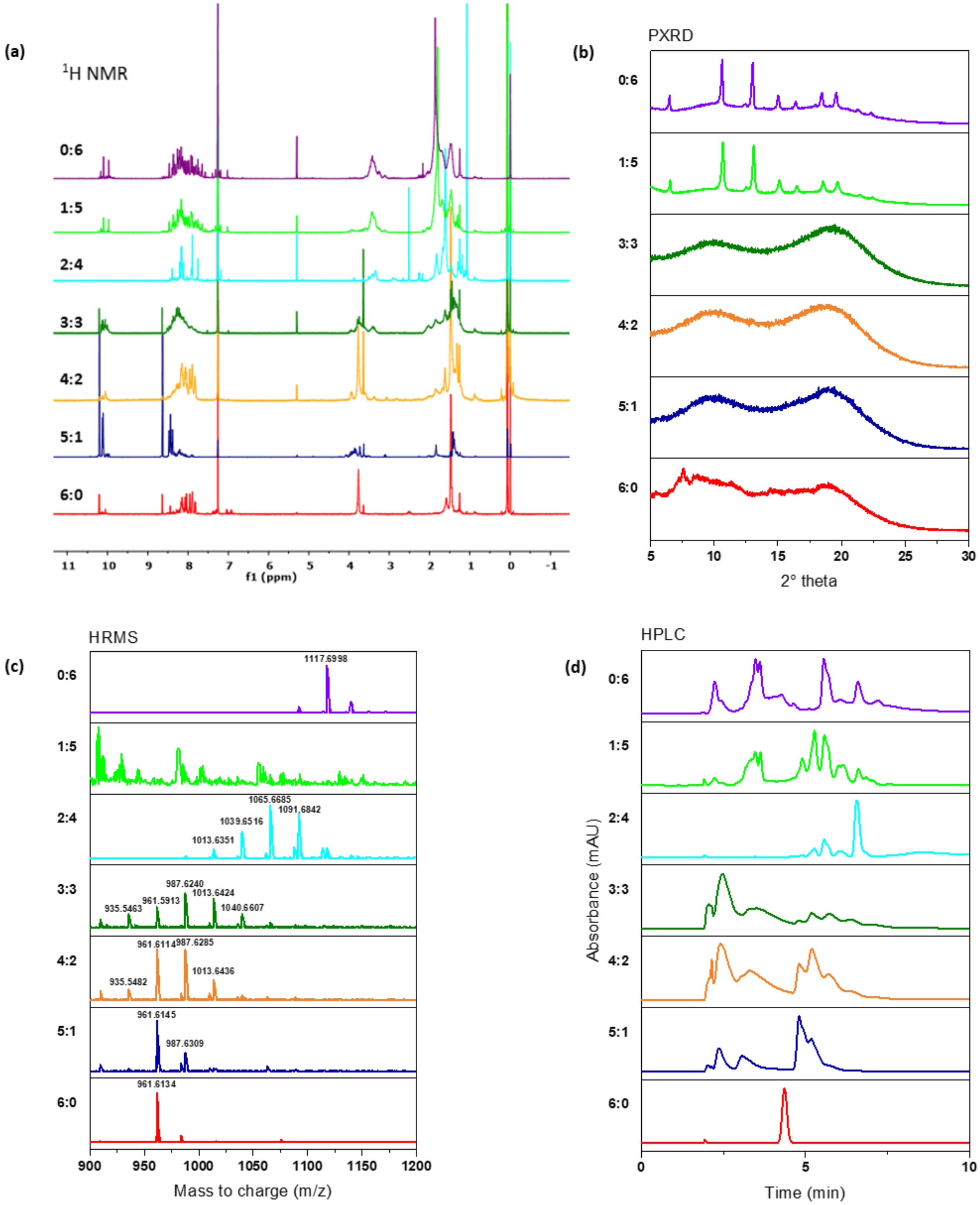

Fig. S10: Experimental data for the scrambled $\mathbf{A}^n\mathbf{:D}^{6\text{-}n}$ cage family: (a) Stacked ^{1}H NMR spectra in $CDCl_3$; (b) Stacked PXRD showing the formation of mainly amorphous material; (c) Stacked mass spectra with expected masses observed for $\mathbf{A}^6\mathbf{D}^0$, $\mathbf{A}^5\mathbf{D}^1$, $\mathbf{A}^4\mathbf{D}^2$, $\mathbf{A}^3\mathbf{D}^3$, $\mathbf{A}^2\mathbf{D}^4$, $\mathbf{A}^1\mathbf{D}^5$, and $\mathbf{A}^0\mathbf{D}^6$ at 960.6003, 986.6159, 1012.6316, 1038.6472, 1064.6629, 1090.6785 and 1116.6942; (d) Stacked HPLC spectra.

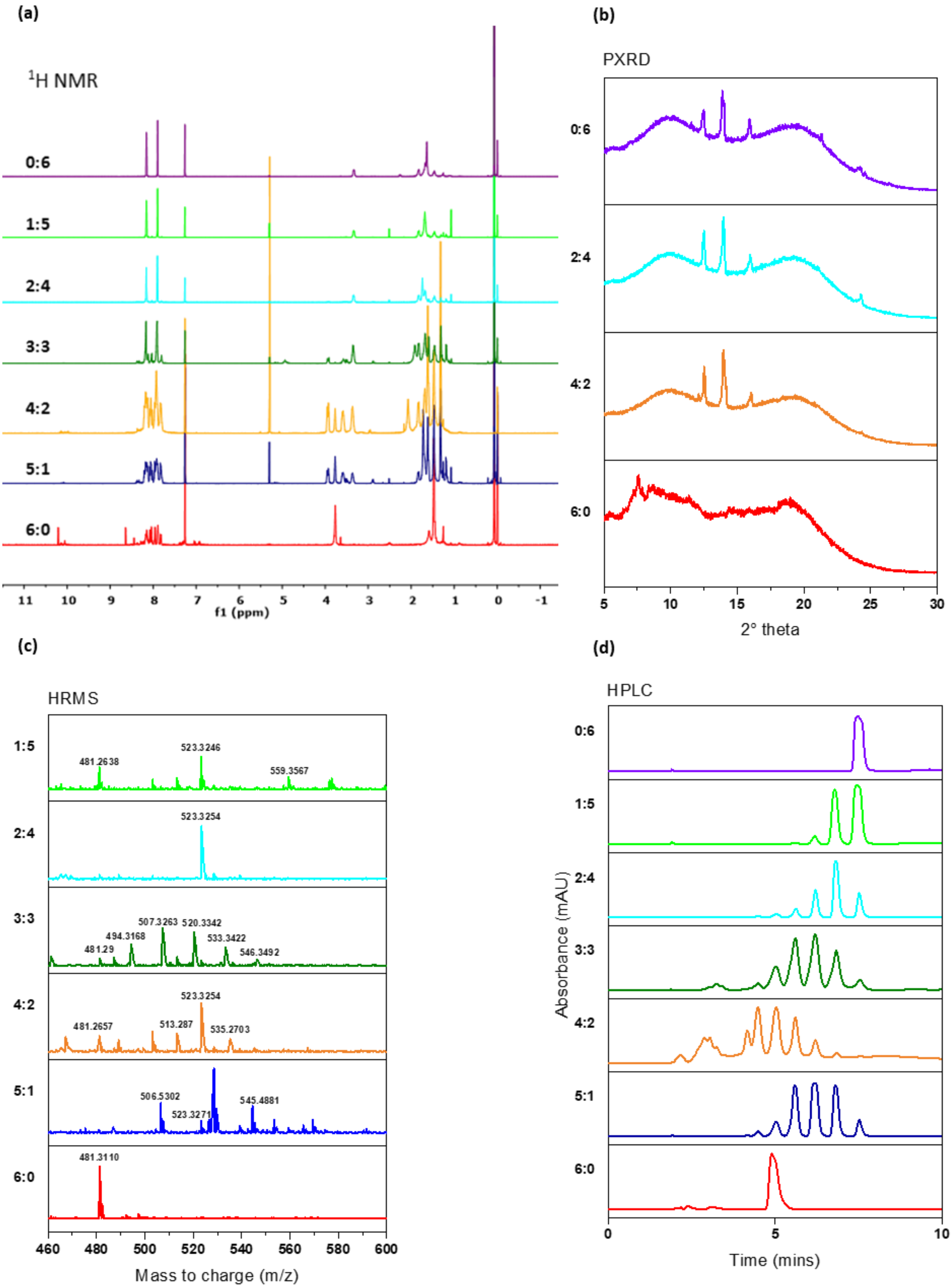

Fig. S11: Experimental data for the scrambled $\mathbf{A^n{:}E^{6-n}}$ cage family: (a) Stacked ^{1}H NMR spectra in CDCl$_3$; (b) Stacked PXRD showing the formation of mainly amorphous material; (c) Stacked mass spectra with expected masses observed for $\mathbf{A^6E^0}$, $\mathbf{A^5E^1}$, $\mathbf{A^4E^2}$, $\mathbf{A^3E^3}$, $\mathbf{A^2E^4}$, $\mathbf{A^1E^5}$, and $\mathbf{A^0E^6}$ at 960.6003, 986.6159, 1012.6316, 1038.6472, 1064.6629, 1090.6785 and 1116.6942; (d) Stacked HPLC spectra showing the formation of scrambled cages.

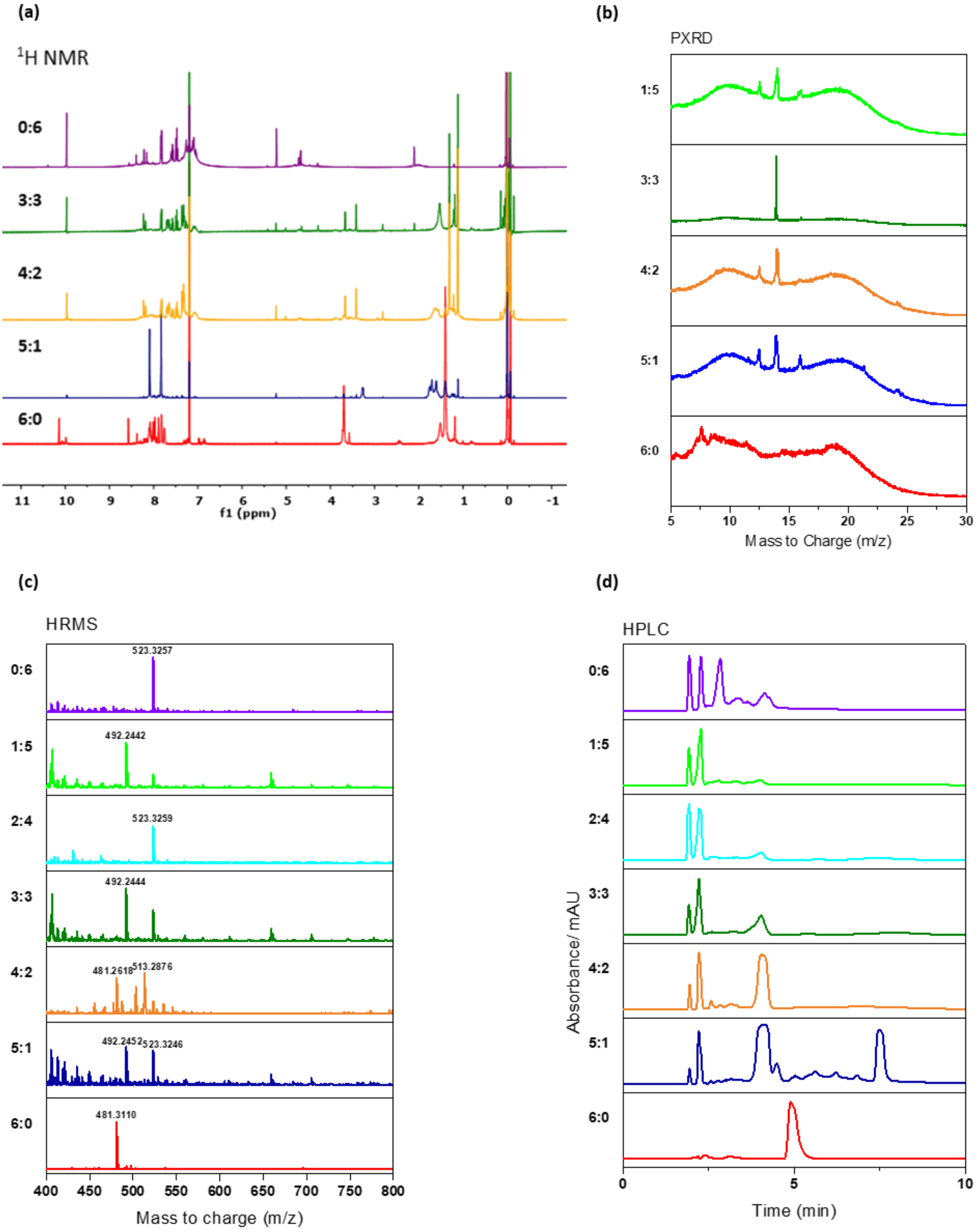

Fig. S12: Experimental data for the scrambled **A^n:F^{6-n}** cage family: (a) Stacked ^{1}H NMR spectra in $CDCl_3$; (b) Stacked PXRD showing the formation of mainly amorphous material; (c) Stacked mass spectra with expected masses observed for **A^6F^0**, **A^5F^1**, **A^4F^2**, **A^3F^3**, **A^2F^4**, **A^1F^5**, and **A^0F^6** at 960.6003, 1084.6316, 1208.6629, 1332.6942, 1456.7255, 1580.7568 and 1704.7881 (d) Stacked HPLC spectra.

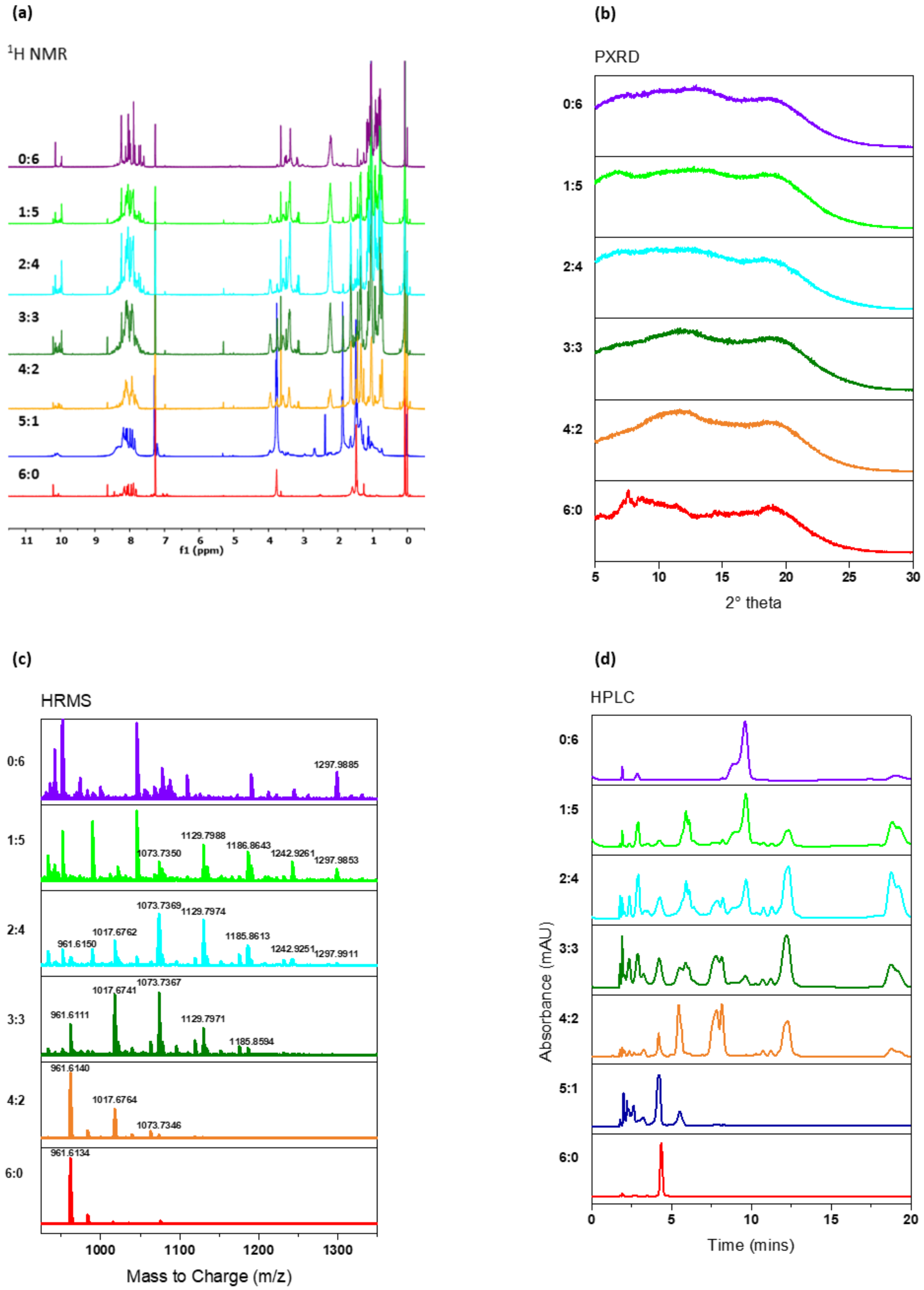

Fig. S13: Experimental data for the scrambled $\mathbf{A^n{:}G^{6-n}}$ cage family: (a) Stacked ^{1}H NMR spectra in $CDCl_3$; (b) Stacked PXRD showing the formation of amorphous material; (c) Stacked mass spectra with expected masses observed for $\mathbf{A^6G^0}$, $\mathbf{A^5G^1}$, $\mathbf{A^4G^2}$, $\mathbf{A^3G^3}$, $\mathbf{A^2G^4}$, $\mathbf{A^1G^5}$, and $\mathbf{A^0G^6}$ at 960.6003, 1016.6629, 1072.7255, 1128.7881, 1184.8507, 1240.9133 and 1296.9759; (d) Stacked HPLC spectra.

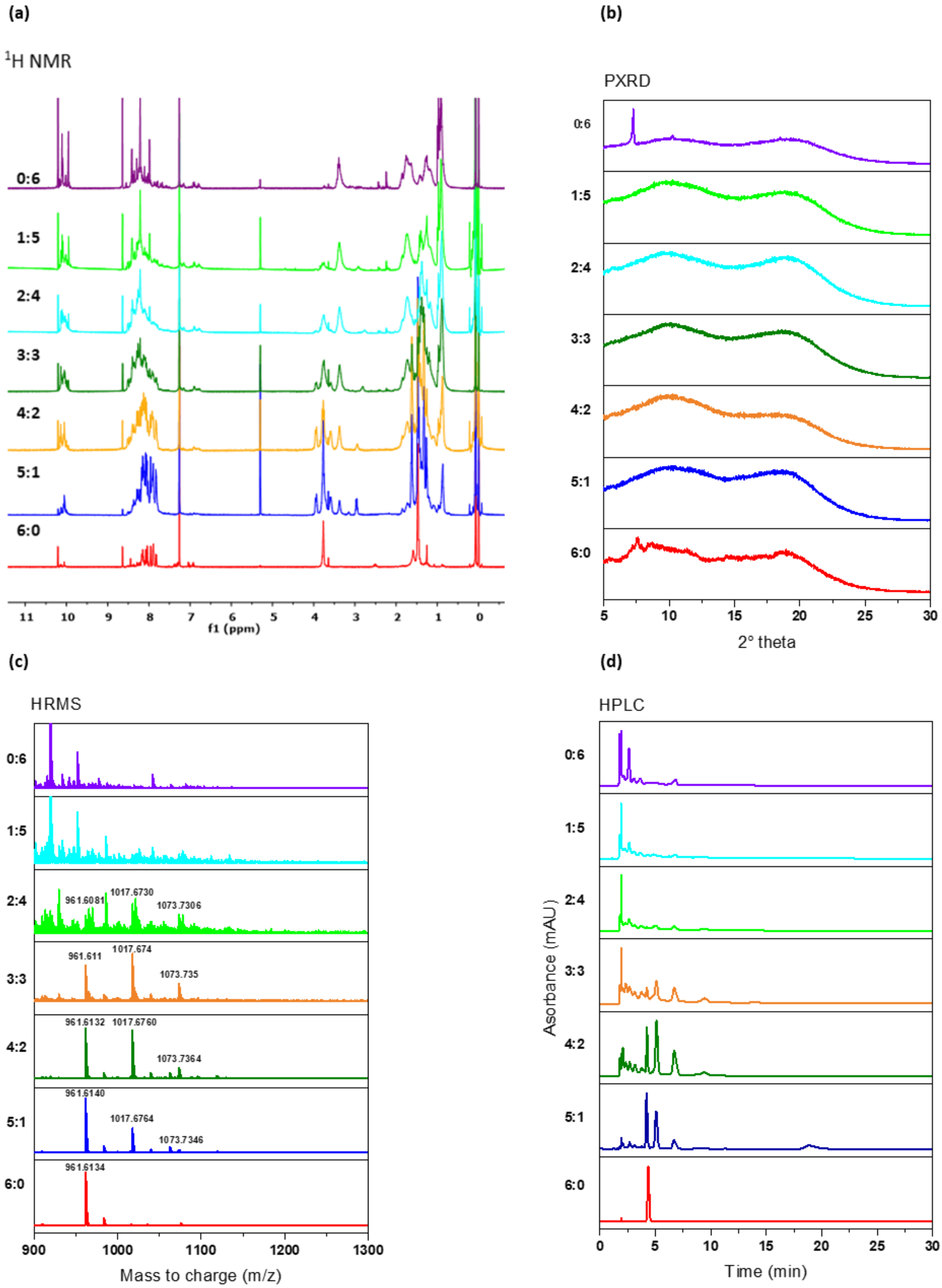

Fig. S14: Experimental data for the scrambled **A^n:H^{6-n}** cage family: (a) Stacked ^1H NMR spectra in $CDCl_3$; (b) Stacked PXRD showing the formation of amorphous material; (c) Stacked mass spectra with expected masses for **A^6H^0**, **A^5H^1**, **A^4H^2**, **A^3H^3**, **A^2H^4**, **A^1H^5**, and **A^0H^6** at 960.6003, 1016.6629, 1072.7255, 1128.7881, 1184.8507, 1240.9133 and 1296.9759; (d) Stacked HPLC spectra.

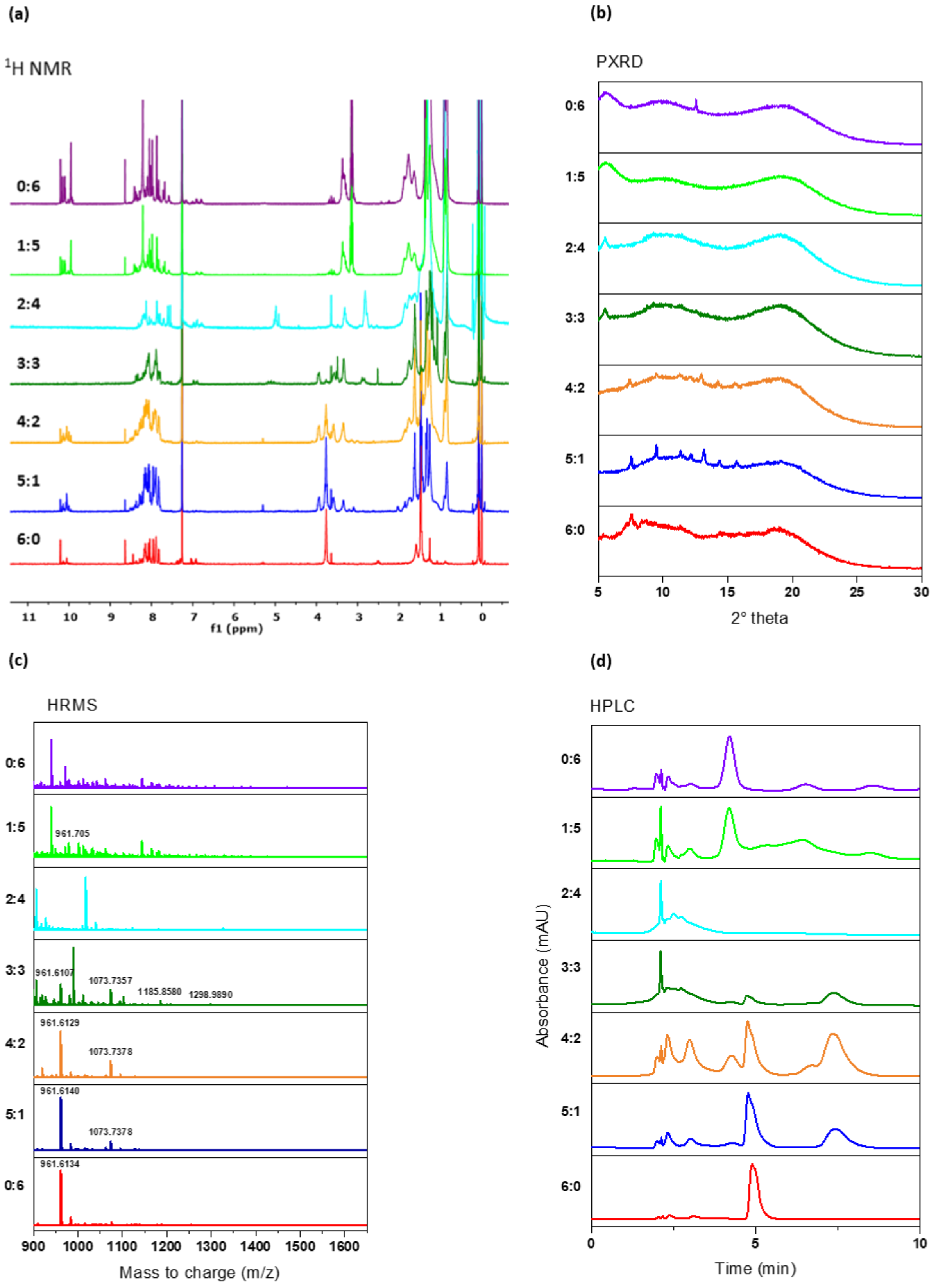

Fig. S15: Experimental data for the scrambled $\mathbf{A^n{:}I^{6-n}}$ cage family: (a) Stacked ^{1}H NMR spectra in $CDCl_3$; (b) Stacked PXRD showing the formation of mainly amorphous material; (c) Stacked mass spectra with expected masses observed for $\mathbf{A^6I^0}$, $\mathbf{A^5I^1}$, $\mathbf{A^4I^2}$, $\mathbf{A^3I^3}$, $\mathbf{A^2I^4}$, $\mathbf{A^1I^5}$, and $\mathbf{A^0I^6}$ at 960.6003, 1072.7255, 1184.8507, 1296.9759, 1409.1011, 1521.2263 and 1633.3515; (d) Stacked HPLC spectra.

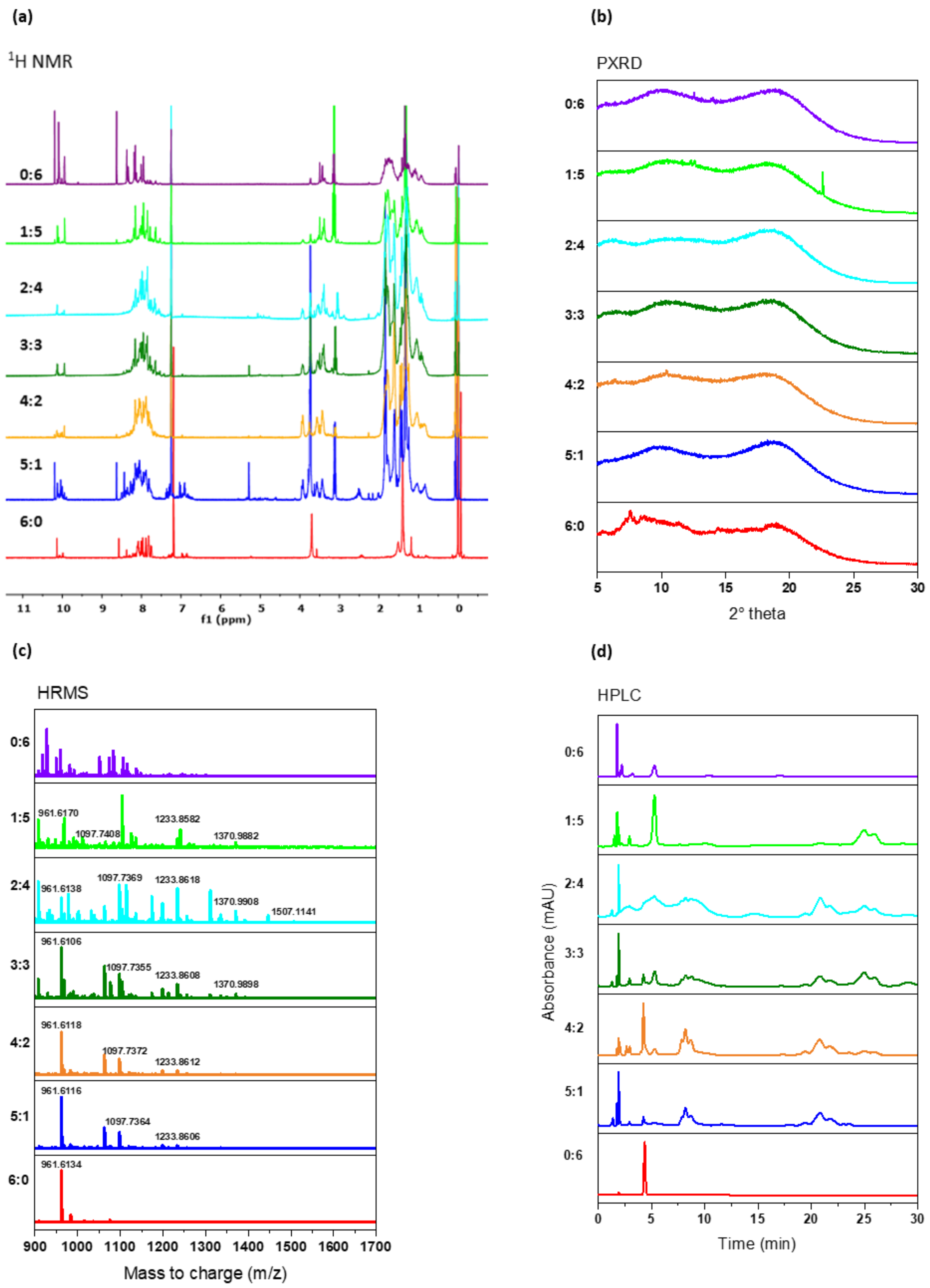

Fig. S16: Experimental data for the scrambled **A^n:J^{6-n}** cage family: (a) Stacked ^{1}H NMR spectra in CDCl$_3$; (b) Stacked PXRD showing the formation of mainly amorphous material; (c) Stacked mass spectra with expected masses observed for **A^{6}J^0**, **A^{5}J^1**, **A^{4}J^2**, **A^{3}J^3**, **A^{2}J^4**, **A^{1}J^5**, and **A^{0}J^6** at 960.6003, 1096.7255, 1232.8507, 1368.9759, 1505.1011, 1641.2263 and 1777.3515; (d) Stacked HPLC spectra.

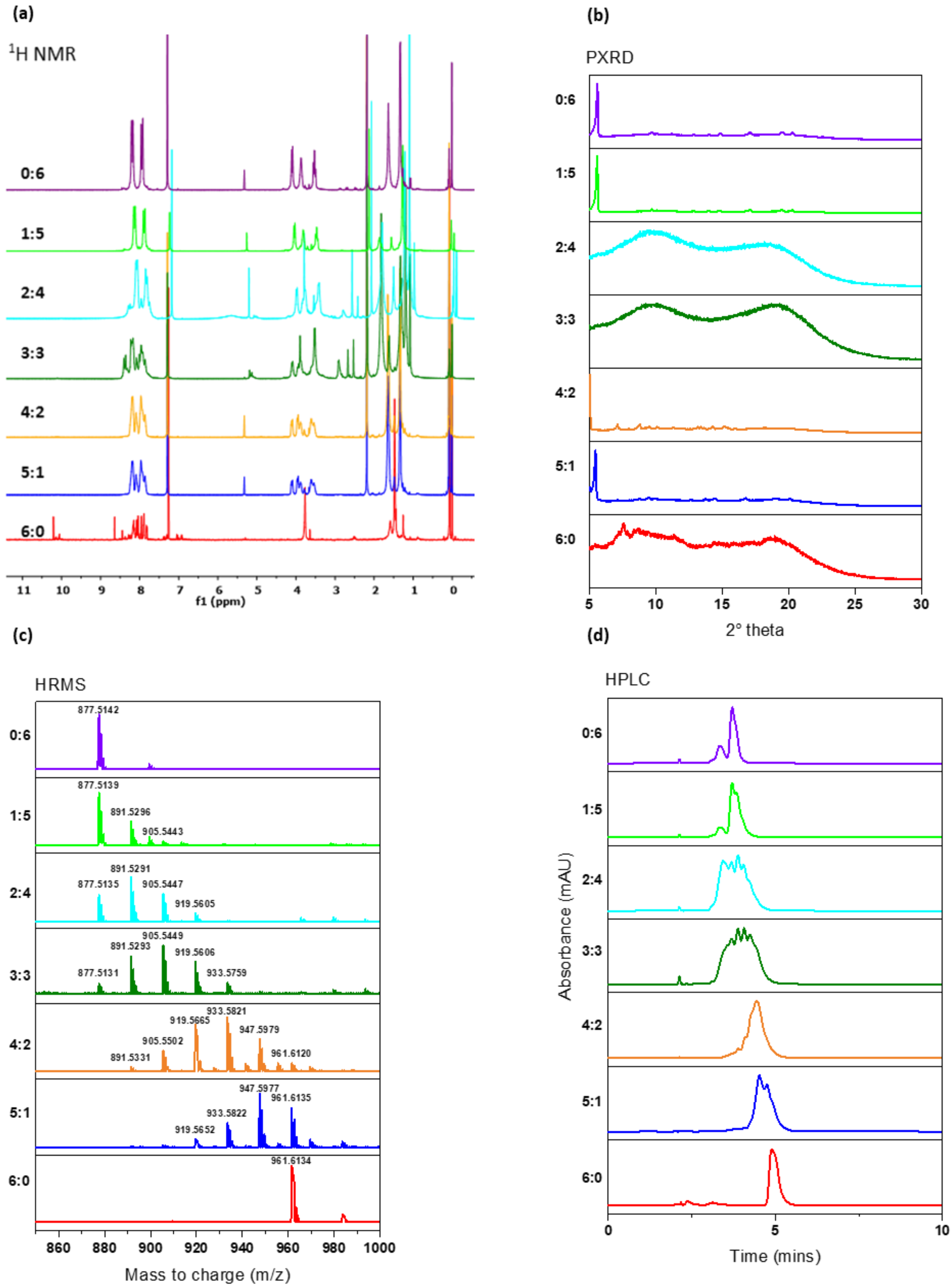

Fig. S17: Experimental data for the scrambled **A^n:K$^{6\text{-}n}$** cage family: (a) Stacked ^{1}H NMR spectra in $CDCl_3$; (b) Stacked PXRD showing the formation of amorphous material; (c) Stacked mass spectra with expected masses observed for **A^{6}K^0**, **A^{5}K^1**, **A^{4}K^2**, **A^{3}K^3**, **A^{2}K^4**, **A^{1}K^5**, and **A^{0}K^6** at 960.6003, 946.5846, 932.569, 918.5533, 904.5377, 890.522 and 876.5064; (d) Stacked HPLC spectra.

4. Selection of solvents

4.1. Common laboratory and non-size excluded solvent solubility screen

The initial investigations for selecting potential porous liquid solvents were carried out manually, and once selected, the methodology was translated onto a HT platform for the high-throughput solubility screen.

General procedure: Scrambled **3^3:13^3** (**A^3:E^3**) cage (30 mg) was manually weighed into a 2 mL vial and solvent was added in 0.1 mL increments using a disposable syringe. Between each addition, the sample was sonicated for 30 minutes and visually inspected to see if the solid had dissolved. If not, the procedure was repeated until dissolved or the lower threshold limit of 50 mg/mL had been reached. For a summary of the results see Table S6 and Fig. S18.

Table S6: Summary of results for solubility testing of **3^3:13^3** in common laboratory solvents

Vial number	**Mass of 3^3:13^3 cage (mg)**	**Solvent**	**Total volume added (mL)**						**Solubility (mg/mL)**
			0.1	0.2	0.3	0.4	0.5	0.6	
1	26.1	Chloroform	✓						261.0
2	26.6	DCM	✘	✘	✓				88.7
3	25.5	Chlorobenzene	✓						255.0
4	26.9	1,1,1,3,3,3-Hexafluoro-2-propanol	✓						269.0
5	26.4	Trifluoroethanol	✓						264.0
6	27.5	Hexane	✘	✘	✘	✘	✘	✘	<50
7	27.5	Toluene	✘	✘	✘	✓			68.8
8	27.5	*p*-xylene	✘	✓					137.5
9	28	Methanol	✘	✘	✘	✘	✘	✘	<50
10	27.4	Ethanol	✘	✘	✘	✘	✘	✘	<50
11	28.3	Isopropanol	✘	✘	✘	✘	✘	✘	<50
12	27.9	Butanol	✘	✘	✘	✘	✘	✘	<50
13	27.7	1,4-Dioxane	✘	✘	✘	✘	✘	✘	<50
14	27.7	Acetonitrile	✘	✘	✘	✘	✘	✘	<50
15	27.9	THF	✘	✘	✘	✘	✘	✘	<50
16	28	Ethyl acetate	✘	✘	✘	✘	✘	✘	<50
17	28.4	Diethyl ether	✘	✘	✘	✘	✘	✘	<50
18	26.8	DMF	✘	✘	✘	✘	✘	✘	<50
19	27.6	DMSO	✘	✘	✘	✘	✘	✘	<50
20	27.5	DMAC	✘	✘	✘	✘	✘	✘	<50
21	26.7	NMP	✘	✘	✘	✘	✘	✘	<50
22	26.9	Acetone	✘	✘	✘	✘	✘	✘	<50
23	27.2	4-Formyl morpholine	✘	✘	✘	✘	✘	✘	<50
24	32.1	2,2-Dimethoxypropane	✘	✘	✘	✘	✘	✘	<50
25	28.5	Cyclohexanone	✘	✘	✘	✘	✘	✘	<50
26	28.4	1-Butyl-3-methylimidazolium tetrafluoroborate	✘	✘	✘	✘	✘	✘	<50
27	26.4	1-Ethyl-3-methylimidazolium bis(trifluoromethylsulfonyl) imide	✘	✘	✘	✘	✘	✘	<50
28	27.1	Anisole (Methoxybenzene)	✘	✓					135.5

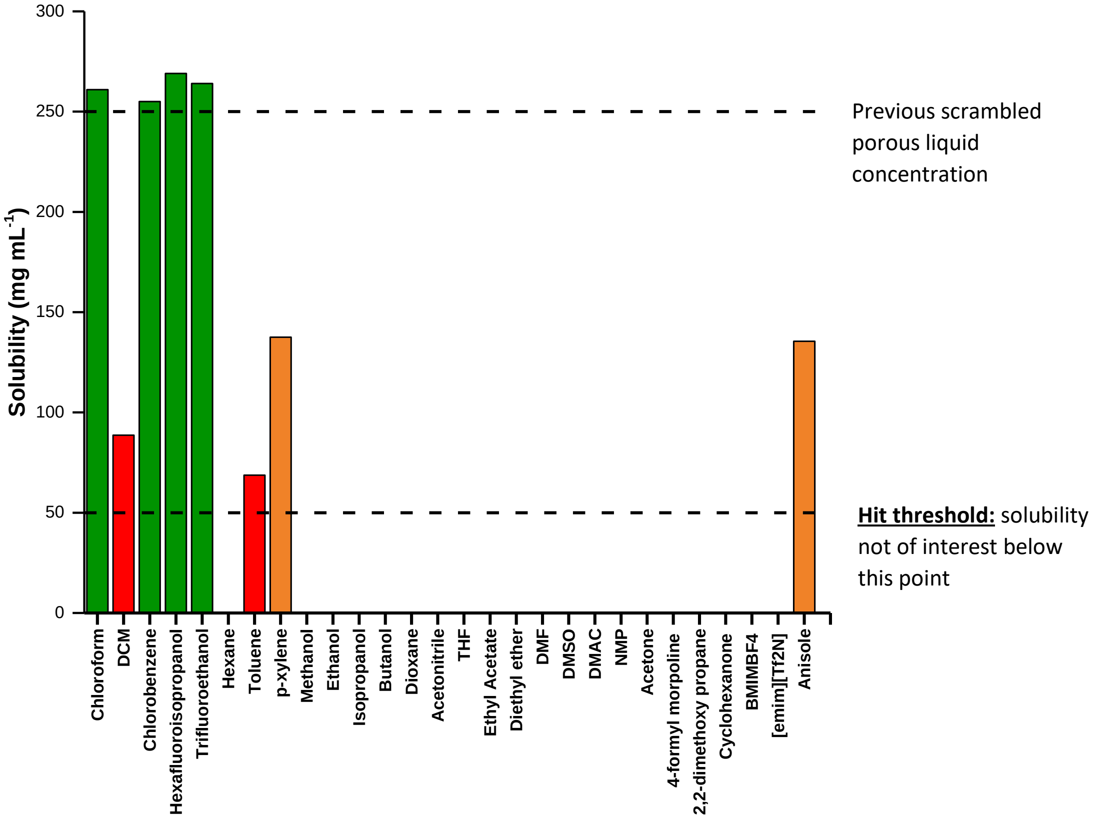

Fig. S18: Comparison of the solubility of scrambled **3^3:13^3** cage in a range of common laboratory solvents. A lower threshold limit of 50 mg/mL was used (shown as a dashed line), and only a solubility above this threshold was classified as a hit – any that fell below this limit are not shown on the graph as an accurate solubility was not recorded. Green = a high solubility, orange = a reasonable solubility, and red = a low solubility.

4.2. Solubility screen of previous scrambled cage (3^3:13^3) in bulkier solvents

The results from the common laboratory solvent solubility tests in Section 4.1 indicated solvent types in which the scrambled **3^3:13^3** cage was highly soluble, and influenced the selection of bulkier solvents that might be suitable for use in a Type II porous liquid. For example, the cage was highly soluble in chlorinated (chloroform, chlorobenzene), fluorinated (hexafluoropropanol, trifluoroethanol), methoxy-substituted (2-methoxybenzene), and certain aromatic solvents (chlorobenzene, p-xylene, 2-methoxybenzene), and therefore bulkier analogues of these were selected (Fig. S19). Further, some analogues with mixed functionality, and also some bulkier analogues of solvents in which the scrambled cage was poorly soluble, were included for comparison. Using this selection of bulkier solvents, a second solubility screen was carried out using the same procedure and scrambled cage to determine if there was a correlation between the smaller common laboratory solvents, and potential size-excluded solvents. For a summary of the results see Table S7.

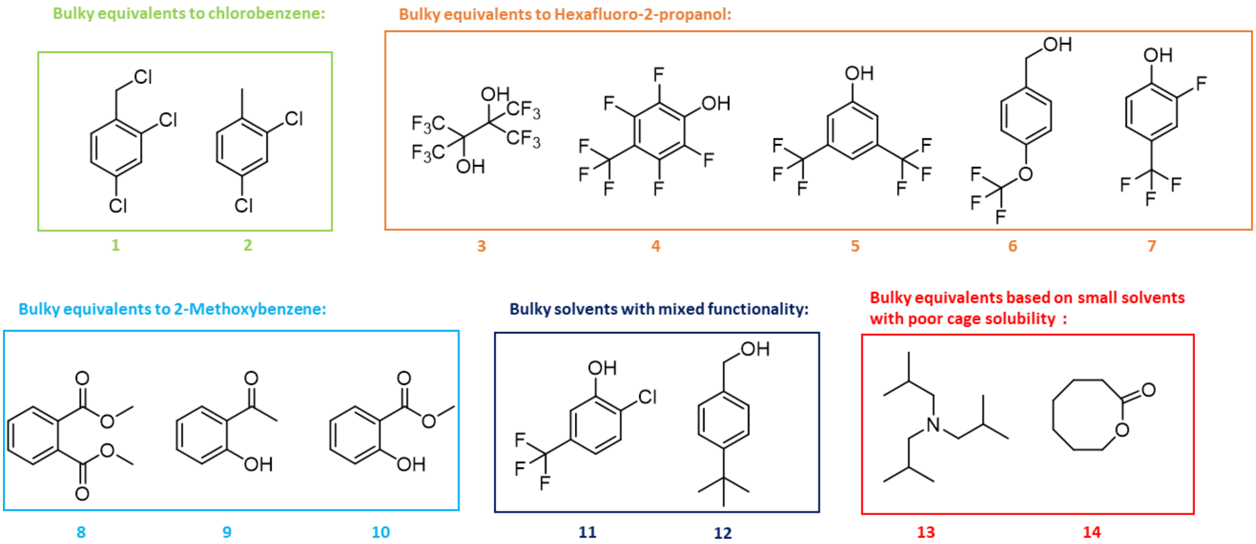

Fig. S19: The structures of the bulky solvents used in the initial solubility screen – solvents are grouped into different families and labelled **1 – 14**

Table S7: Summary of solubility testing of **3^3:13^3** in bulkier solvent analogues

Solvent number	Solvent name	Mass of cage (mg)	Total volume added (mL)				Solubility (mg/mL)
			0.1	0.2	0.3	0.4	
1	2,4-Dichlorobenzyl chloride	29.7	✓				297.0
2	2-Chloro-4-toluene	30.5	✓				305.0
3	Hexafluoro-2,3-bis (trifluoromethyl) butane-2,3-diol	31.7	✗	✗	✗	✓	79.3
4	2,3,5,6-Tetrafluoro-4-(trifluoromethyl)phenol	29.6	✗	✗	✓		98.7
5	3,5-Bis(trifluoromethyl) phenol	31.3	✗	✗	✓		104.3
6	4-(Trifluoromethoxy)benzyl alcohol	30.8	✓				308.0
7	2-Fluoro-5-(trifluoromethyl) phenol	30.3	✗	✗	✓		101.0
8	Dimethyl phathalate	28.7	✗	✗	✗	✗	<50
9	2-Hydroxyacetophenone	30.9	✓				309.0
10	Methyl salicylate	31.0	✓				310.0
11	4-Chloro-3-(trifluoromethyl)phenol	29.4	✗	✗	✓		147.0
12	4-(*tert*Butyl)benzyl alcohol	31.8	✗	✗	✓		106.0
13	Triisobutylamine	30.6	✗	✗	✗	✗	<50
14	ε-Caprolactone	28.8	✗	✗	✗	✗	<50

4.3. Xenon uptake measurements using chemical displacement

To determine if the bulkier solvent 'hits' in which the scrambled **3^3:13^3** cage was highly soluble from Section 4.2 were size-excluded, their use as a displacement solvent in the previously reported gas-loaded scrambled Type II porous liquid[6] was investigated (see Fig. S20). This was used as the cavity size of the cages was the same as those in the high-throughput scrambling screen. Xenon was chosen to be the displaced gas as only a single atom can occupy the cage cavities, meaning a maximum expected uptake can be calculated. If the solvent was not size-excluded, the maximum displacement of xenon would be 4.6 cm^3 on addition of the potential solvent to the xenon-loaded porous liquid.

Maximum expected volume of xenon that could be evolved per sample:

Mass of cage used = 200 mg
Moles of cage = 0.192 mmol
MW = 1039.34

$$V_{Xe} = \frac{nRT}{P} = \frac{(0.192\ x10^{-3})\ x\ 8.31\ x\ 298}{101325} = 4.6\ cm^3$$

General procedure: Samples of porous liquid were prepared by dissolving scrambled **3^3:13^3** cage (200 mg), desolvated in a vacuum oven at 90 °C overnight, in purified perchloropropene (1 mL) by vortexing – see *Chem. Sci.*, **2017**, *8*, 2640 for further details. Xenon was then added to the porous liquid by bubbling the gas through the sample at ~50-60 mL/min (60-66 on Gilmont flowmeter scale with a stainless steel float) for 10 min. The potential size-excluded solvent (1.0 eq. relative to cage) was then added and the displacement of water measured in an inverted burette over 10 minutes. Chloroform (16 µL, 1.0 eq. relative to cage) was then added to evolve the remaining xenon and the displacement of water was again measured over 10 minutes (see Table S8 and Fig. S21).

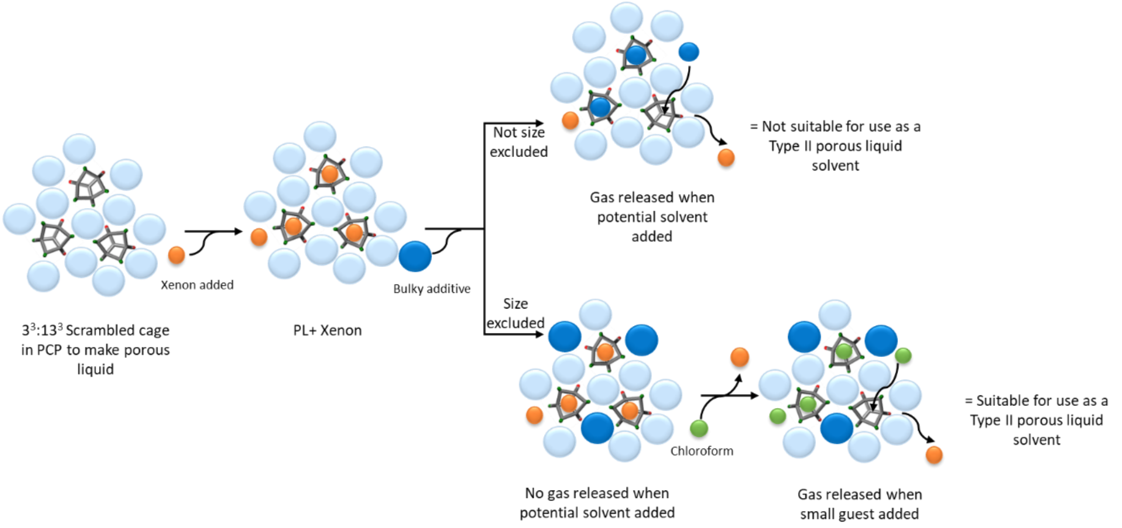

Fig. S20: General scheme to show the gas evolution experiments carried out using the previously reported scrambled porous liquid and the potential new porous liquid solvents as bulky additives

Table S8: Summary of the gas evolution screen on addition of bulky additives, with the volumes of xenon evolved to determine size-exclusivity of new potential porous liquid solvents

Bulky Additive (Bulky solvent from 4.2	**Solvent number**	**Total volume of gas evolved from porous liquid (cm^3)**		**Total volume of gas evolved from perchloropropene (cm^3)**	
		After addition of bulky additive	After addition of bulky additive and then $CHCl_3$	After addition of bulky additive	After addition of bulky additive and then $CHCl_3$
2,4-Dichlorobenzyl chloride	1	0.5	2.4	0.5	0.1
2-Chloro-4-toluene	2	0.6	1.6	0.1	0.0
Hexafluoro-2,3-bis (trifluoromethyl) butane-2,3-diol	3	0.1	2.3	0.3	0.1
2,3,5,6-Tetrafluoro-4-(trifluoromethyl)phenol	4	0.0	1.5	0.1	0.2
3,5-Bis(trifluoromethyl) phenol	5	0.1	2.3	0.3	0.1
4-(Trifluoromethoxy)benzyl alcohol	6	0.7	2.4	0.1	0.2
2-Fluoro-5-(trifluoromethyl) phenol	7	0.4	1.9	0.6	0.3
2-Hydroxyacetophenone	9	0.7	3.9	0.4	0.7
Methyl salicylate	10	0.5	1.2	0.1	0.2
4-Chloro-3-(trifluoromethyl)phenol	11	0.9	2.2	0.5	0.2
4-(*tert*Butyl)benzyl alcohol	12	0.3	2.2	1.0	0.4

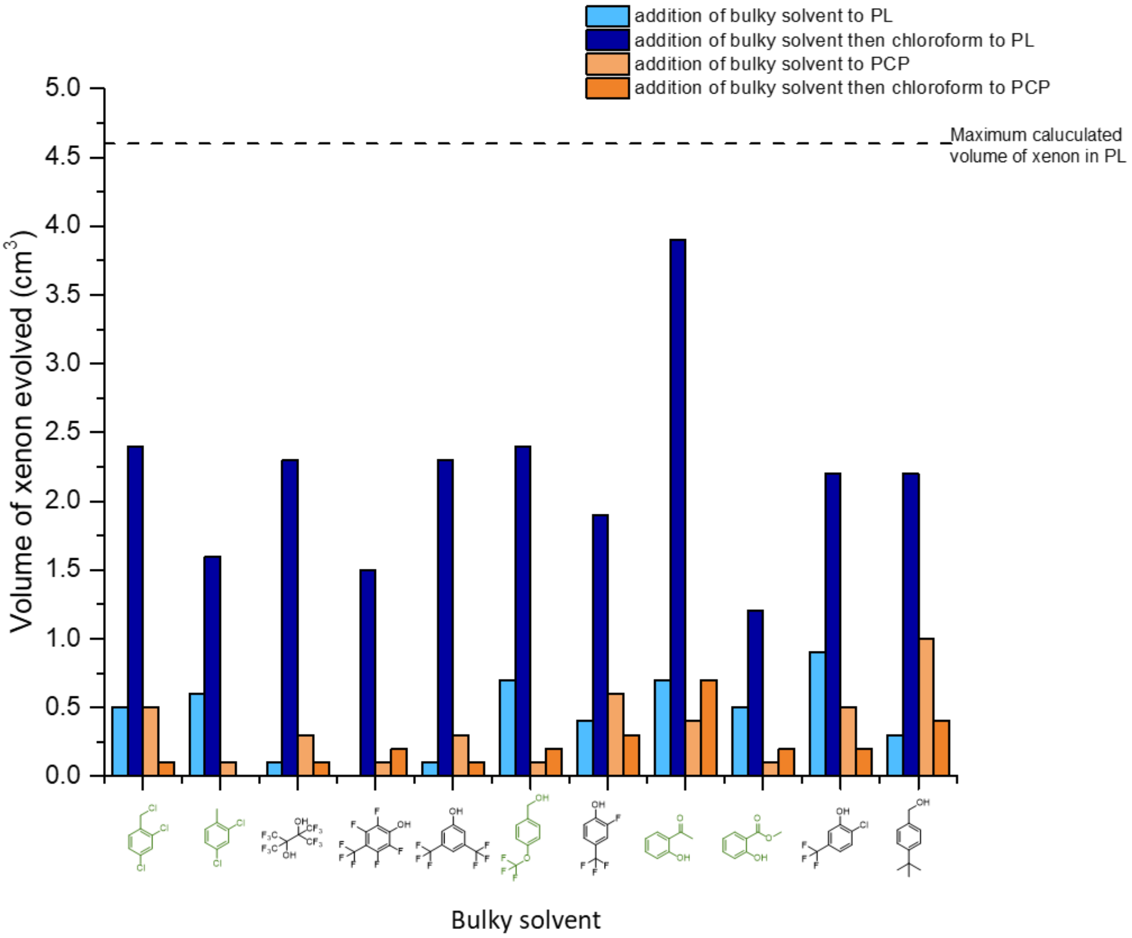

Fig. S21: Comparison of the amount of xenon evolved when a series of potential porous liquid solvents (shown along the bottom axes) were added to the original scrambled **3^3:13^3** porous liquid (20% w/v) and the neat solvent, perchloropropene (PCP). Green = solvents that were both highly solubilising and size excluded.

5. High-throughput solubility testing

General procedure: Stock solutions of the scrambled cage hits (300 mg) in chloroform (10 mL) were prepared and 1 mL of each stock solution was liquid dispensed into 250 pre-weighed vials using a Chemspeed Swing platform. The solvent was then removed under reduced pressure and the scrambled cage samples dried overnight in a vacuum oven at 90 °C, before the dispensed mass of cage was recorded – these were re-adjusted if needed to ensure ~30 mg of sample was in each vial. Using the Chemspeed Swing platform, the six size-excluded solvents (0.1 mL, Fig. S22) were then added to the samples in the vials using liquid dispensing, before the resulting mixture was sonicated for 30 minutes (if samples heated up during sonication, they were left to cool to room temperature). The mixture was visually inspected to determine if the solid had dissolved and the outcome recorded. If the solid had not fully dissolved, further increments of solvent (0.1 mL) were added *via* liquid dispensing, followed by sonication for 30 minutes, until the solid dissolved or the lower threshold of 100 mg/mL was reached (see Fig. S23). *NB.* The **3^3:13^3** (**A^3:E^3**) cage used in the reported original scrambled porous liquid[6] was included as a control to ensure the solubility screen was successful, as it is known to be soluble at 200 mg/mL in perchloropropene (PCP).

As the scrambled cages used were a mixture, there is a distribution of cages with different molecular weights – in order to take this into account in the screen, the molecular weight of the cage species formed using the diamine feed ratio was calculated and used as the average molecular weight in solubility calculations, for example, for the scrambled cage **A^3:E^3**:

Table S9: Methodology for calculating average molecular weight for scrambled cage **A^3:E^3**

Precursor	Chemical formula	Equivalents	MW in cage
TFB	$C_9H_6O_3$	4	264.462
Amine A	$C_4H_{12}N_2$	3	342.576
Amine E	$C_6H_{14}N_2$	3	648.576
		Sum =	1255.614
		Minus 12H_2O	1039.434

With each scrambled cage mixture having a different average molecular weight, there will be a different number of cavities per mL even if the mass/mL is the same (e.g. 20% w/v = 200 mg/1 mL). Therefore, the solubility of each cage in mmol/mL was also calculated to allow a more accurate comparison of the different scrambled cage solubilities in the size-excluded solvents.

For a summary of the high-throughput solubility screen see Table S10.

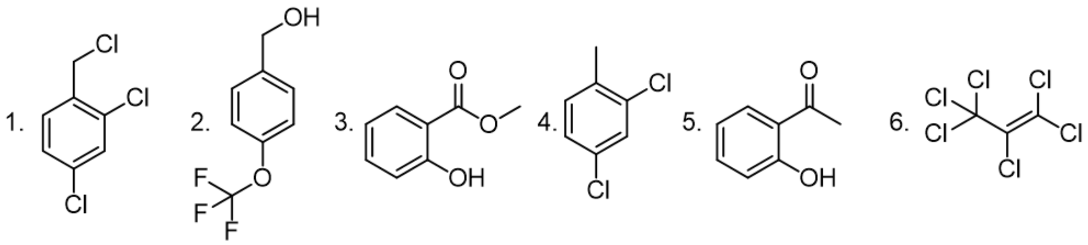

2,4-Dichlorobenzyl chloride (DCBC) **4-(Trifluoromethoxy)benzyl alcohol (TBA)** **Methyl salicylate (MS)** **2-Chloro-4-toluene (DCT)** **2-Hydroxyacetophenone (HAP)** **Perchloropropene (PCP)**

Fig. S22: The six size-excluded solvents used during the high-throughput solubility screen

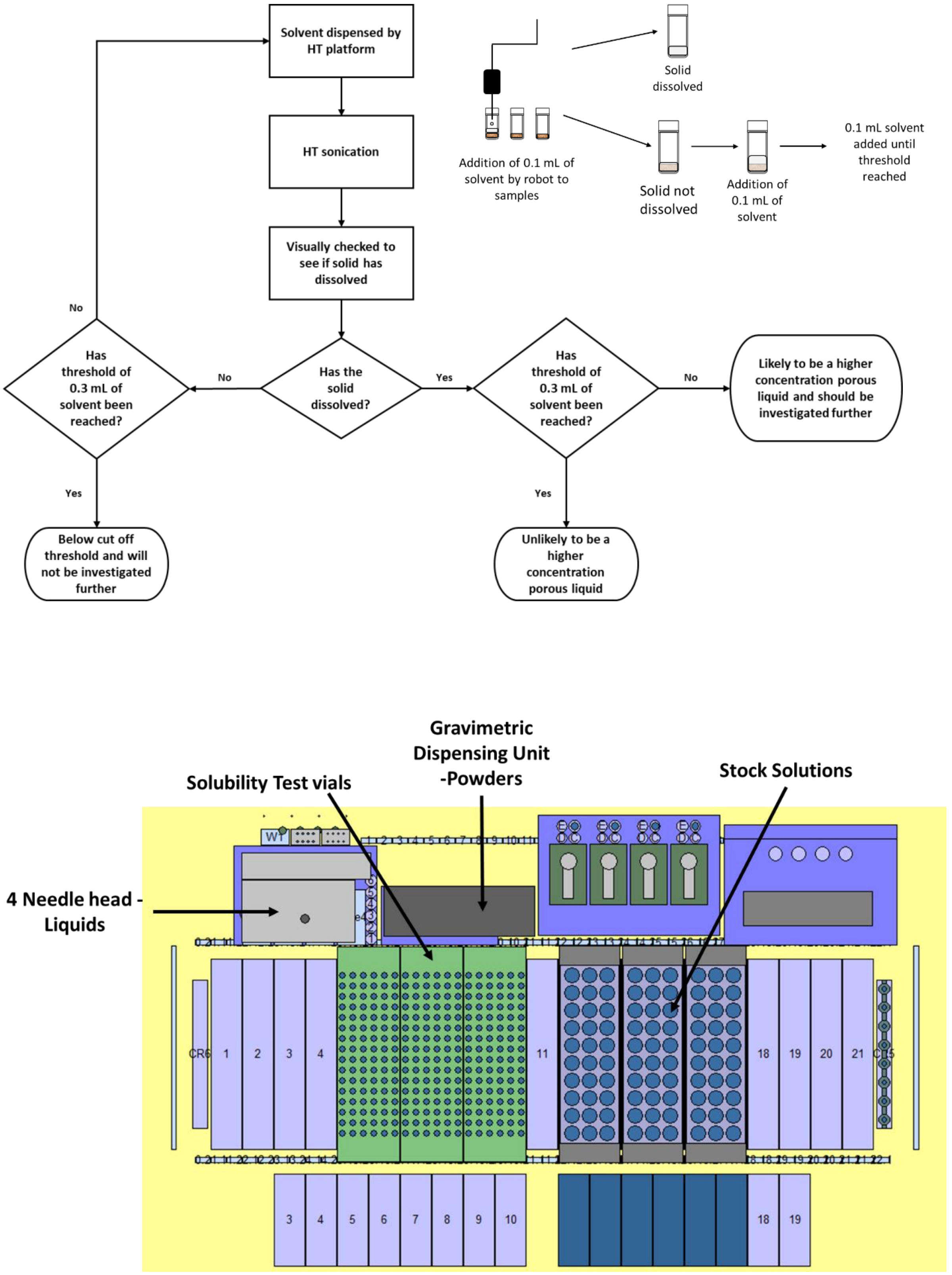

Fig. S23: Graphical representation of the methodology used during the high-throughput solubility screen with size-excluded solvents (upper), and a graphical layout of the Chemspeed Swing platform used during the high-throughput solubility testing (lower)

Table S10: Summary of results from the high-throughput solubility screen

Reaction Code	Scrambled cage (Amine A: Amine X)	Chemical formula	Average MW	Mass (mg)	Solvent	Fully dissolved in: 0.1 mL?	0.2 mL?	0.3 mL?	Overall solubility (mg/mL)	Overall solubility (mmol/mL)
A6	$A^6:B^0$	$C_{60}H_{72}N_{12}$	961.320	31.4	1	✘	✘	✘	<50	-
A12	$A^6:B^0$	$C_{60}H_{72}N_{12}$	961.320	29.3	2	✘	✓		146.5	0.152
A18	$A^6:B^0$	$C_{60}H_{72}N_{12}$	961.320	32.3	3	✘	✘	✘	<50	-
A24	$A^6:B^0$	$C_{60}H_{72}N_{12}$	961.320	31.2	4	✘	✘	✘	<50	-
A30	$A^6:B^0$	$C_{60}H_{72}N_{12}$	961.320	28.7	5	✘	✘	✓	95.7	0.100
A36	$A^6:B^0$	$C_{60}H_{72}N_{12}$	961.320	31.1	6	✘	✘	✘	<50	-
B1	$A^5:B^1$	$C_{58}H_{68}N_{12}$	933.266	29.0	1	✘	✘	✘	<50	-
B2	$A^4:B^2$	$C_{56}H_{64}N_{12}$	905.212	29.4	1	✘	✘	✘	<50	-
B3	$A^3:B^3$	$C_{54}H_{60}N_{12}$	877.158	30.8	1	✘	✘	✘	<50	-
B4	$A^2:B^4$	$C_{52}H_{56}N_{12}$	849.104	29.3	1	✘	✘	✘	<50	-
B5	$A^1:B^5$	$C_{50}H_{52}N_{12}$	821.05	28.6	1	✘	✘	✘	<50	-
B6	$A^0:B^6$	$C_{48}H_{48}N_{12}$	792.996	30.8	1	✘	✘	✘	<50	-
B7	$A^5:B^1$	$C_{58}H_{68}N_{12}$	933.266	29.5	2	✘	✘	✓	98.3	0.152
B8	$A^4:B^2$	$C_{56}H_{64}N_{12}$	905.212	31.2	2	✘	✘	✓	104.0	0.115
B9	$A^3:B^3$	$C_{54}H_{60}N_{12}$	877.158	30.5	2	✘	✘	✓	101.7	0.116
B10	$A^2:B^4$	$C_{52}H_{56}N_{12}$	849.104	28.6	2	✘	✘	✓	95.3	0.112
B11	$A^1:B^5$	$C_{50}H_{52}N_{12}$	821.05	29.5	2	✘	✘	✓	98.3	0.120
B12	$A^0:B^6$	$C_{48}H_{48}N_{12}$	792.996	30.9	2	✘	✘	✓	103.0	0.130
B13	$A^5:B^1$	$C_{58}H_{68}N_{12}$	933.266	31.8	3	✘	✘	✘	<50	-
B14	$A^4:B^2$	$C_{56}H_{64}N_{12}$	905.212	30.8	3	✘	✘	✘	<50	-
B15	$A^3:B^3$	$C_{54}H_{60}N_{12}$	877.158	30.7	3	✘	✘	✘	<50	-
B16	$A^2:B^4$	$C_{52}H_{56}N_{12}$	849.104	28.3	3	✘	✘	✘	<50	-
B17	$A^1:B^5$	$C_{50}H_{52}N_{12}$	821.05	29.3	3	✘	✘	✘	<50	-
B18	$A^0:B^6$	$C_{48}H_{48}N_{12}$	792.996	31.2	3	✘	✘	✘	<50	-
B19	$A^5:B^1$	$C_{58}H_{68}N_{12}$	933.266	30.2	4	✘	✘	✘	<50	-
B20	$A^4:B^2$	$C_{56}H_{64}N_{12}$	905.212	29.4	4	✘	✘	✘	<50	-
B21	$A^3:B^3$	$C_{54}H_{60}N_{12}$	877.158	30.2	4	✘	✘	✘	<50	-
B22	$A^2:B^4$	$C_{52}H_{56}N_{12}$	849.104	31.2	4	✘	✘	✘	<50	-
B23	$A^1:B^5$	$C_{50}H_{52}N_{12}$	821.05	27.9	4	✘	✘	✘	<50	-
B24	$A^0:B^6$	$C_{48}H_{48}N_{12}$	792.996	29.2	4	✘	✘	✘	<50	-
B25	$A^5:B^1$	$C_{58}H_{68}N_{12}$	933.266	29.3	5	✘	✘	✘	<50	-
B26	$A^4:B^2$	$C_{56}H_{64}N_{12}$	905.212	30.1	5	✘	✘	✘	<50	-
B27	$A^3:B^3$	$C_{54}H_{60}N_{12}$	877.158	31.0	5	✘	✘	✘	<50	-
B28	$A^2:B^4$	$C_{52}H_{56}N_{12}$	849.104	25.0	5	✘	✘	✓	83.3	0.100
B29	$A^1:B^5$	$C_{50}H_{52}N_{12}$	821.05	29.6	5	✘	✘	✘	<50	-
B30	$A^0:B^6$	$C_{48}H_{48}N_{12}$	792.996	30.6	5	✘	✘	✘	<50	-
B31	$A^5:B^1$	$C_{58}H_{68}N_{12}$	933.266	31.2	6	✘	✘	✘	<50	-
B32	$A^4:B^2$	$C_{56}H_{64}N_{12}$	905.212	30.6	6	✘	✘	✘	<50	-
B33	$A^3:B^3$	$C_{54}H_{60}N_{12}$	877.158	31.6	6	✘	✘	✘	<50	-
B34	$A^2:B^4$	$C_{52}H_{56}N_{12}$	849.104	20.1	6	✘	✘	✘	<50	-
B35	$A^1:B^5$	$C_{50}H_{52}N_{12}$	821.05	29.5	6	✘	✘	✘	<50	-
B36	$A^0:B^6$	$C_{48}H_{48}N_{12}$	792.996	31.1	6	✘	✘	✘	<50	-
C1	$A^5:C^1$	$C_{59}H_{70}N_{12}$	947.293	27.4	1	✘	✘	✘	<50	-
C2	$A^4:C^2$	$C_{58}H_{68}N_{12}$	933.266	27.6	1	✘	✘	✘	<50	-
C3	$A^3:C^3$	$C_{57}H_{66}N_{12}$	919.239	31.1	1	✘	✘	✘	<50	-
C4	$A^2:C^4$	$C_{56}H_{64}N_{12}$	905.212	29.2	1	✘	✘	✓	97.3	0.108
C5	$A^1:C^5$	$C_{55}H_{62}N_{12}$	891.185	30.4	1	✘	✓		152.0	0.171
C6	$A^0:C^6$	$C_{54}H_{60}N_{12}$	877.158	30.3	1	✘	✘	✘	<50	-
C7	$A^5:C^1$	$C_{59}H_{70}N_{12}$	947.293	27.9	2	✘	✘	✓	93.0	0.0982
C8	$A^4:C^2$	$C_{58}H_{68}N_{12}$	933.266	29.8	2	✘	✘	✓	99.3	0.106
C9	$A^3:C^3$	$C_{57}H_{66}N_{12}$	919.239	29.8	2	✘	✓		149.0	0.162
C10	$A^2:C^4$	$C_{56}H_{64}N_{12}$	905.212	27.2	2	✘	✓		136.0	0.150
C11	$A^1:C^5$	$C_{55}H_{62}N_{12}$	891.185	30.8	2	✘	✘	✓	102.7	0.115
C12	$A^0:C^6$	$C_{54}H_{60}N_{12}$	877.158	28.9	2	✘	✓		144.5	0.165
C13	$A^5:C^1$	$C_{59}H_{70}N_{12}$	947.293	22.2	3	✘	✘	✘	<50	-
C14	$A^4:C^2$	$C_{58}H_{68}N_{12}$	933.266	28.7	3	✘	✘	✘	<50	-
C15	$A^3:C^3$	$C_{57}H_{66}N_{12}$	919.239	30.2	3	✘	✓		151.0	0.164
C16	$A^2:C^4$	$C_{56}H_{64}N_{12}$	905.212	29.7	3	✘	✓		148.5	0.164
C17	$A^1:C^5$	$C_{55}H_{62}N_{12}$	891.185	29.4	3	✘	✘	✓	98.0	0.110
C18	$A^0:C^6$	$C_{54}H_{60}N_{12}$	877.158	30.9	3	✘	✘	✓	103.0	0.117
C19	$A^5:C^1$	$C_{59}H_{70}N_{12}$	947.293	15.5	4	✘	✘	✘	<50	-

C20	A^4:C^2	$C_{58}H_{68}N_{12}$	933.266	29.3	4	✗	✗	✗	<50	-
C21	A^3:C^3	$C_{57}H_{66}N_{12}$	919.239	30.2	4	✗	✗	✗	<50	-
C22	A^2:C^4	$C_{56}H_{64}N_{12}$	905.212	30.4	4	✗	✗	✓	101.3	0.112
C23	A^1:C^5	$C_{55}H_{62}N_{12}$	891.185	31.5	4	✗	✗	✗	<50	-
C24	A^0:C^6	$C_{54}H_{60}N_{12}$	877.158	30.3	4	✗	✗	✗	<50	-
C25	A^5:C^1	$C_{59}H_{70}N_{12}$	947.293	10.4	5	✗	✓		52.0	0.0555
C26	A^4:C^2	$C_{58}H_{68}N_{12}$	933.266	9.3	5	✗	✗	✓	31.0	0.0332
C27	A^3:C^3	$C_{57}H_{66}N_{12}$	919.239	9.3	5	✗	✗	✓	30.7	0.0334
C28	A^2:C^4	$C_{56}H_{64}N_{12}$	905.212	12.5	5	✗	✗	✓	41.7	0.0460
C29	A^1:C^5	$C_{55}H_{62}N_{12}$	891.185	-	5	✗	✗	✗	<50	-
C30	A^0:C^6	$C_{54}H_{60}N_{12}$	877.158	17.0	5	✗	✓		85.0	0.0969
C31	A^5:C^1	$C_{59}H_{70}N_{12}$	947.293	10.3	6	✗	✗	✓	34.3	0.0362
C32	A^4:C^2	$C_{58}H_{68}N_{12}$	933.266	29.5	6	✗	✗	✗	<50	-
C33	A^3:C^3	$C_{57}H_{66}N_{12}$	919.239	30.2	6	✗	✗	✗	<50	-
C34	A^2:C^4	$C_{56}H_{64}N_{12}$	905.212	30.3	6	✗	✗	✗	<50	-
C35	A^1:C^5	$C_{55}H_{62}N_{12}$	891.185	33	6	✗	✗	✗	<50	-
C36	A^0:C^6	$C_{54}H_{60}N_{12}$	877.158	30.7	6	✗	✗	✗	<50	-
E1	A^5:E^1	$C_{62}H_{74}N_{12}$	987.358	29.3	1	✗	✗	✗	<50	-
E2	A^4:E^2	$C_{64}H_{76}N_{12}$	1013.396	31.1	1	✗	✓		155.5	0.153
E3	A^3:E^3	$C_{66}H_{78}N_{12}$	1039.434	30.4	1	✓			304.0	0.292
E4	A^2:E^4	$C_{68}H_{80}N_{12}$	1065.472	30.6	1	✗	✗	✗	<50	-
E5	A^1:E^5	$C_{70}H_{82}N_{12}$	1091.510	28.4	1	✗	✗	✗	<50	-
E6	A^0:E^6	$C_{72}H_{84}N_{12}$	1117.548	30.4	1	✗	✗	✗	<50	-
E7	A^5:E^1	$C_{62}H_{74}N_{12}$	987.358	29.7	2	✗	✓		148.5	0.150
E8	A^4:E^2	$C_{64}H_{76}N_{12}$	1013.396	31.4	2	✗	✓		157.0	0.155
E9	A^3:E^3	$C_{66}H_{78}N_{12}$	1039.434	29.1	2	✓			291.0	0.280
E10	A^2:E^4	$C_{68}H_{80}N_{12}$	1065.472	30.4	2	✗	✗	✓	101.3	0.0951
E11	A^1:E^5	$C_{70}H_{82}N_{12}$	1091.510	31.7	2	✗	✗	✓	105.7	0.0968
E12	A^0:E^6	$C_{72}H_{84}N_{12}$	1117.548	30.3	2	✗	✗	✗	<50	-
E13	A^5:E^1	$C_{62}H_{74}N_{12}$	987.358	30.5	3	✗	✗	✗	<50	-
E14	A^4:E^2	$C_{64}H_{76}N_{12}$	1013.396	29.6	3	✗	✗	✗	<50	-
E15	A^3:E^3	$C_{66}H_{78}N_{12}$	1039.434	30.8	3	✓			308.0	0.296
E16	A^2:E^4	$C_{68}H_{80}N_{12}$	1065.472	29.7	3	✗	✗	✓	99.0	0.0929
E17	A^1:E^5	$C_{70}H_{82}N_{12}$	1091.510	31	3	✗	✗	✗	<50	-
E18	A^0:E^6	$C_{72}H_{84}N_{12}$	1117.548	32	3	✗	✗	✗	<50	-
E19	A^5:E^1	$C_{62}H_{74}N_{12}$	987.358	29.8	4	✗	✗	✗	<50	-
E20	A^4:E^2	$C_{64}H_{76}N_{12}$	1013.396	29.7	4	✗	✗	✗	<50	-
E21	A^3:E^3	$C_{66}H_{78}N_{12}$	1039.434	29.7	4	✓			297.0	0.286
E22	A^2:E^4	$C_{68}H_{80}N_{12}$	1065.472	29.9	4	✗	✗	✗	<50	-
E23	A^1:E^5	$C_{70}H_{82}N_{12}$	1091.510	29.9	4	✗	✗	✗	<50	-
E24	A^0:E^6	$C_{72}H_{84}N_{12}$	1117.548	28.5	4	✗	✗	✗	<50	-
E25	A^5:E^1	$C_{62}H_{74}N_{12}$	987.358	24.0	5	✗	✓		120.0	0.122
E26	A^4:E^2	$C_{64}H_{76}N_{12}$	1013.396	28.3	5	✗	✗	✗	<50	-
E27	A^3:E^3	$C_{66}H_{78}N_{12}$	1039.434	28.6	5	✓			286.0	0.275
E28	A^2:E^4	$C_{68}H_{80}N_{12}$	1065.472	29.1	5	✗	✓		145.5	0.137
E29	A^1:E^5	$C_{70}H_{82}N_{12}$	1091.510	29.4	5	✗	✗	✓	98.0	0.0900
E30	A^0:E^6	$C_{72}H_{84}N_{12}$	1117.548	30.9	5	✗	✗	✓	103.0	0.0921
E31	A^5:E^1	$C_{62}H_{74}N_{12}$	987.358	30.5	6	✗	✗	✗	<50	-
E32	A^4:E^2	$C_{64}H_{76}N_{12}$	1013.396	29.1	6	✗	✗	✗	<50	-
E33	A^3:E^3	$C_{66}H_{78}N_{12}$	1039.434	129	6	✗	✓		109.5	0.105
E34	A^2:E^4	$C_{68}H_{80}N_{12}$	1065.472	29.6	6	✗	✗	✗	<50	-
E35	A^1:E^5	$C_{70}H_{82}N_{12}$	1091.510	28.1	6	✗	✗	✗	<50	-
E36	A^0:E^6	$C_{72}H_{84}N_{12}$	1117.548	31.7	6	✗	✗	✗	<50	-
F1	A^5:F^1	$C_{70}H_{76}N_{12}$	1085.462	28.9	1	✗	✗	✗	<50	-
F7	A^5:F^1	$C_{70}H_{76}N_{12}$	1085.462	28.8	2	✗	✗	✗	<50	-
F13	A^5:F^1	$C_{70}H_{76}N_{12}$	1085.462	28.7	3	✗	✗	✗	<50	-
F19	A^5:F^1	$C_{70}H_{76}N_{12}$	1085.462	22.4	4	✗	✗	✗	<50	-
F25	A^5:F^1	$C_{70}H_{76}N_{12}$	1085.462	-	5	✗	✗	✗	<50	-
F31	A^5:F^1	$C_{70}H_{76}N_{12}$	1085.462	29.4	6	✗	✗	✗	<50	-
G1	A^5:G^1	$C_{64}H_{80}N_{12}$	1017.428	31.3	1	✗	✗	✗	<50	-
G2	A^4:G^2	$C_{68}H_{88}N_{12}$	1073.536	28.2	1	✗	✓		141.0	0.131
G3	A^3:G^3	$C_{72}H_{96}N_{12}$	1129.644	30.6	1	✓			306.0	0.271
G4	A^2:G^4	$C_{76}H_{104}N_{12}$	1185.752	29.9	1	✓			299.0	0.252
G5	A^1:G^5	$C_{80}H_{112}N_{12}$	1241.86	29.1	1	✓			291.0	0.234
G6	A^0:G^6	$C_{84}H_{120}N_{12}$	1297.968	30.6	1	✓			306.0	0.236
G7	A^5:G^1	$C_{64}H_{80}N_{12}$	1017.428	30.3	2	✗	✓		151.5	0.149
G8	A^4:G^2	$C_{68}H_{88}N_{12}$	1073.536	26.4	2	✓			264.0	0.246

G9	$A^{3}:G^{3}$	$C_{72}H_{96}N_{12}$	1129.644	29.2	2	✓			292.0	0.259
G10	$A^{2}:G^{4}$	$C_{76}H_{104}N_{12}$	1185.752	29.0	2	✓			290.0	0.245
G11	$A^{1}:G^{5}$	$C_{80}H_{112}N_{12}$	1241.86	28.8	2	✓			288.0	0.232
G12	$A^{0}:G^{6}$	$C_{84}H_{120}N_{12}$	1297.968	30.9	2	✖	✖	✖	<50	-
G13	$A^{5}:G^{1}$	$C_{64}H_{80}N_{12}$	1017.428	30.6	3	✖	✖	✖	<50	-
G14	$A^{4}:G^{2}$	$C_{68}H_{88}N_{12}$	1073.536	19.0	3	✓			190.0	0.177
G15	$A^{3}:G^{3}$	$C_{72}H_{96}N_{12}$	1129.644	29.2	3	✓			292.0	0.258
G16	$A^{2}:G^{4}$	$C_{76}H_{104}N_{12}$	1185.752	30.8	3	✓			308.0	0.260
G17	$A^{1}:G^{5}$	$C_{80}H_{112}N_{12}$	1241.86	30.2	3	✓			302.0	0.243
G18	$A^{0}:G^{6}$	$C_{84}H_{120}N_{12}$	1297.968	29	3	✓			290.0	0.223
G19	$A^{5}:G^{1}$	$C_{64}H_{80}N_{12}$	1017.428	30.2	4	✖	✖	✖	<50	-
G20	$A^{4}:G^{2}$	$C_{68}H_{88}N_{12}$	1073.536	17.5	4	✖	✓		87.5	0.0815
G21	$A^{3}:G^{3}$	$C_{72}H_{96}N_{12}$	1129.644	27.2	4	✓			272.0	0.241
G22	$A^{2}:G^{4}$	$C_{76}H_{104}N_{12}$	1185.752	29.9	4	✓			299.0	0.252
G23	$A^{1}:G^{5}$	$C_{80}H_{112}N_{12}$	1241.86	29.3	4	✓			293.0	0.236
G24	$A^{0}:G^{6}$	$C_{84}H_{120}N_{12}$	1297.968	31.5	4	✓			315.0	0.243
G25	$A^{5}:G^{1}$	$C_{64}H_{80}N_{12}$	1017.428	17.2	5	✖	✖	✓	57.3	0.0563
G26	$A^{4}:G^{2}$	$C_{68}H_{88}N_{12}$	1073.536	29.2	5	✖	✓		145.5	0.136
G27	$A^{3}:G^{3}$	$C_{72}H_{96}N_{12}$	1129.644	30.6	5	✓			306.0	0.271
G28	$A^{2}:G^{4}$	$C_{76}H_{104}N_{12}$	1185.752	29.9	5	✓			299.0	0.252
G29	$A^{1}:G^{5}$	$C_{80}H_{112}N_{12}$	1241.86	32.1	5	✓			321.0	0.258
G30	$A^{0}:G^{6}$	$C_{84}H_{120}N_{12}$	1297.968	30.9	5	✓			309.0	0.238
G31	$A^{5}:G^{1}$	$C_{64}H_{80}N_{12}$	1017.428	30.4	6	✖	✖	✖	<50	-
G32	$A^{4}:G^{2}$	$C_{68}H_{88}N_{12}$	1073.536	18.2	6	✖	✖	✓	60.7	0.0565
G33	$A^{3}:G^{3}$	$C_{72}H_{96}N_{12}$	1129.644	20.3	6	✓			203.0	0.180
G34	$A^{2}:G^{4}$	$C_{76}H_{104}N_{12}$	1185.752	30.8	6	✓			308.0	0.260
G35	$A^{1}:G^{5}$	$C_{80}H_{112}N_{12}$	1241.86	29.2	6	✓			292.0	0.235
G36	$A^{0}:G^{6}$	$C_{84}H_{120}N_{12}$	1297.968	29.4	6	✖	✖	✖	<50	-
H1	$A^{5}:H^{1}$	$C_{64}H_{80}N_{12}$	1017.428	29.4	1	✖	✖	✖	<50	-
H2	$A^{4}:H^{2}$	$C_{68}H_{88}N_{12}$	1073.536	27.5	1	✖	✖	✖	<50	-
H3	$A^{3}:H^{3}$	$C_{72}H_{96}N_{12}$	1129.644	31.1	1	✖	✖	✖	<50	-
H7	$A^{5}:H^{1}$	$C_{64}H_{80}N_{12}$	1017.428	29.8	2	✖	✖	✓	99.3	0.0976
H8	$A^{4}:H^{2}$	$C_{68}H_{88}N_{12}$	1073.536	29.8	2	✖	✖	✓	99.3	0.0925
H9	$A^{3}:H^{3}$	$C_{72}H_{96}N_{12}$	1129.644	30.9	2	✖	✖	✖	<50	-
H13	$A^{5}:H^{1}$	$C_{64}H_{80}N_{12}$	1017.428	25.4	3	✖	✖	✖	<50	-
H14	$A^{4}:H^{2}$	$C_{68}H_{88}N_{12}$	1073.536	29.3	3	✖	✖	✖	<50	-
H15	$A^{3}:H^{3}$	$C_{72}H_{96}N_{12}$	1129.644	31.6	3	✖	✖	✖	<50	-
H19	$A^{5}:H^{1}$	$C_{64}H_{80}N_{12}$	1017.428	23.8	4	✖	✖	✓	79.3	0.0780
H20	$A^{4}:H^{2}$	$C_{68}H_{88}N_{12}$	1073.536	28.6	4	✖	✖	✖	<50	-
H21	$A^{3}:H^{3}$	$C_{72}H_{96}N_{12}$	1129.644	32.4	4	✖	✖	✖	<50	-
H25	$A^{5}:H^{1}$	$C_{64}H_{80}N_{12}$	1017.428	28.8	5	✓			288.0	0.283
H26	$A^{4}:H^{2}$	$C_{68}H_{88}N_{12}$	1073.536	15.5	5	✖	✖	✖	<50	-
H27	$A^{3}:H^{3}$	$C_{72}H_{96}N_{12}$	1129.644	28.8	5	✖	✓		96.0	0.0850
H31	$A^{5}:H^{1}$	$C_{64}H_{80}N_{12}$	1017.428	23.9	6	✖	✖	✖	<50	-
H32	$A^{4}:H^{2}$	$C_{68}H_{88}N_{12}$	1073.536	29.9	6	✖	✖	✖	<50	-
H33	$A^{3}:H^{3}$	$C_{72}H_{96}N_{12}$	1129.644	31.3	6	✖	✖	✖	<50	-
I1	$A^{5}:I^{1}$	$C_{68}H_{88}N_{12}$	1073.536	28.1	1	✖	✖	✖	<50	-
I2	$A^{4}:I^{2}$	$C_{76}H_{104}N_{12}$	1185.752	28.9	1	✖	✖	✖	<50	-
I3	$A^{3}:I^{3}$	$C_{84}H_{120}N_{12}$	1297.968	29.6	1	✖	✓		148.0	0.114
I4	$A^{2}:I^{4}$	$C_{92}H_{136}N_{12}$	1410.184	30.0	1	✓			300.0	0.106
I7	$A^{5}:I^{1}$	$C_{68}H_{88}N_{12}$	1073.536	29.8	2	✖	✖	✖	<50	-
I8	$A^{4}:I^{2}$	$C_{76}H_{104}N_{12}$	1185.752	29.8	2	✖	✓		149.0	0.0838
I9	$A^{3}:I^{3}$	$C_{84}H_{120}N_{12}$	1297.968	31.2	2	✖	✓		156.0	0.0801
I10	$A^{2}:I^{4}$	$C_{92}H_{136}N_{12}$	1410.184	31.1	2	✓			311.0	0.0735
I12	$A^{5}:I^{1}$	$C_{68}H_{88}N_{12}$	1073.536	22.6	3	✖	✖	✖	<50	-
I14	$A^{4}:I^{2}$	$C_{76}H_{104}N_{12}$	1185.752	31.8	3	✖	✖	✖	<50	-
I15	$A^{3}:I^{3}$	$C_{84}H_{120}N_{12}$	1297.968	29.9	3	✖	✖	✖	<50	-
I16	$A^{2}:I^{4}$	$C_{92}H_{136}N_{12}$	1410.184	21.5	3	✓			215.0	0.152
I19	$A^{5}:I^{1}$	$C_{68}H_{88}N_{12}$	1073.536	22.6	4	✖	✖	✖	<50	-
I20	$A^{4}:I^{2}$	$C_{76}H_{104}N_{12}$	1185.752	31.8	4	✖	✖	✖	<50	-
I21	$A^{3}:I^{3}$	$C_{84}H_{120}N_{12}$	1297.968	29.9	4	✖	✖	✖	<50	-
I22	$A^{2}:I^{4}$	$C_{92}H_{136}N_{12}$	1410.184	28.7	4	✓			290.0	0.206
I25	$A^{5}:I^{1}$	$C_{68}H_{88}N_{12}$	1073.536	16.0	5	**?**	✓		80.0	0.0745
I26	$A^{4}:I^{2}$	$C_{76}H_{104}N_{12}$	1185.752	30.2	5	✓			302.0	0.254
I27	$A^{3}:I^{3}$	$C_{84}H_{120}N_{12}$	1297.968	22.1	5	✓			220.0	0.169
I28	$A^{2}:I^{4}$	$C_{92}H_{136}N_{12}$	1410.184	28.7	5	✓			287.0	0.203
I31	$A^{5}:I^{1}$	$C_{68}H_{88}N_{12}$	1073.536	n	6	✖	✖	✖	<50	-

I32	$A^4:I^2$	$C_{76}H_{104}N_{12}$	1185.752	30.9	6	✗	✗	✗	<50	-
I33	$A^3:I^3$	$C_{84}H_{120}N_{12}$	1297.968	31.2	6	✗	✗	✗	<50	-
I34	$A^2:I^4$	$C_{92}H_{136}N_{12}$	1410.184	29.8	6	✗	✗	✗	<50	-
J1	$A^5:J^1$	$C_{70}H_{88}N_{12}$	1097.558	30.8	1	✗	✓		154.0	0.140
J2	$A^4:J^2$	$C_{80}H_{104}N_{12}$	1233.796	31.0	1	✗	✓		155.0	0.126
J3	$A^3:J^3$	$C_{90}H_{120}N_{12}$	1370.034	31.1	1	✗	✓		155.5	0.113
J7	$A^5:J^1$	$C_{70}H_{88}N_{12}$	1097.558	28.9	2	✗	✓		144.5	0.132
J8	$A^4:J^2$	$C_{80}H_{104}N_{12}$	1233.796	30.9	2	✗	✓		154.5	0.125
J9	$A^3:J^3$	$C_{90}H_{120}N_{12}$	1370.034	29.8	2	✗	✗	✓	100.7	0.073
J13	$A^5:J^1$	$C_{70}H_{88}N_{12}$	1097.558	29.3	3	✗	✗	✗	<50	-
J14	$A^4:J^2$	$C_{80}H_{104}N_{12}$	1233.796	31.9	3	✗	✗	✗	<50	-
J15	$A^3:J^3$	$C_{90}H_{120}N_{12}$	1370.034	30	3	✓			300.0	0.219
J19	$A^5:J^1$	$C_{70}H_{88}N_{12}$	1097.558	30	4	✗	✓		150.0	0.137
J20	$A^4:J^2$	$C_{80}H_{104}N_{12}$	1233.796	28.8	4	✓			288.0	0.233
J21	$A^3:J^3$	$C_{90}H_{120}N_{12}$	1370.034	31.3	4	✗	✗	✗	<50	-
J25	$A^5:J^1$	$C_{70}H_{88}N_{12}$	1097.558	28.6	5	✗	✗	✓	95.3	0.0868
J26	$A^4:J^2$	$C_{80}H_{104}N_{12}$	1233.796	30.2	5	✗	✗	✗	<50	-
J27	$A^3:J^3$	$C_{90}H_{120}N_{12}$	1370.034	32.9	5	✗	✗	✗	<50	-
J31	$A^5:J^1$	$C_{70}H_{88}N_{12}$	1097.558	28.8	6	✗	✗	✗	<50	-
J32	$A^4:J^2$	$C_{80}H_{104}N_{12}$	1233.796	31.3	6	✗	✗	✗	<50	-
J33	$A^3:J^3$	$C_{90}H_{120}N_{12}$	1370.034	30.6	6	✗	✗	✗	<50	-
K1	$A^5:K^1$	$C_{59}H_{70}N_{12}$	947.293	30.3	1	✗	✗	✗	<50	-
K2	$A^4:K^2$	$C_{58}H_{68}N_{12}$	933.266	29.9	1	✗	✗	✗	<50	-
K3	$A^3:K^3$	$C_{57}H_{66}N_{12}$	919.239	31.1	1	✗	✓		155.5	0.169
K4	$A^2:K^4$	$C_{56}H_{64}N_{12}$	905.212	28.1	1	✗	✗	✗	<50	-
K5	$A^1:K^5$	$C_{55}H_{62}N_{12}$	891.185	29.9	1	✗	✗	✗	<50	-
K6	$A^0:K^6$	$C_{54}H_{60}N_{12}$	877.158	29.8	1	✗	✗	✗	<50	-
K7	$A^5:K^1$	$C_{59}H_{70}N_{12}$	947.293	28.9	2	✗	✗	✓	96.3	0.102
K8	$A^4:K^2$	$C_{58}H_{68}N_{12}$	933.266	29.8	2	✗	✗	✓	99.3	0.104
K9	$A^3:K^3$	$C_{57}H_{66}N_{12}$	919.239	30.8	2	✓			308.0	0.335
K10	$A^2:K^4$	$C_{56}H_{64}N_{12}$	905.212	30.0	2	✗	✗	✓	142.5	0.160
K11	$A^1:K^5$	$C_{55}H_{62}N_{12}$	891.185	28.5	2	✗	✗	✗	<50	-
K12	$A^0:K^6$	$C_{54}H_{60}N_{12}$	877.158	29.5	2	✗	✗	✗	<50	-
K13	$A^5:K^1$	$C_{59}H_{70}N_{12}$	947.293	28.4	3	✗	✗	✗	<50	-
K14	$A^4:K^2$	$C_{58}H_{68}N_{12}$	933.266	29.8	3	✗	✗	✗	<50	-
K15	$A^3:K^3$	$C_{57}H_{66}N_{12}$	919.239	31	3	✗	✗	✗	<50	-
K16	$A^2:K^4$	$C_{56}H_{64}N_{12}$	905.212	29	3	✗	✗	✗	<50	-
K17	$A^1:K^5$	$C_{55}H_{62}N_{12}$	891.185	31	3	✗	✗	✗	<50	-
K18	$A^0:K^6$	$C_{54}H_{60}N_{12}$	877.158	30.1	3	✗	✗	✗	<50	-
K19	$A^5:K^1$	$C_{59}H_{70}N_{12}$	947.293	31.1	4	✗	✗	✗	<50	-
K20	$A^4:K^2$	$C_{58}H_{68}N_{12}$	933.266	29.7	4	✗	✗	✗	<50	-
K21	$A^3:K^3$	$C_{57}H_{66}N_{12}$	919.239	28.8	4	✗	✗	✗	<50	-
K22	$A^2:K^4$	$C_{56}H_{64}N_{12}$	905.212	29.6	4	✗	✗	✗	<50	-
K23	$A^1:K^5$	$C_{55}H_{62}N_{12}$	891.185	31.4	4	✗	✗	✗	<50	-
K24	$A^0:K^6$	$C_{54}H_{60}N_{12}$	877.158	28.7	4	✗	✗	✗	<50	-
K25	$A^5:K^1$	$C_{59}H_{70}N_{12}$	947.293	29.4	5	✗	✗	✗	<50	-
K26	$A^4:K^2$	$C_{58}H_{68}N_{12}$	933.266	29.7	5	✗	✗	✗	<50	-
K27	$A^3:K^3$	$C_{57}H_{66}N_{12}$	919.239	29.1	5	✗	✗	✗	<50	-
K28	$A^2:K^4$	$C_{56}H_{64}N_{12}$	905.212	28.1	5	✗	✗	✗	<50	-
K29	$A^1:K^5$	$C_{55}H_{62}N_{12}$	891.185	30.5	5	✗	✗	✗	<50	-
K30	$A^0:K^6$	$C_{54}H_{60}N_{12}$	877.158	27.5	5	✗	✗	✗	<50	-
K31	$A^5:K^1$	$C_{59}H_{70}N_{12}$	947.293	29.8	6	✗	✗	✗	<50	-
K32	$A^4:K^2$	$C_{58}H_{68}N_{12}$	933.266	30.1	6	✗	✗	✗	<50	-
K33	$A^3:K^3$	$C_{57}H_{66}N_{12}$	919.239	32.3	6	✗	✗	✗	<50	-
K34	$A^2:K^4$	$C_{56}H_{64}N_{12}$	905.212	30.1	6	✗	✗	✗	<50	-
K35	$A^1:K^5$	$C_{55}H_{62}N_{12}$	891.185	31.3	6	✗	✗	✗	<50	-
K36	$A^0:K^6$	$C_{54}H_{60}N_{12}$	877.158	32.2	6	✗	✗	✗	<50	-

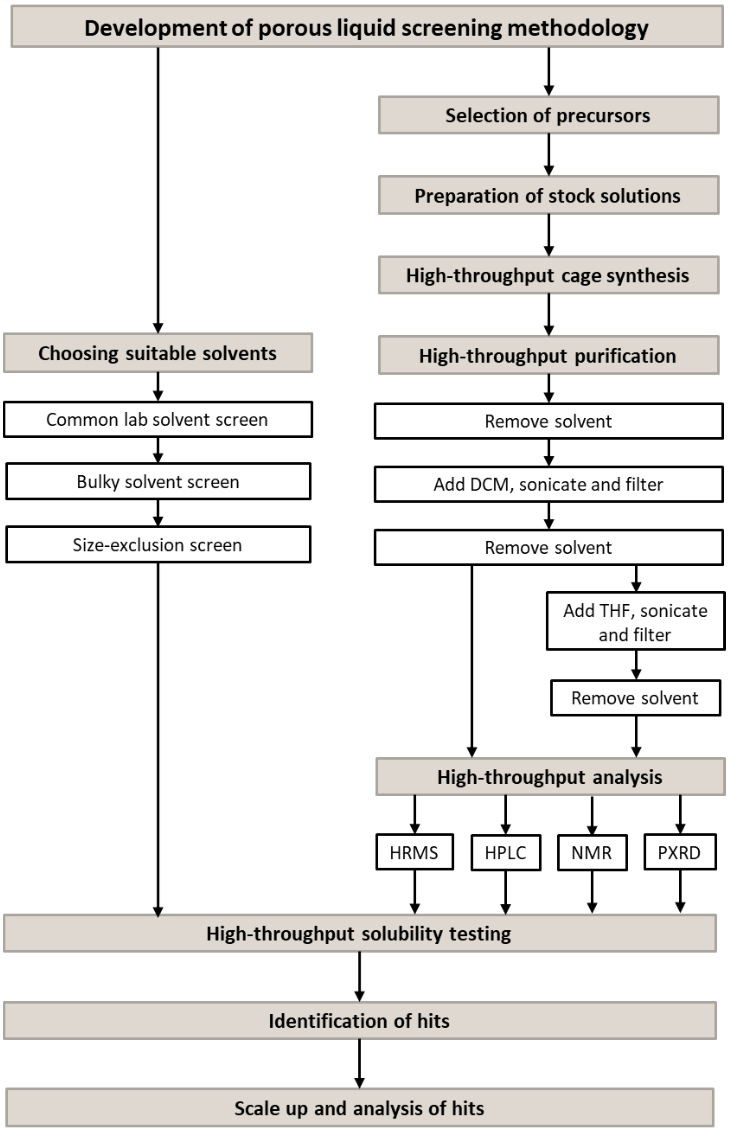

Fig. S24: Overall workflow for the high-throughput discovery of Type II scrambled porous liquids

6. Scale-up of hits

6.1. Synthesis of scrambled cages

For the successful hits from the high-throughput solubility screen using the five size-excluded solvents, the highly soluble scrambled cages were scaled up using conventional batch synthesis (minimum 95% purity targeted for the isolated product) - **A^3:E^3**, **A^4:G^2**, **A^3:G^3**, **A^2:G^4**, **A^1:G^5**, **A^5:H^1**, **A^4:I^2**, **A^3:I^3**, **A^2:I^4** and **A^3:K^3** (Fig. S25).

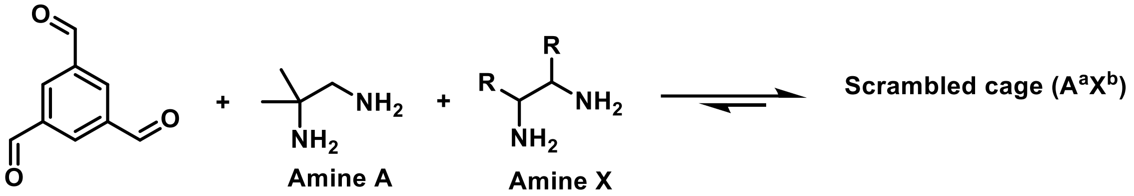

Fig. S25: General scheme for the formation of scrambled cages from 1,3,5-triformylbenzene (TFB, 4.0 equiv.) and two vicinal diamines in varying ratios (total = 6.0 equiv.). The result is a distribution of [4+6] cages.

A^3:E^3 (3^3:13^3)

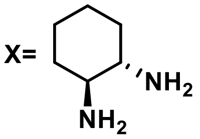

In a 5 L jacketed vessel equipped with an overhead stirrer, TFB (30.0 g, 185 mmol, 4.0 eq.) was dissolved in DCM (2.5 L). A solution of 1,2-diamino-2-methyl-propane (Amine **A**, 12.23 g, 138.7 mmol, 3.0 eq.) and (*R,R*)-1,2-diaminocyclohexane (Amine **E**, 15.87 g, 138.7 mmol, 3.0 eq.) in DCM (1.5 L) was then added. The reaction mixture was stirred for 72 h at room temperature. The resulting solution was dried ($MgSO_4$) and the solvent removed under reduced pressure. The crude product was re-dissolved in DCM (500 mL) and the solution filtered to remove any insoluble precipitate. The solvent was removed under reduced pressure and the resulting solid washed with ethyl acetate (500 mL) to afford **A^3:E^3** (35.61 g, 34.3 mmol, 74%) as an off-white power.

^{1}H NMR (400 MHz, $CDCl_3$): δ 8.18–7.80 (24H, m, N=C**H** and Ar**H**), 3.92–3.35 (12H, m, C**H**N=CH and C**H**$_2$N=CH), 1.82–1.31 (42H, m, C**H**$_2$ and C**H**$_3$). Data in agreement with literature values.[6]

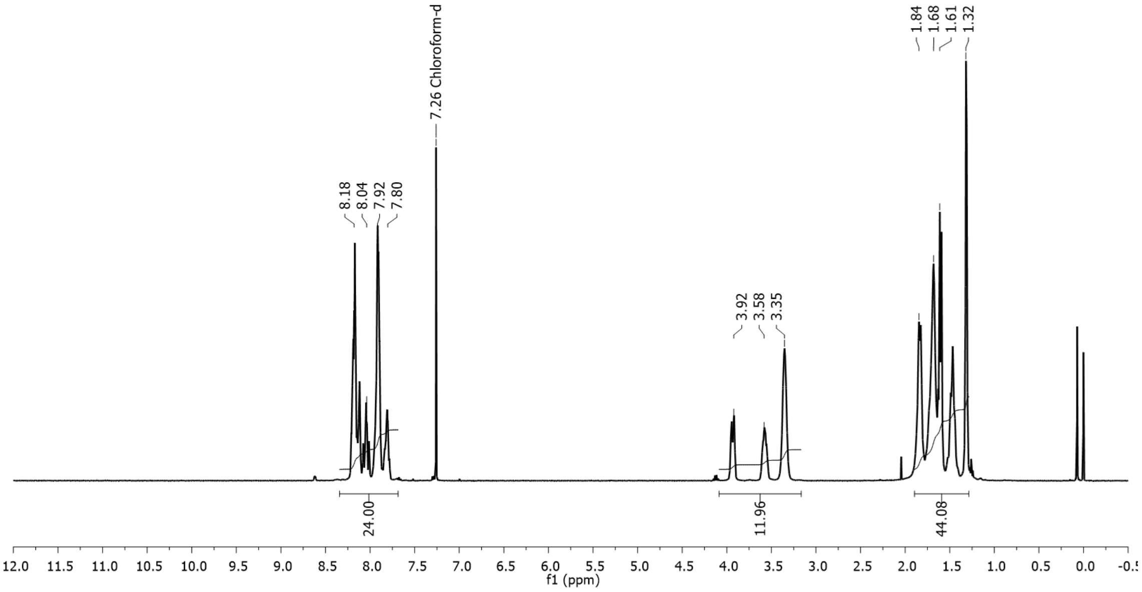

Fig. S26: ^{1}H NMR ($CDCl_3$) spectrum of scrambled **A^3:E^3** cage

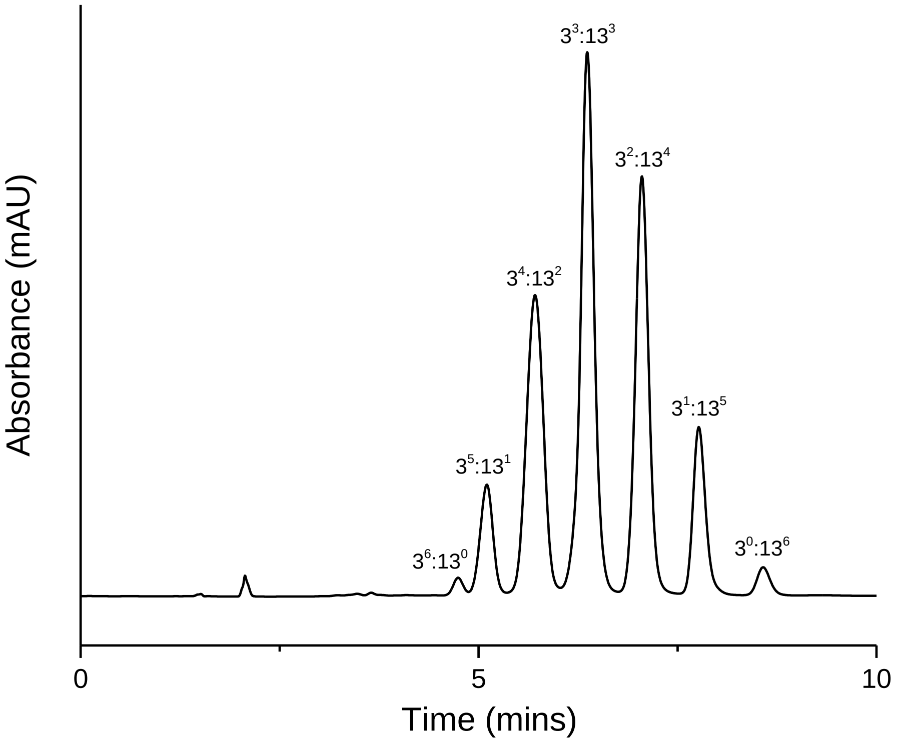

Fig. S27: HPLC of scrambled **A^3:E^3** cage showing the distribution of cage species present

$\mathbf{A^4}$:$\mathbf{G^2}$

X=

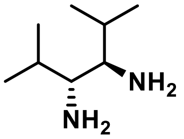

To a solution of TFB (0.33 g, 2.04 mmol, 4.0 eq.) dissolved in chloroform (30 mL), was added solutions of 1,2-diamino-2-methyl-propane (Amine **A**, 0.18 g, 2.04 mmol, 4.0 eq.) in chloroform (15 mL), and (3*R*,4*R*)-2,5-dimethylhexane-3,4-diamine dihydrochloride (Amine **G**, 0.22 g, 1.03 mmol, 2.0 eq.) in chloroform (15 mL), followed by triethylamine (0.2 mL, 1.7 mmol, 3.3 eq.). The reaction mixture was stirred for 72 h at room temperature before the solvent was removed under reduced pressure. The crude product was dissolved in THF (50 mL), filtered to remove triethylamine hydrochloride salts, and the solvent removed under reduced pressure. The crude product was redissolved in DCM (50 mL) and filtered to remove any insoluble polymer. The solvent was removed under reduced pressure to afford the product (0.11 g, 0.1 mmol, 20%) as a cream solid.

IR (ν_{max} /cm^{-1}): 2974, 2860, 1709, 1657 (imine N=C), 1599, 1448, 1367, 1261; **^{1}H NMR** (400 MHz, CDCl$_3$): δ 8.17–7.83 (24H, m, Ar**H** and N=**CH**), 3.94–3.42 (12H, m, C**H**N=CH and C**H**$_2$N=CH), 2.22- 2.20 (4H, m, C**H**), (15H, m, C**H**), 1.62-0.72 (48H, m, C**H**$_3$) (*NB.* **X**= residual solvent); **^{13}C NMR** (101 MHz, CDCl$_3$): (due to scrambling, all singlets appear as broad multiplets) δ 161.71, 160.21, 155.93, 137.08, 129.87, 125.98, 72.88, 61.69, 46.25, 30.78, 28.93, 21.84, 16.20; **HRMS** (ES+) calc. for scrambled cages $\mathbf{A^6G^0}$, $\mathbf{A^5G^1}$, $\mathbf{A^4G^2}$, $\mathbf{A^3G^3}$, $\mathbf{A^2G^4}$, $\mathbf{A^1G^5}$, $\mathbf{A^0G^6}$ = 960.6003, 1016.6629, 1072.7255, 1128.7881, 1184.8507, 1240.9133, 1296.9759; found [M+H]$^+$ at: 961.5915, 1017.6505, 1073.7108, 1129.7697, 1185.8276, 1241.8854, 1298.9463.

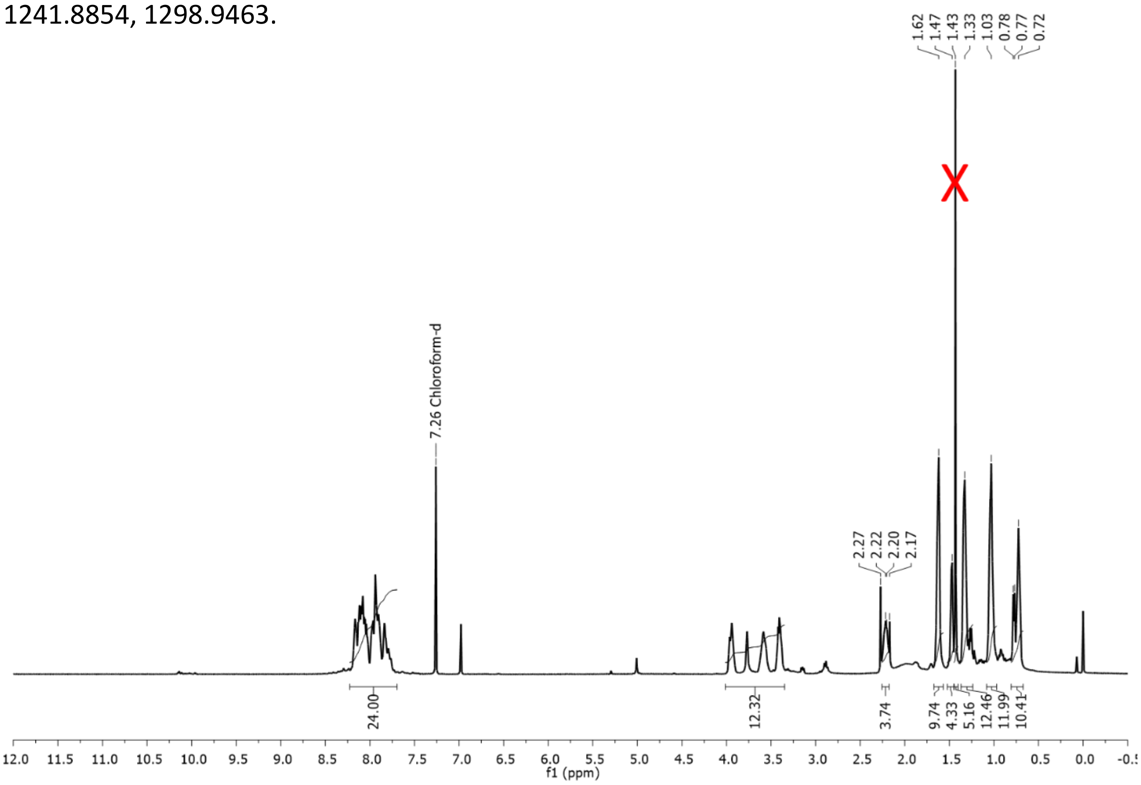

Fig. S28: ^{1}H NMR (CDCl$_3$) spectrum of scrambled $\mathbf{A^4}$:$\mathbf{G^2}$ cage

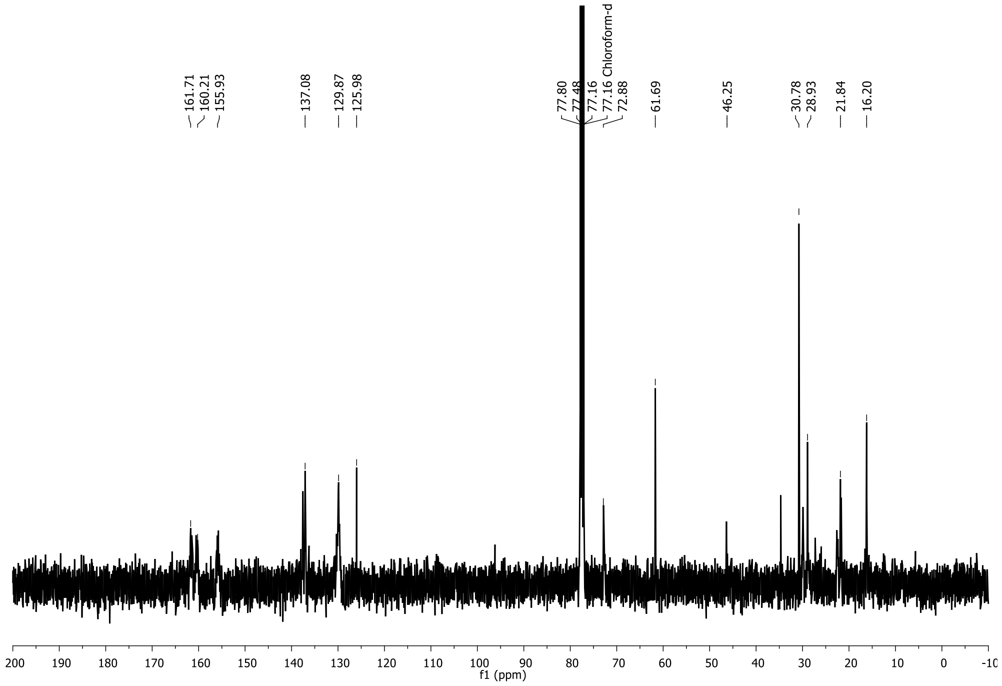

Fig. S29: ^{13}C NMR (CDCl$_3$) spectrum of scrambled **A^4:G^2** cage

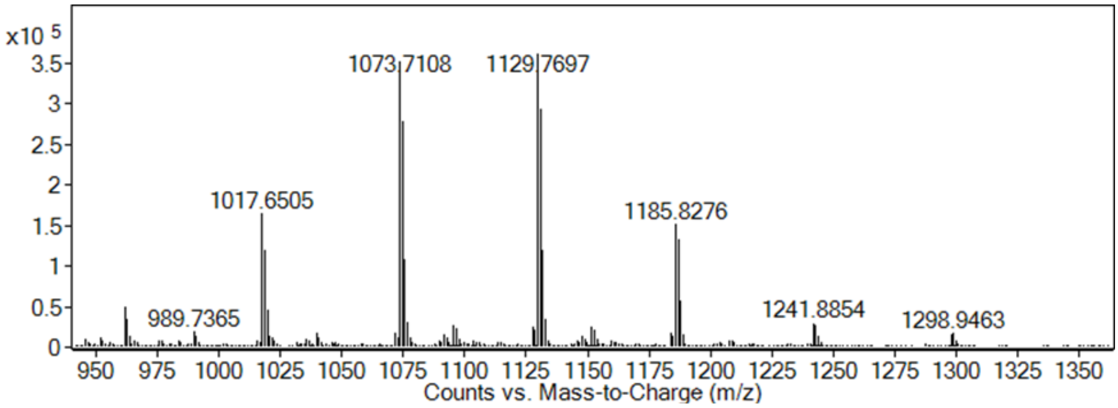

Fig. S30: HRMS spectra for the scrambled **A^4:G^2** cage

A^3:G^3

X=

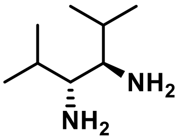

To a solution of TFB (0.60 g, 3.7 mmol, 4.0 eq.) dissolved in chloroform (60 mL), was added solutions of 1,2-diamino-2-methyl-propane (Amine, **A**, 0.24 g, 2.8 mmol, 3.0 eq.) in chloroform (30 mL), and (3*R*,4*R*)-2,5-dimethylhexane-3,4-diamine dihydrochloride (Amine **G**, 0.60 g, 2.8 mmol, 3.0 eq.) in chloroform (30 mL), followed by triethylamine (0.39 mL, 2.8 mmol, 3.3 eq.). The reaction mixture was stirred for 72 h at room temperature before the solvent was removed under reduced pressure. The crude product was dissolved in THF (60 mL), filtered to remove triethylamine hydrochloride salts, and the solvent removed under reduced pressure. The resulting oil was triturated in methanol (50 mL) and the purified scrambled cage collected as a colourless solid by filtration (0.76 g, 6.8 mmol, 73%).

IR (ν_{max} /cm^{-1}): 2949, 2841, 1709, 1655 (imine N=C), 1599, 1456, 1259; **^{1}H NMR** (400 MHz, CDCl$_3$): δ 8.32–7.72, (24H, m, N=C**H** and Ar**H**), 3.95–3.24 (12H, m, C**H**N=CH and C**H**$_2$N=CH), 2.20-1.62 (6H, m, C**H**), 1.09-0.77 (54H, m, C**H**$_3$) (*NB.* **X**= residual solvent); **^{13}C NMR** (101 MHz, CDCl$_3$): (due to scrambling, all singlets appear as broad multiplets) δ 160.19, 159.70, 137.55, 136.60, 129.62, 50.87, 28.49, 28.27, 21.61, 21.44, 15.87; **HRMS** (ES+) calc. for scrambled cages **A**^{6}**G**^{0}, **A**^{5}**G**^{1}, **A**^{4}**G**^{2}, **A**^{3}**G**^{3}, **A**^{2}**G**^{4}, **A**^{1}**G**^{5}, **A**^{0}**G**^{6} = 960.6003, 1016.6629, 1072.7255, 1128.7881, 1184.8507, 1240.9133, 1296.9759; found [M+H]$^+$ at: 1073.7226, 1129.7846, 1185.8456, 1241.9053, 1297.9669.

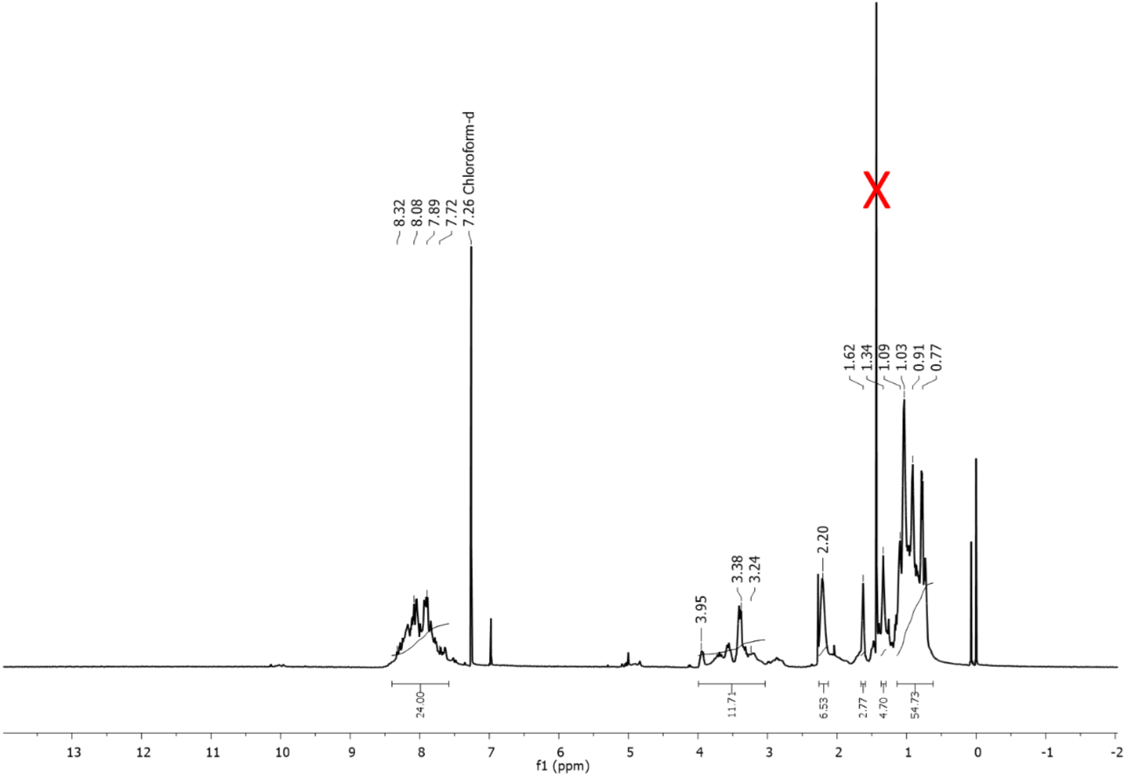

Fig. S31: ^{1}H NMR (CDCl$_3$) spectrum of scrambled **A^3:G^3** cage

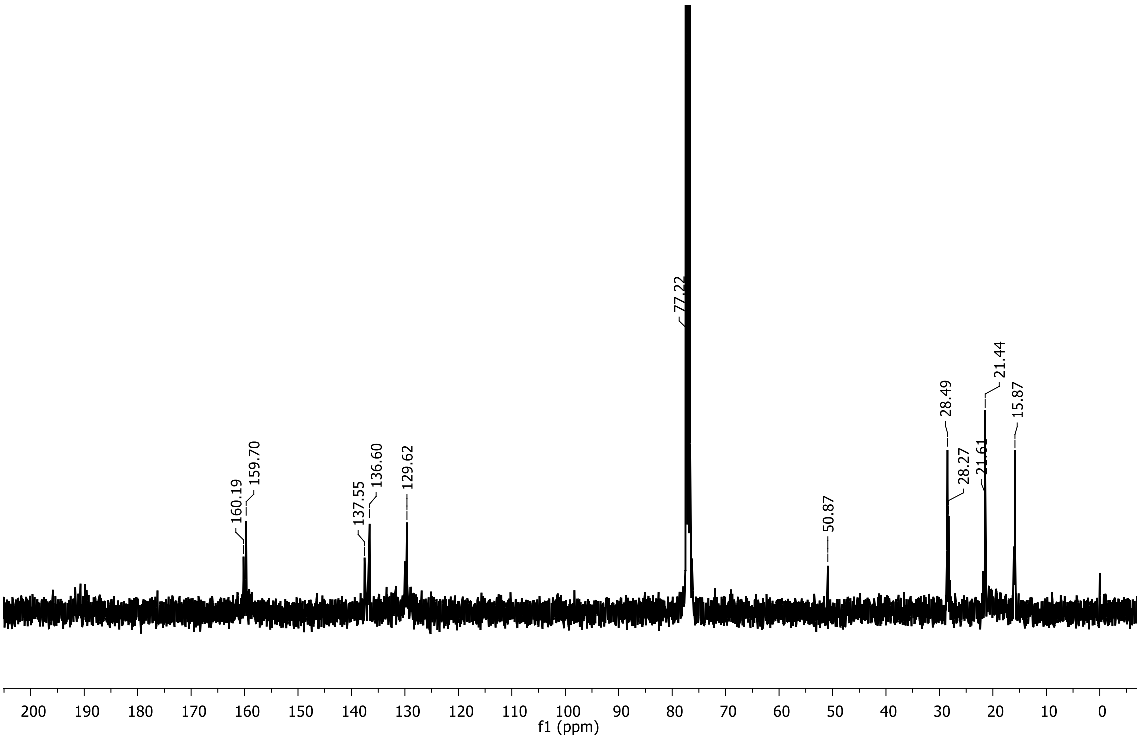

Fig. S32: ^{13}C NMR (CDCl$_3$) spectrum of scrambled **A^3:G^3** cage

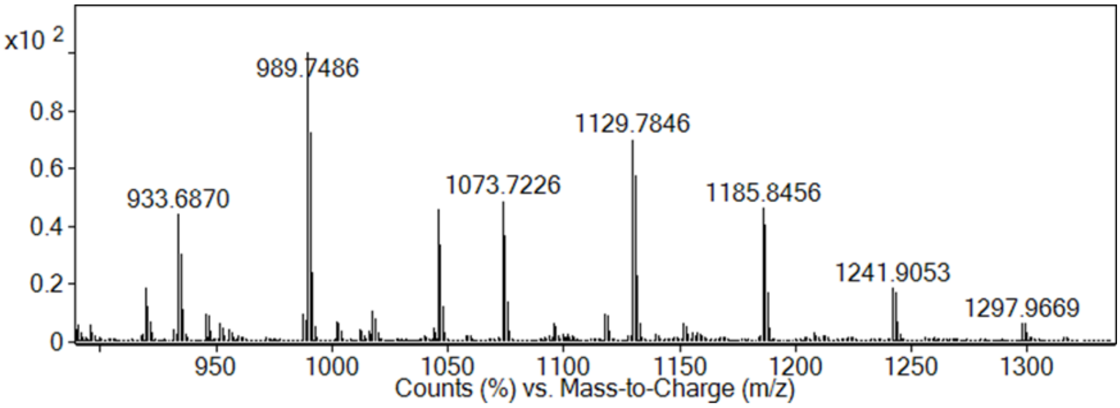

Fig. S33: HRMS spectra for **A^3:G^3** scrambled cage

A^{2}:G^{4}

X=

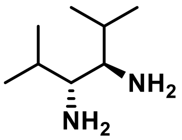

To a solution of TFB (0.50 g, 3.1 mmol, 4.0 eq.) dissolved in chloroform (30 mL), was added solutions of 1,2-diamino-2-methyl-propane (Amine **A**, 0.14 g, 1.55 mmol, 2.0 eq.) in chloroform (15 mL), and (3*R*,4*R*)-2,5-dimethylhexane-3,4-diamine dihydrochloride (Amine **G**, 0.75 g, 3.1 mmol, 4.0 eq.) in chloroform (15 mL), followed by triethylamine (0.30 mL, 2.6 mmol, 3.3 eq.). The reaction mixture was stirred for 72 h at room temperature before the solvent was removed under reduced pressure. The crude product was dissolved in THF (50 mL), filtered to remove triethylamine hydrochloride salts, and the solvent removed under reduced pressure. The resulting oil was triturated in methanol (50 mL) and the purified scrambled cage was collected as a colourless solid (0.44 g, 3.7 mmol, 48%).

IR (ν_{max} /cm^{-1}): 2970, 2860, 1709, 1641 (imine N=C), 1595, 1452, 1381, 1267; **^{1}H NMR** (400 MHz, CDCl$_3$): δ 8.20–7.63 (24H, m, N=C**H** and Ar**H**), 3.75–2.87 (12H, m, C**H**N=CH and C**H**$_2$N=CH),2.20 (8H, br s, C**H**), 1.10-0.79 (60H, m, C**H**$_3$); **^{13}C NMR** (101 MHz, CDCl$_3$): (due to scrambling, all singlets appear as broad multiplets) 161.61, 159.84, 136.73, 129.76, 76.42, 67.59, 61.29, 32.20, 28.62, 28.41, 28.15, 21.96, 21.76, 21.57, 20.92, 18.82, 16.23, 15.99; **HRMS** (ES+) calc. for scrambled cages **A^{6}G^{0}**, **A^{5}G^{1}**, **A^{4}G^{2}**, **A^{3}G^{3}**, **A^{2}G^{4}**, **A^{1}G^{5}**, **A^{0}G^{6}** = 960.6003, 1016.6629, 1072.7255, 1128.7881, 1184.8507, 1240.9133, 1296.9759; found [M+H]$^{+}$ at: 1073.7506, 1129.8139, 1185.8771, 1241.9393, 1298.0007.

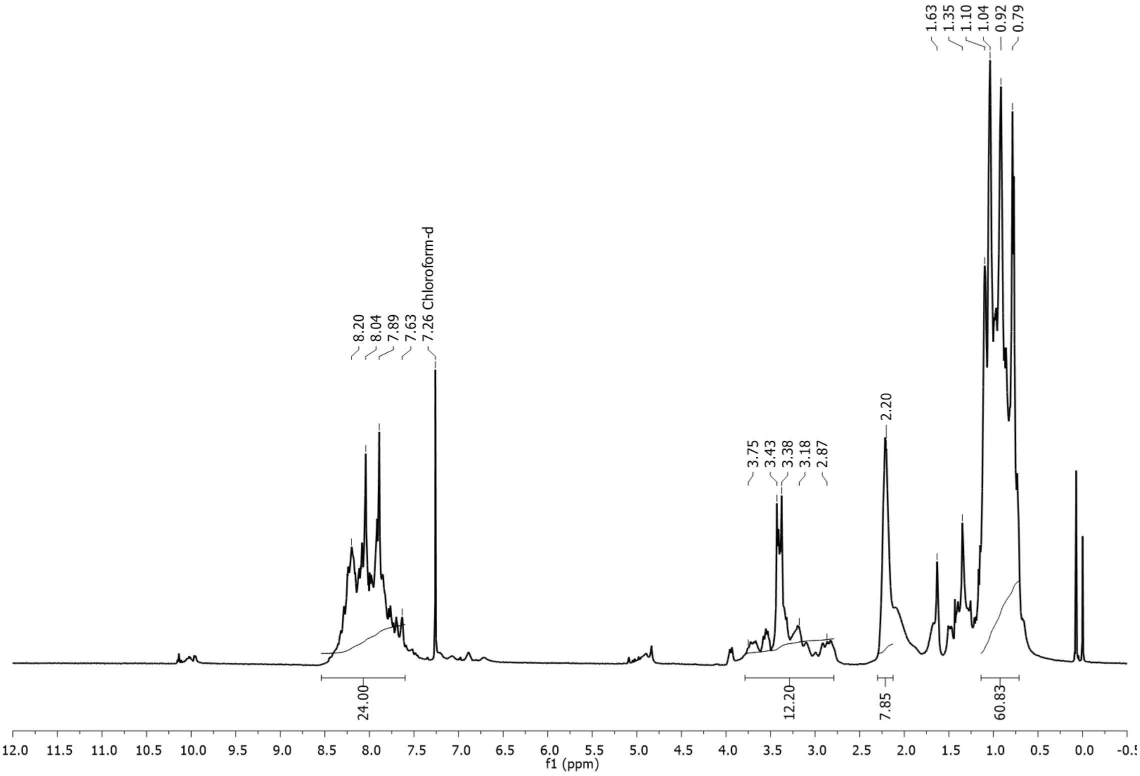

Fig. S34: ^{1}H NMR (CDCl$_3$) spectrum of scrambled **A^{2}:G^{4}** cage

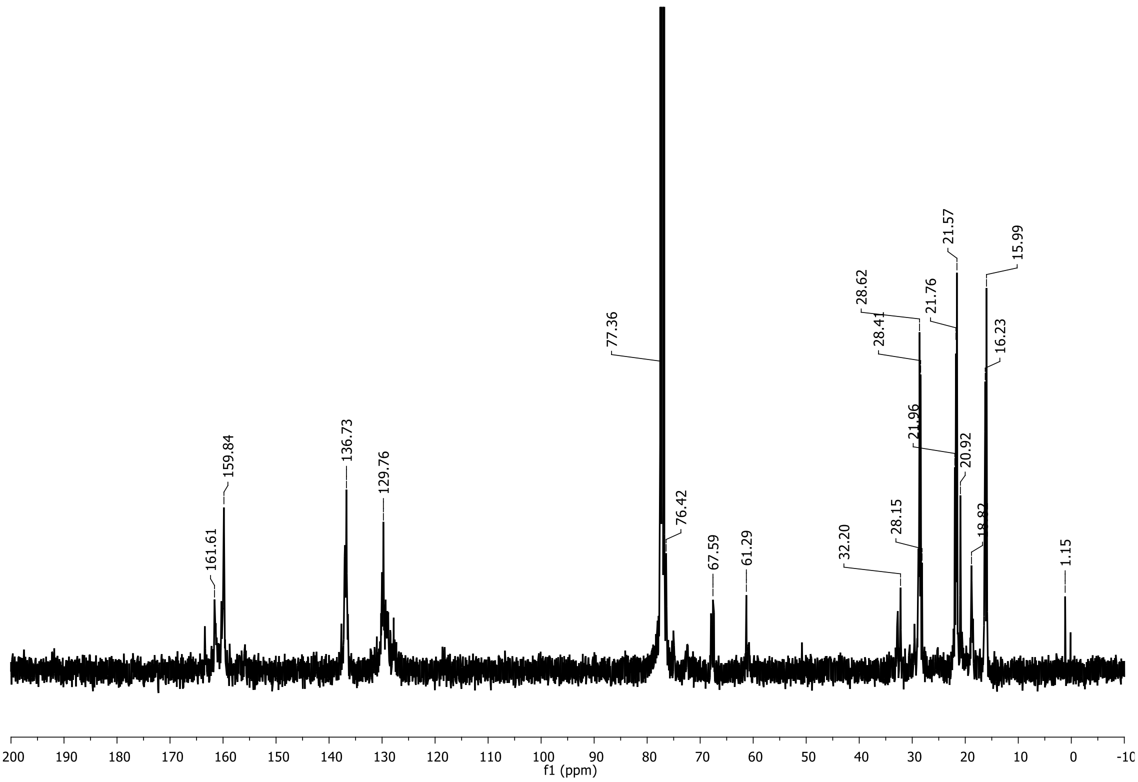

Fig. S35: ^{13}C NMR ($CDCl_3$) spectrum of scrambled $\mathbf{A^2{:}G^4}$ cage

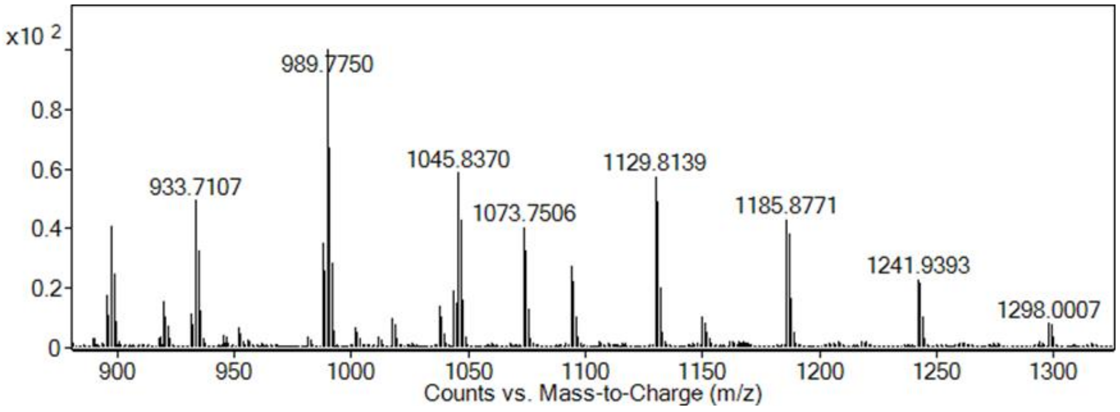

Fig. S36: HRMS spectra for the scrambled $\mathbf{A^2{:}G^4}$ cage

A^1:G^5

X=

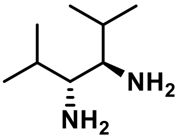

To a solution of TFB (0.50 g, 3.1 mmol, 4.0 eq.) dissolved in DCM (50 mL), was added solutions of 1,2-diamino-2-methyl-propane (Amine **A**, 0.07 g, 0.8 mmol, 1.0 eq.) in DCM (25 mL), and (3*R*,4*R*)-2,5-dimethylhexane-3,4-diamine dihydrochloride (Amine **G**, 0.84 g, 3.9 mmol, 5.0 eq.) in DCM (25 mL), followed by triethylamine (0.4 mL, 5.1 mmol, 3.3 eq.). The reaction mixture was stirred for 72 h at room temperature before the solvent was removed under reduced pressure. The crude product was dissolved in THF (50 mL), filtered to remove the triethylamine hydrochloride salts, and the solvent removed under reduced pressure. The crude material was then re-dissolved in DCM, filtered to remove any polymer, and the solvent removed under reduced pressure. Methanol (50 mL) was added to precipitate the scrambled cage which was collected by filtration as a colourless powder (0.40 g, 0.3 mmol, 42%).

IR (ν_{max} /cm^{-1}): 2968, 2860, 1701, 1659 (imine N=C), 1595, 1466, 1364, 1259; ^{1}**H NMR** (400 MHz, $CDCl_3$): δ 8.24–7.68 (24H, m, N=C**H** and Ar**H**), 3.96–3.18 (12H, m, C**H**N=CH and C**H**$_2$N=CH), 2.21 and 1.35 (10H, m, C**H**), 1.11–0.77 (60H, m, C**H**$_3$); ^{13}**C NMR** (101 MHz, $CDCl_3$): (due to scrambling chemical shifts appear as multiplets) 159.70, 136.59, 129.87, 61.16, 28.49, 28.28, 21.61, 21.43, 16.12, 15.85; **HRMS** (ES+) calc. for scrambled cages **A^{6}G^0**, **A^{5}G^1**, **A^{4}G^2**, **A^{3}G^3**, **A^{2}G^4**, **A^{1}G^5**, **A^{0}G^6** = 960.6003, 1016.6629, 1072.7255, 1128.7881, 1184.8507, 1240.9133, 1296.9759; found $[M+H]^+$ at: 1129.8253, 1185.8900, 1241.9539, 1298.0147.

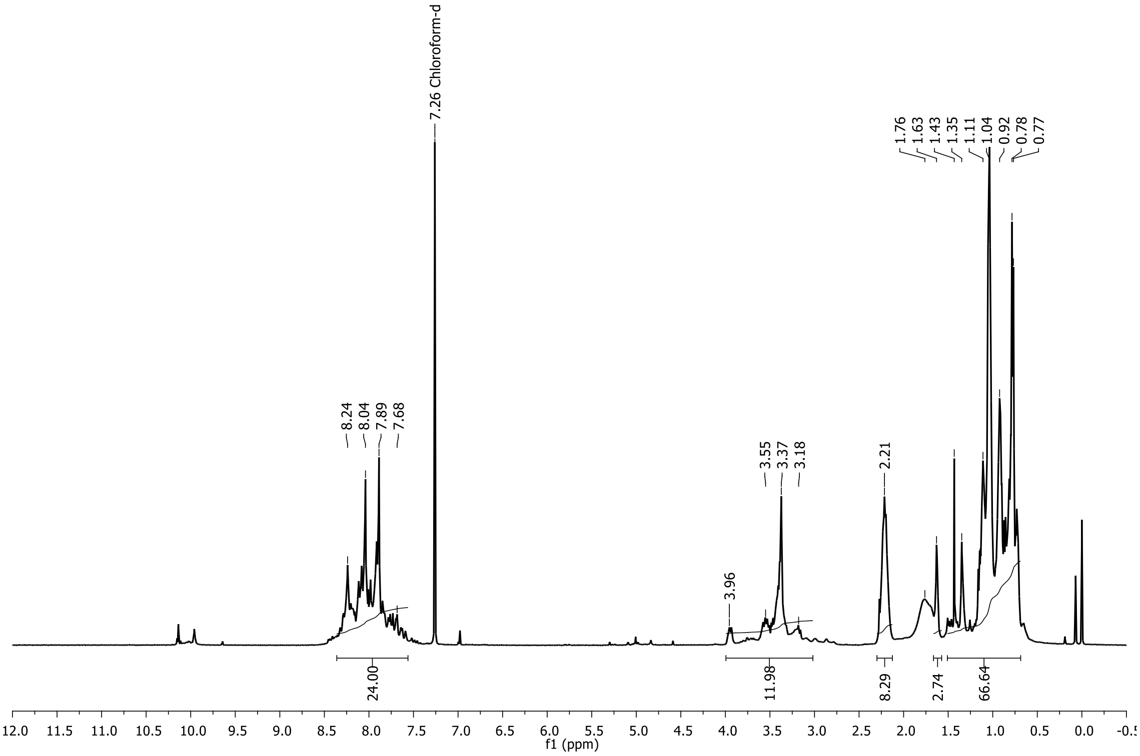

Fig. S37: ^{1}H NMR ($CDCl_3$) spectrum of scrambled **A^1:G^5** cage

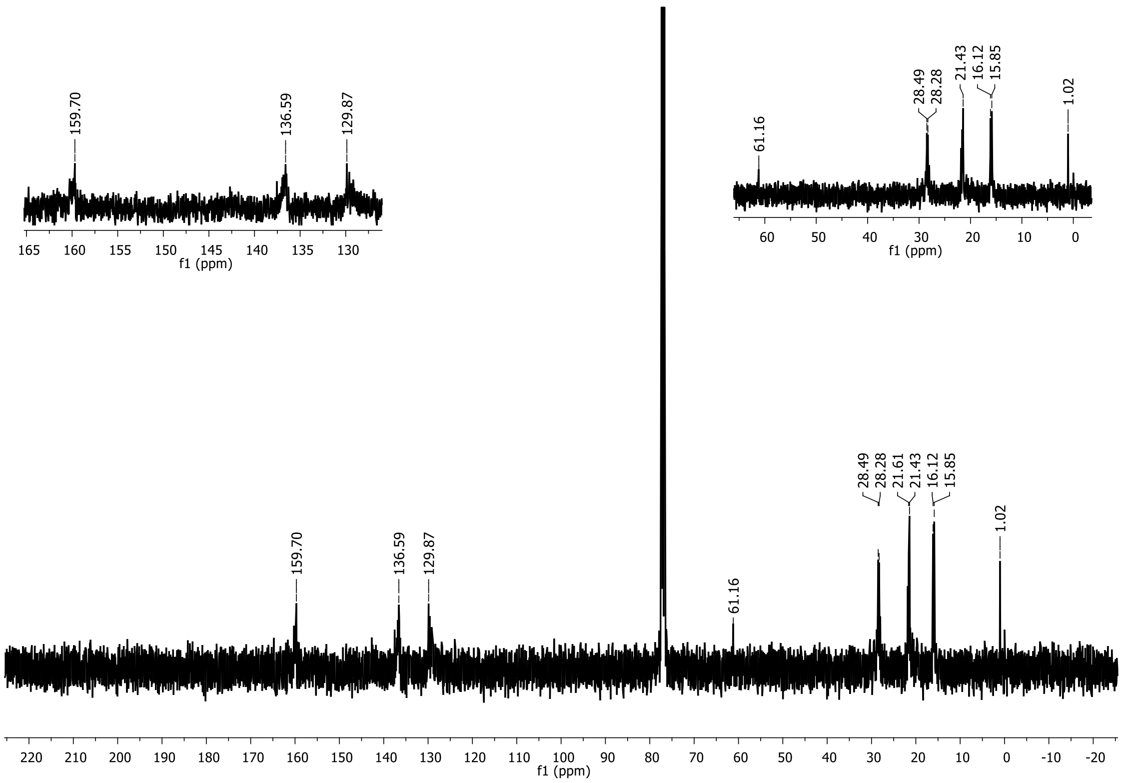

Fig. S38: ^{13}C NMR (CDCl$_3$) spectrum of scrambled **A^1:G^5** cage

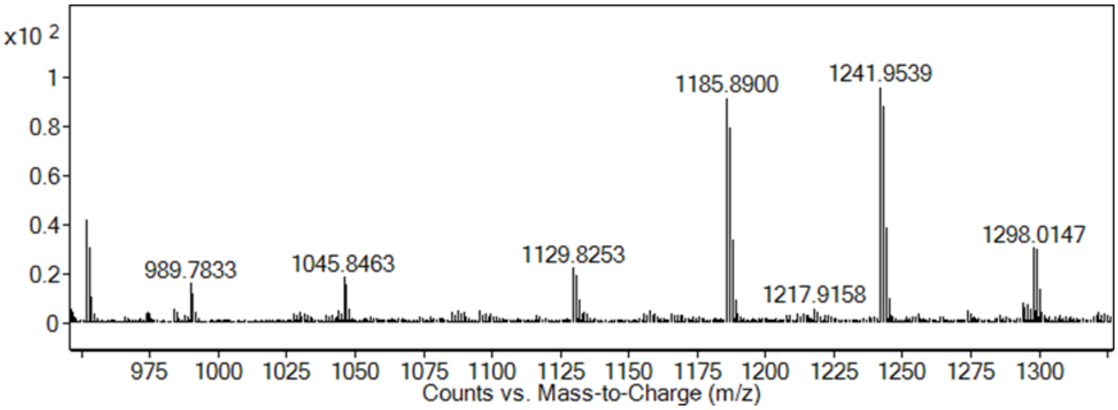

Fig. S39: HRMS spectra for the scrambled **A^1:G^5** cage

A^5:H^1

X=

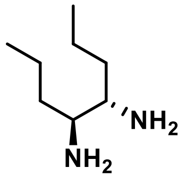

To a solution of TFB (0.64 g, 4.0 mmol, 4.0 eq.) dissolved in chloroform (30 mL), was added solutions of 1,2-diamino-2-methyl-propane (Amine **A**, 0.44 g, 5.0 mmol, 5.0 eq.) in chloroform (15 mL), and (4*S*,5*S*)-octane-4,5-diamine (Amine **H**, 0.19 g, 1.3 mmol, 1.0 eq.) in chloroform (15mL). The reaction mixture was stirred at 60 °C for 72 h before being allowed to cool to room temperature, and the solvent was removed under reduced pressure. The crude product was re-dissolved in DCM (40 mL), filtered to remove insoluble polymer, and the solvent removed under reduced pressure. Acetone (50 mL) was added to precipitate the scrambled cage product which was collected by filtration as a colourless powder (0.16 g, 0.2 mmol, 16%).

IR (ν_{max}/cm^{-1}): 2960, 2856, 1705, 1651 (imine N=C), 1456, 1250; **^{1}H NMR** (400 MHz, CDCl$_3$): δ 8.15–7.83 (24H, m, N=C**H** and Ar**H**), 3.95–3.35 (12H, m, C**H**N=CH and C**H**$_2$N=CH), 1.74–1.25 (44H, m, C**H**$_2$ and C**H**$_3$); **^{13}C NMR** (101 MHz, CDCl$_3$): (due to scrambling, all singlets appear as broad multiplets) δ 161.38, 155.67, 137.04, 129.68, 75.91, 72.82, 61.64, 53.83, 32.33, 26.29, 23.02, 14.52; **HRMS** (ES+): calc. for scrambled cages **A^6H^0**, **A^5H^1**, **A^4H^2**, **A^3H^3**, **A^2H^4**, **A^1H^5**, **A^0H^6** = 960.6003, 1016.6629, 1072.7255, 1128.7881, 1184.8507, 1240.9133, 1296.9759; found [M+H]$^+$ at: 961.6157, 1015.6232, 1073.7418, 1127.7487, 1185.8712, 1297.9926.

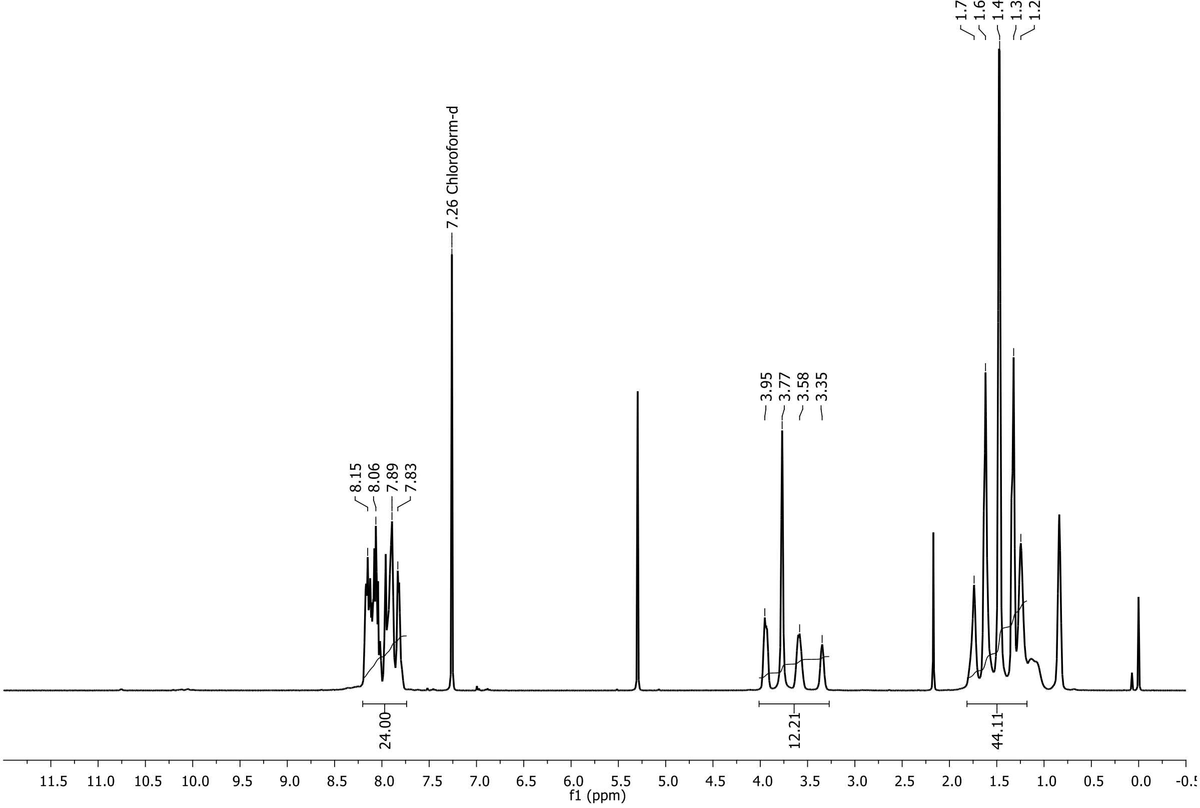

Fig. S40: ^{1}H NMR (CDCl$_3$) spectrum of scrambled **A^5:H^1** cage

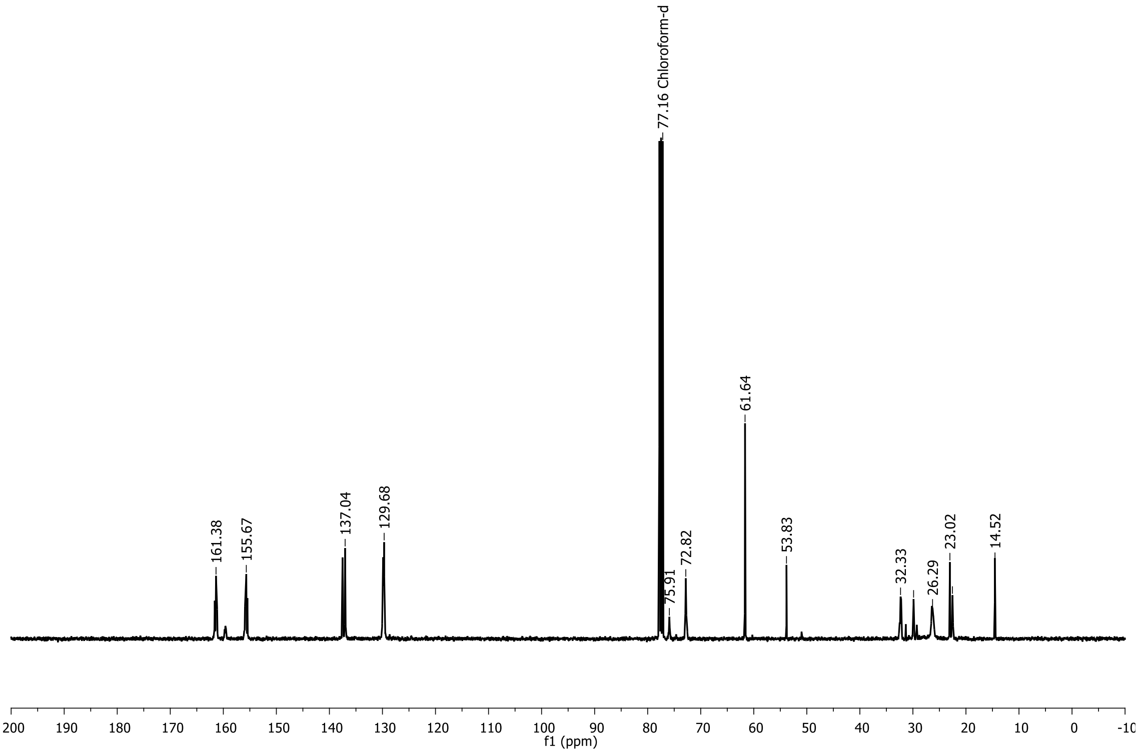

Fig. S41: ^{13}C NMR (CDCl$_3$) spectrum of parent **A^5:H^1** cage

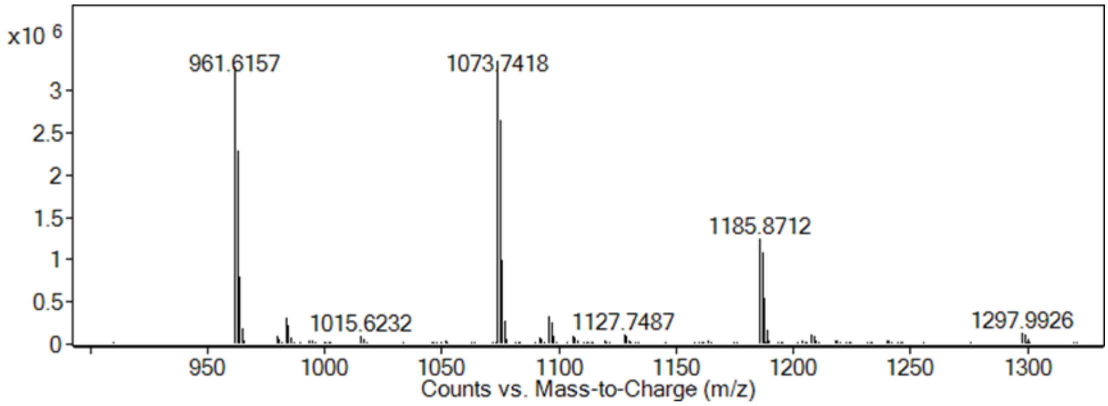

Fig. S42: HRMS spectra for the scrambled **A^5:H^1** cage

A^4:I^2

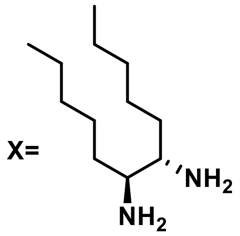

To a solution of TFB (0.46 g, 2.9 mmol, 4.0 eq.) dissolved in chloroform (30 mL), was added solutions of 1,2-diamino-2-methyl-propane (Amine **A**, 0.25 g, 2.9 mmol, 4.0 eq.) in chloroform (15 mL), and (6*S*,7*S*)-dodecane-6,7-diamine (Amine **I**, 0.27 g, 1.4 mmol, 2.0 eq.) in chloroform (15mL). The reaction mixture was stirred at 60 °C for 72 h before being allowed to cool to room temperature, and the solvent was removed under reduced pressure. The crude product was re-dissolved in DCM (40 mL), filtered to remove insoluble polymer, and the solvent removed under reduced pressure. Acetone (50 mL) was added to precipitate the scrambled cage product which was collected by filtration as a colourless powder (0.11 g, 0.093 mmol, 18%).

IR (ν_{max}/cm^{-1}): 2968, 2849, 1705, 1643 (imine N=C), 1448, 1379, 1263; ^{1}**H NMR** (400 MHz, CDCl$_3$): δ 8.15–7.83 (24H, m, N=C**H** and Ar**H**), 3.93–3.34 (12H, m, , C**H**N=CH and C**H**$_2$N=CH), 1.75–0.84 (68H, m, C**H**$_2$ and C**H**$_3$); ^{13}**C NMR** (101 MHz, CDCl$_3$): (due to scrambling, all singlets appear as broad multiplets) δ 161.70, 137.55, 129.86, 61.70, 31.39, 29.84, 23.04, 14.55; **HRMS** (ES+): calc. for scrambled cages **A^{6}I^0**, **A^{5}I^1**, **A^{4}I^2**, **A^{3}I^3**, **A^{2}I^4**, **A^{1}I^5**, **A^{0}I^6** = 960.6003, 1072.7255, 1184.8507, 1296.9759, 1409.1011, 1521.2263 and 1633.3515; found [M+H]$^+$ at: 961.6129, 1073.7396, 1185.8681, 1297.9899.

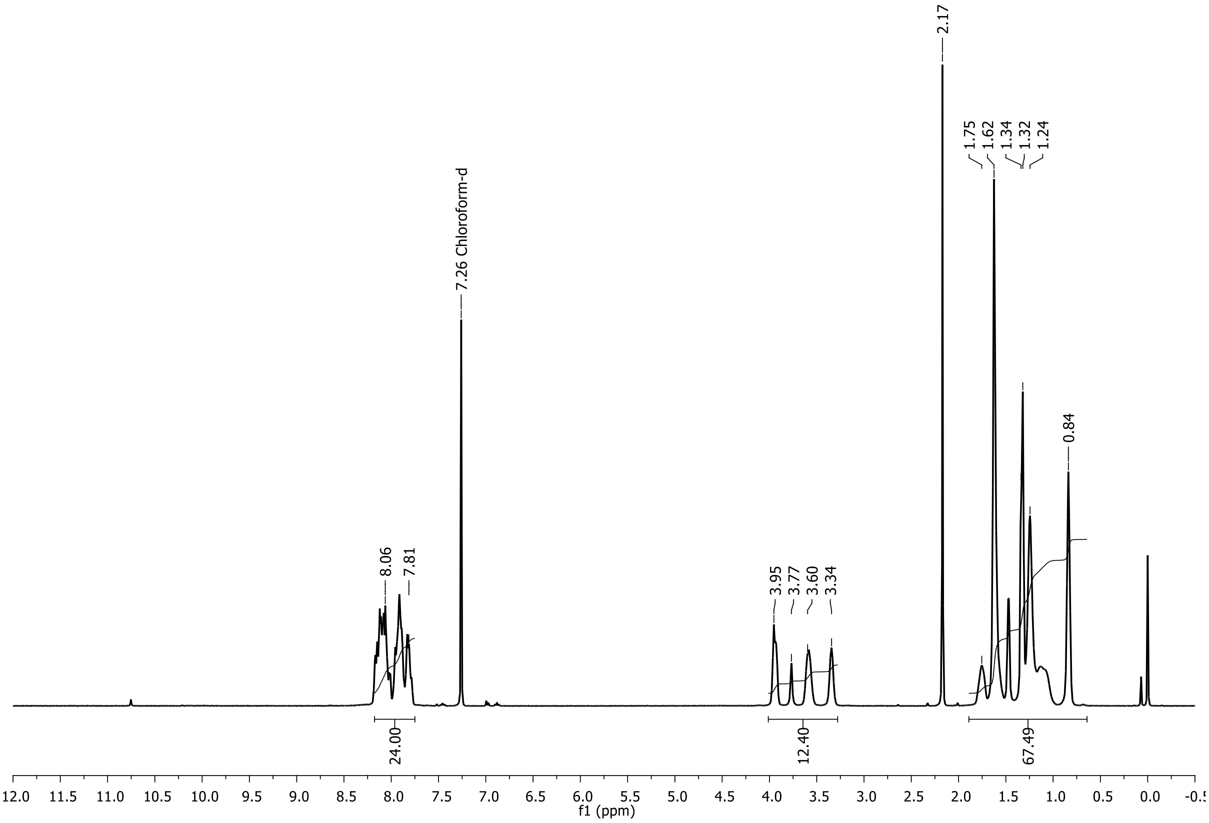

Fig. S43: ^{1}H NMR (CDCl$_3$) spectrum of scrambled **A^4:I^2** cage

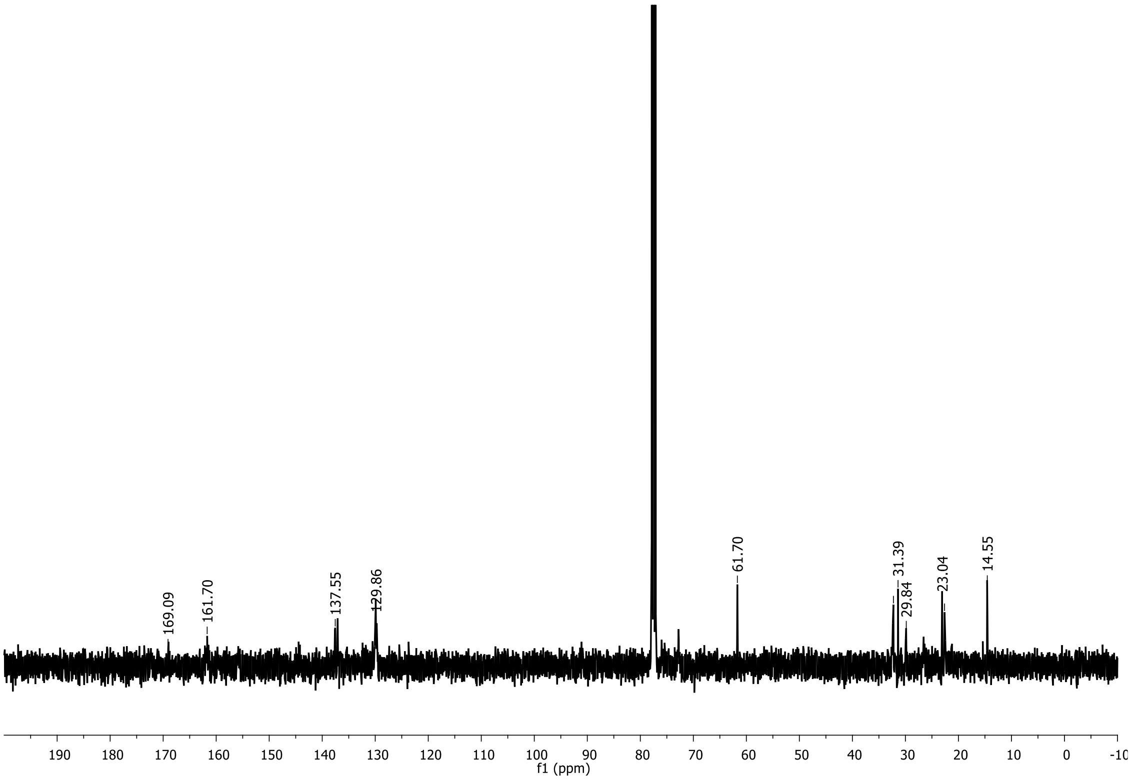

Fig. S44: ^{13}C NMR ($CDCl_3$) spectrum of parent **A⁴:I²** cage

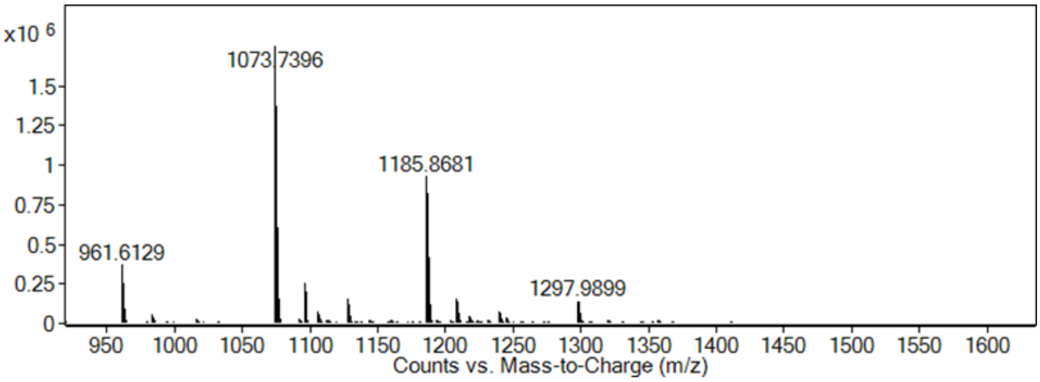

Fig. S45: HRMS spectra for the scrambled **A⁴:I²** cage

A^3:I^3

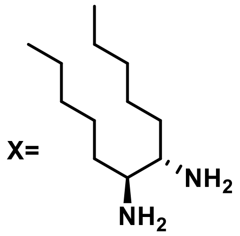

To a solution of TFB (0.46 g, 2.9 mmol, 4.0 eq.) dissolved in chloroform (30 mL), was added solutions of 1,2-diamino-2-methyl-propane (Amine **A**, 0.19 g, 2.2 mmol, 3.0 eq.) in chloroform (15 mL), and (6*S*,7*S*)-dodecane-6,7-diamine (Amine **I**, 0.43 g, 2.2 mmol, 3.0 eq.) in chloroform (15mL). The reaction mixture was stirred at 60 °C for 72 h before being allowed to cool to room temperature, and the solvent was removed under reduced pressure. The crude product was re-dissolved in DCM (40 mL), filtered to remove insoluble polymer, and the solvent removed under reduced pressure. Acetone (50 mL) was added to precipitate the scrambled cage product which was collected by filtration as a colourless powder (0.27 g, 0.2 mmol, 29%).

IR (ν_{max}/cm^{-1}): 2968, 2854, 1647 (imine N=C), 1445, 1364, 1261; **^{1}H NMR** (400 MHz, CDCl$_3$): δ 8.17–7.83 (24H, m, N=C**H** and Ar**H**), 3.94–3.34 (12H, m, C**H**N=CH and C**H**$_2$N=CH), 1.76–0.84* (77H, m, C**H**$_2$ and C**H**$_3$); **^{13}C NMR** (101 MHz, CDCl$_3$): (due to scrambling, all singlets appear as broad multiplets) δ 161.14, 155.52, 137.20, 129.59, 61.38, 31.98, 22.31, 14.26; **HRMS** (ES+): calc. for scrambled cages **A^{6}I^0**, **A^{5}I^1**, **A^{4}I^2**, **A^{3}I^3**, **A^{2}I^4**, **A^{1}I^5**, **A^{0}I^6** = 960.6003, 1072.7255, 1184.8507, 1296.9759, 1409.1011, 1521.2263 and 1633.3515; found [M+H]$^+$ at: 1073.7399, 1073.7399, 1185.8644, 1297.9908, 1411.1186.

*85H expected but 77H observed, possibly due to a slightly different scrambling distribution forming over the that targeted

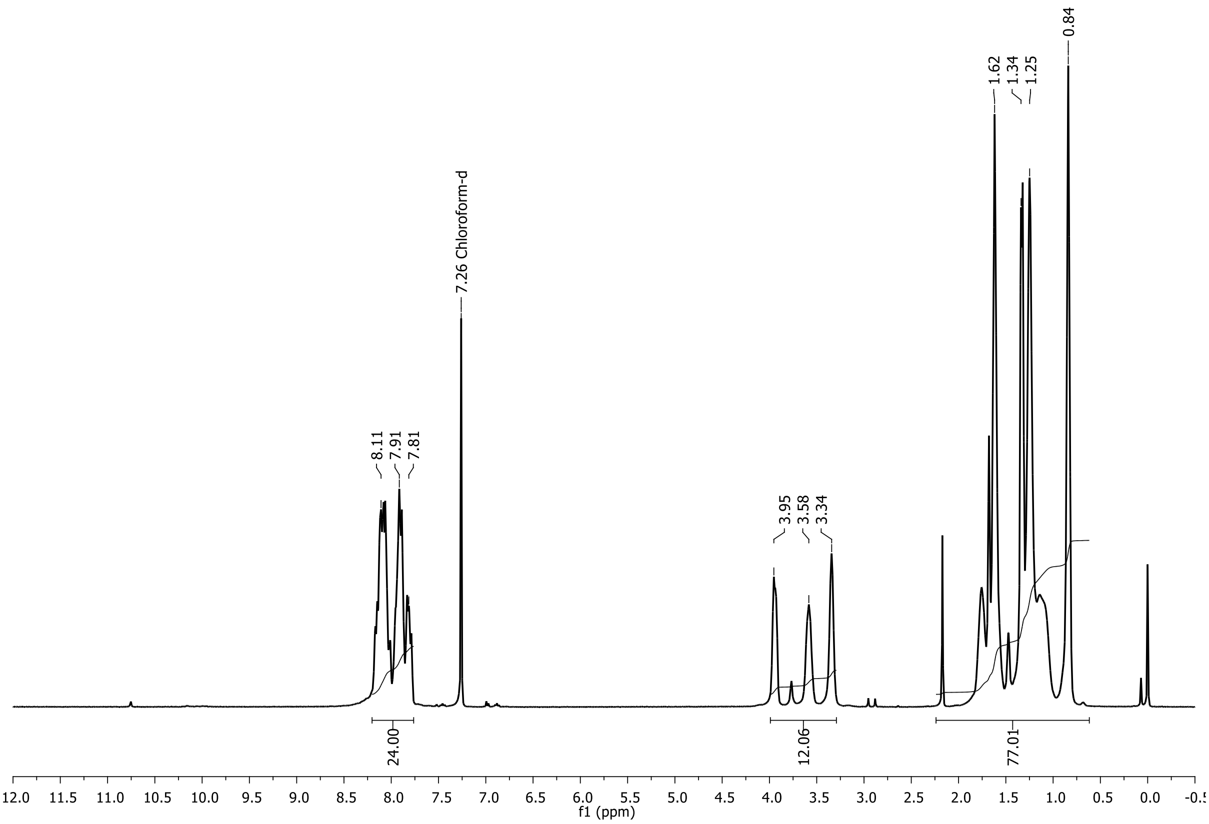

Fig. S46: ^{1}H NMR (CDCl$_3$) spectrum of scrambled **A^3:I^3** cage

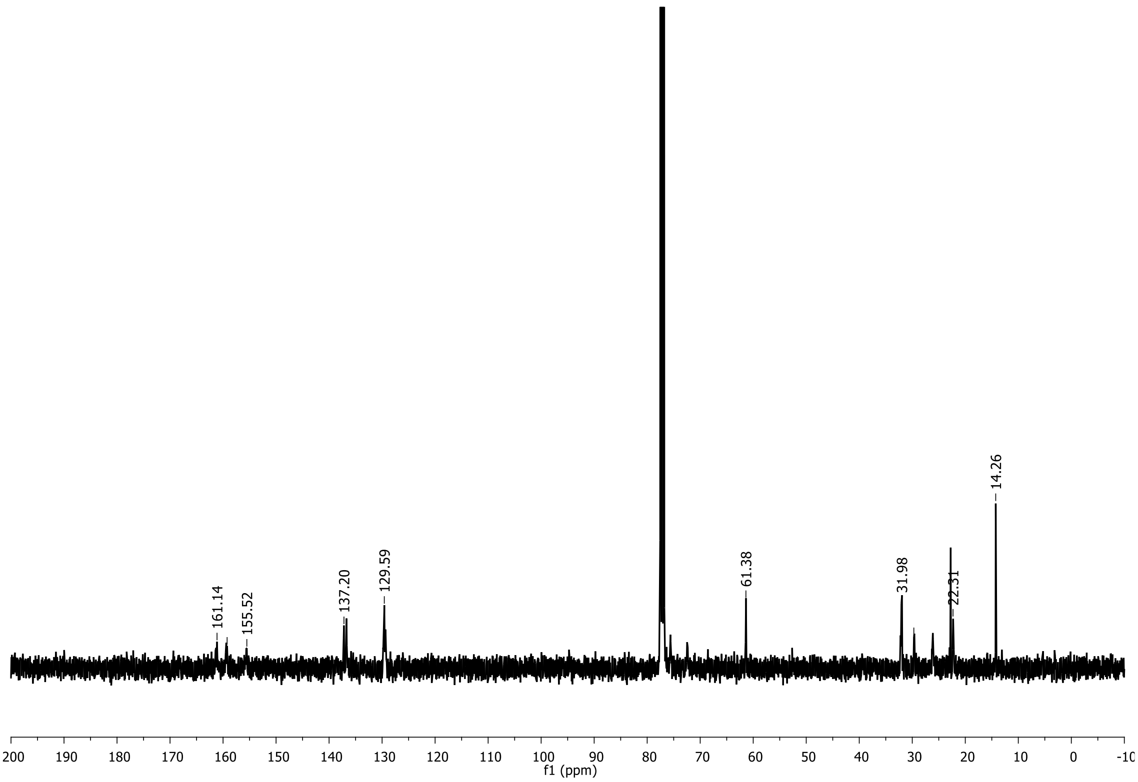

Fig. S47: ^{13}C NMR ($CDCl_3$) spectrum of parent **A^3:I^3** cage

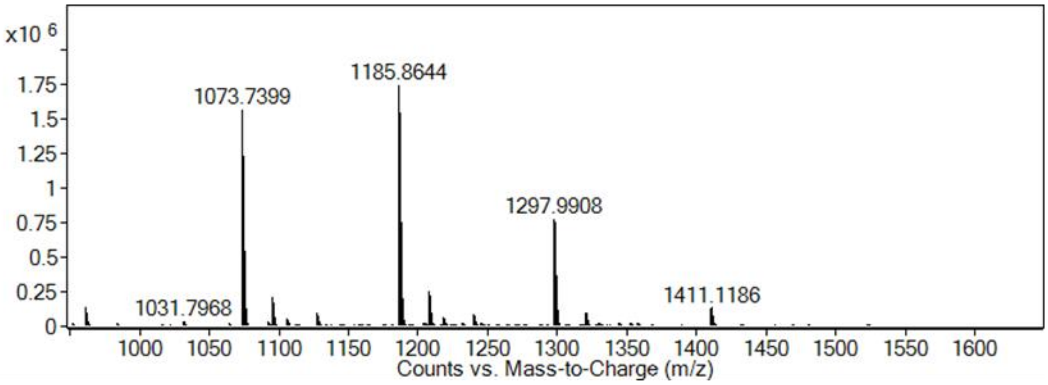

Fig. S48: HRMS spectra for the scrambled **A^3:I^3** cage

A^2:I^4

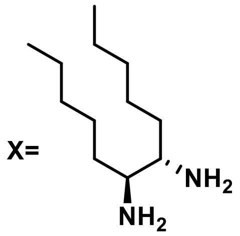

To a solution of TFB (0.46 g, 2.9 mmol, 4.0 eq.) dissolved in chloroform (30 mL), was added solutions of 1,2-diamino-2-methyl-propane (Amine **A**, 0.13 g, 1.4 mmol, 2.0 eq.) in chloroform (15 mL), and (6*S*,7*S*)-dodecane-6,7-diamine (Amine **I**, 0.60 g, 2.9 mmol, 4.0 eq.) in chloroform (15mL). The reaction mixture was stirred at 60 °C for 72 h before being allowed to cool to room temperature, and the solvent was removed under reduced pressure. The crude product was re-dissolved in DCM (40 mL), filtered to remove insoluble polymer, and the solvent removed under reduced pressure. Acetone (50 mL) was added to precipitate the scrambled cage which was collected by filtration as a colourless powder (0.16 g, 0.1 mmol, 45%).

IR (ν_{max}/cm^{-1}): 2964, 2851, 1647 (imine N=C), 1456, 1263; **^{1}H NMR** (400 MHz, $CDCl_3$): δ 8.07–7.79 (24H, m, N=C**H** and Ar**H**), 3.94–3.34 (12H, m, C**H**N=CH and C**H**$_2$N=CH), 1.76–0.84 (95H, m, C**H**$_2$ and C**H**$_3$); **^{13}C NMR** (101 MHz, $CDCl_3$): (due to scrambling, all singlets appear as broad multiplets) δ 161.14, 159.46, 137.19, 136.75, 129.65, 129.40, 75.59, 61.41, 31.96, 29.65, 26.17, 22.75, 22.72, 22.27, 14.25; **HRMS** (ES+) calc. for scrambled cages **A^6I^0**, **A^5I^1**, **A^4I^2**, **A^3I^3**, **A^2I^4**, **A^1I^5**, **A^0I^6** = 960.6003, 1072.7255, 1184.8507, 1296.9759, 1409.1011, 1521.2263 and 1633.3515; found $[M+H]^+$ at: 1185.8460, 1297.9703, 1411.0961, 1523.2191.

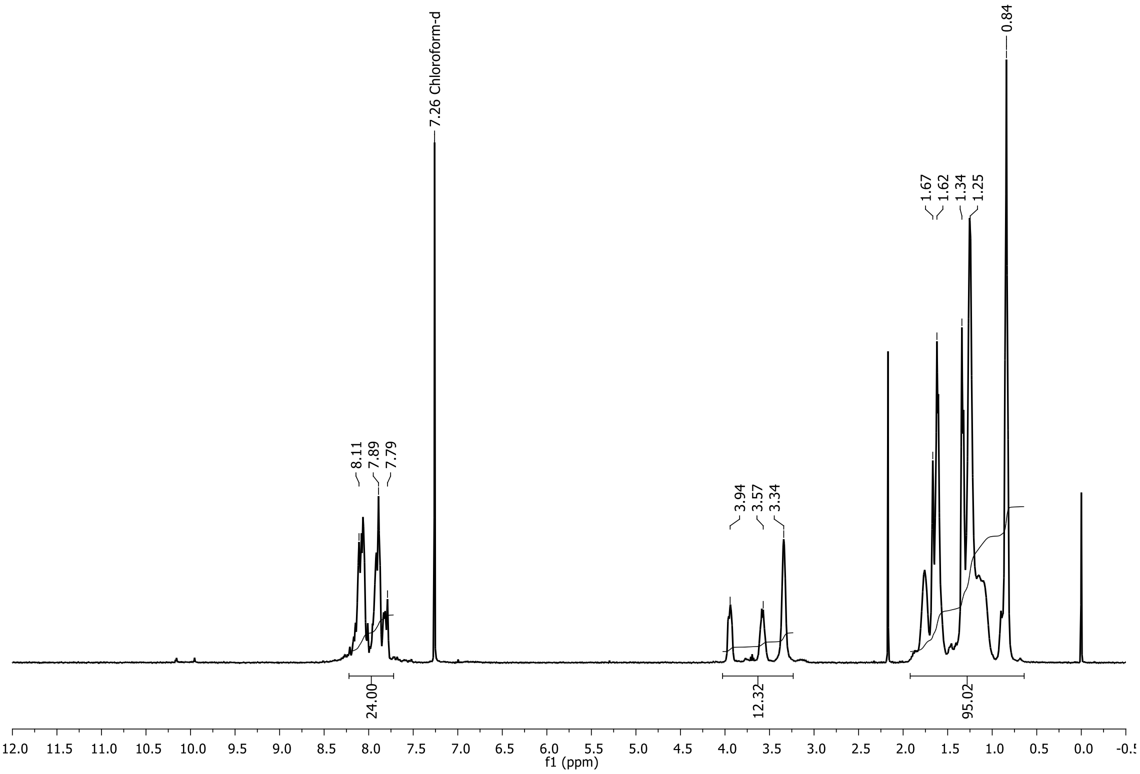

Fig. S49: ^{1}H NMR ($CDCl_3$) spectrum of scrambled **A^2:I^4** cage

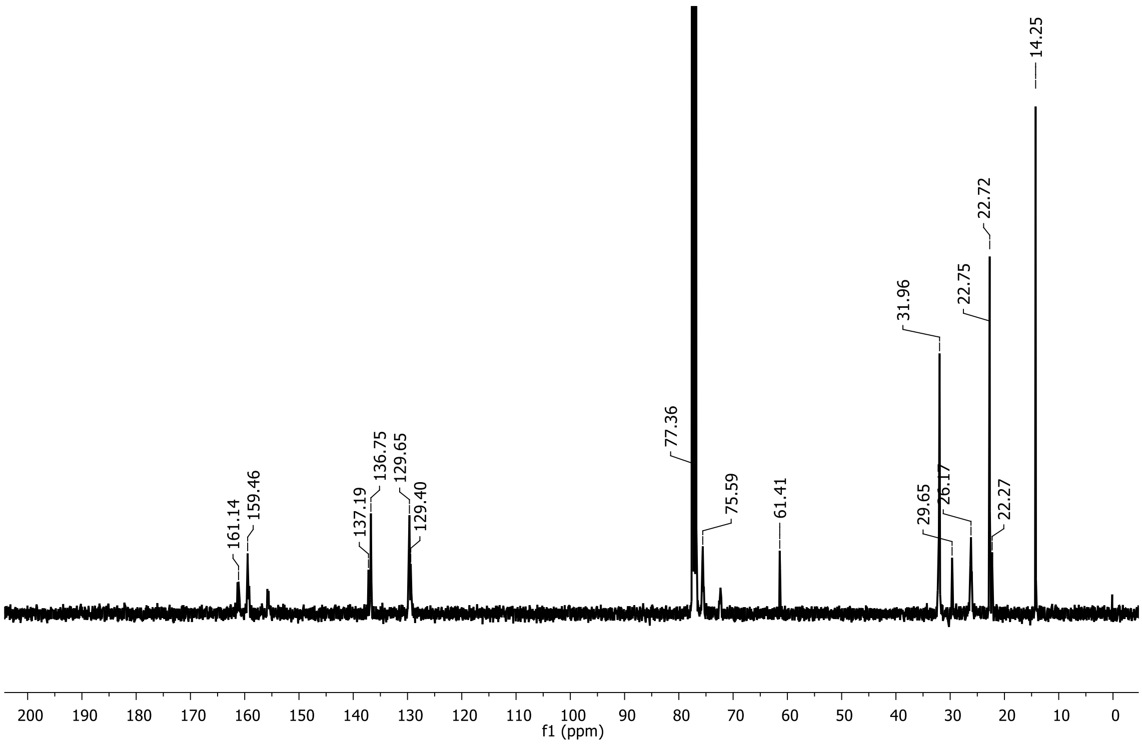

Fig. S50: ^{13}C NMR (CDCl$_3$) spectrum of scrambled **A^2:I^4** cage

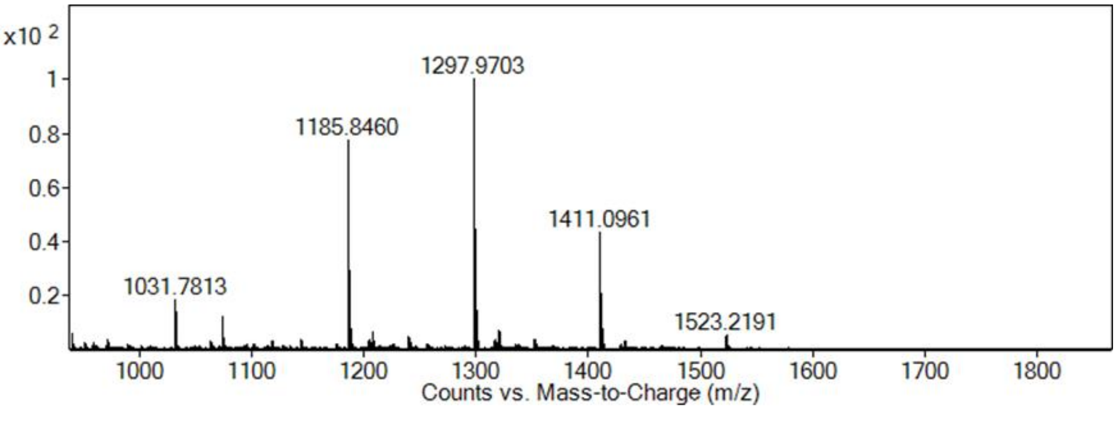

Fig. S51: HRMS spectra for the scrambled **A^2:I^4** cage

A^3:K^3

X=

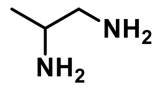

To a solution of TFB (15.00 g, 0.093 mol, 4.0 eq) dissolved in DCM (1.5 L), was added solutions of 1,2-diamino-2-methyl-propane (Amine **A**, 6.11 g, 0.069 mol, 3.0 eq) in DCM (250 mL), and racemic propane-1,2-diamine (Amine **K**, 5.11g, 0.069 mol, 3.0 eq) in DCM (250 mL). The reaction mixture was stirred at room temperature for 72 h before the solvent was removed under reduced pressure. The crude product was re-dissolved in DCM (250 mL), filtered to remove insoluble polymer, and the solvent removed under reduced pressure. The resulting solid was washed with ethyl acetate (250 mL) and collected to give the scrambled cage as a colourless solid (19.0 g, 20.7 mmol, 89%).

IR (ν_{max}/cm^{-1}): 2970, 2851, 1707, 1649 (imine N=C), 1601, 1447, 1383, 1265, 1149; **^{1}H NMR** (400 MHz, CDCl$_3$): δ 8.17–7.83 (24H, m, N=C**H** and Ar**H**) 3.92–3.52 (15H, m, C**H**N=CH and C**H**$_2$N=CH) 1.60–1.19(27H, m, C**H**$_3$); **^{13}C NMR** (101 MHz, CDCl$_3$): (due to scrambling, all singlets appear as broad multiplets) δ 162.79, 159.26, 154.97, 136.98, 136.28, 129.35, 72.13, 68.22, 66.64, 61.03, 60.19, 50.42, 29.22, 28.58, 21.86, 20.75, 14.00; **HRMS** (ES+) calc. for scrambled cages **A^{6}K^0**, **A^{5}K^1**, **A^{4}K^2**, **A^{3}K^3**, **A^{2}K^4**, **A^{1}K^5**, **A^{0}K^6** = 960.6003, 946.5846, 932.569, 918.5533, 904.5377, 890.522 and 876.5064; found [M+H]$^+$ at: 947.5812, 933.5684, 919.5531, 905.5372, 891.5213, 877.5066.

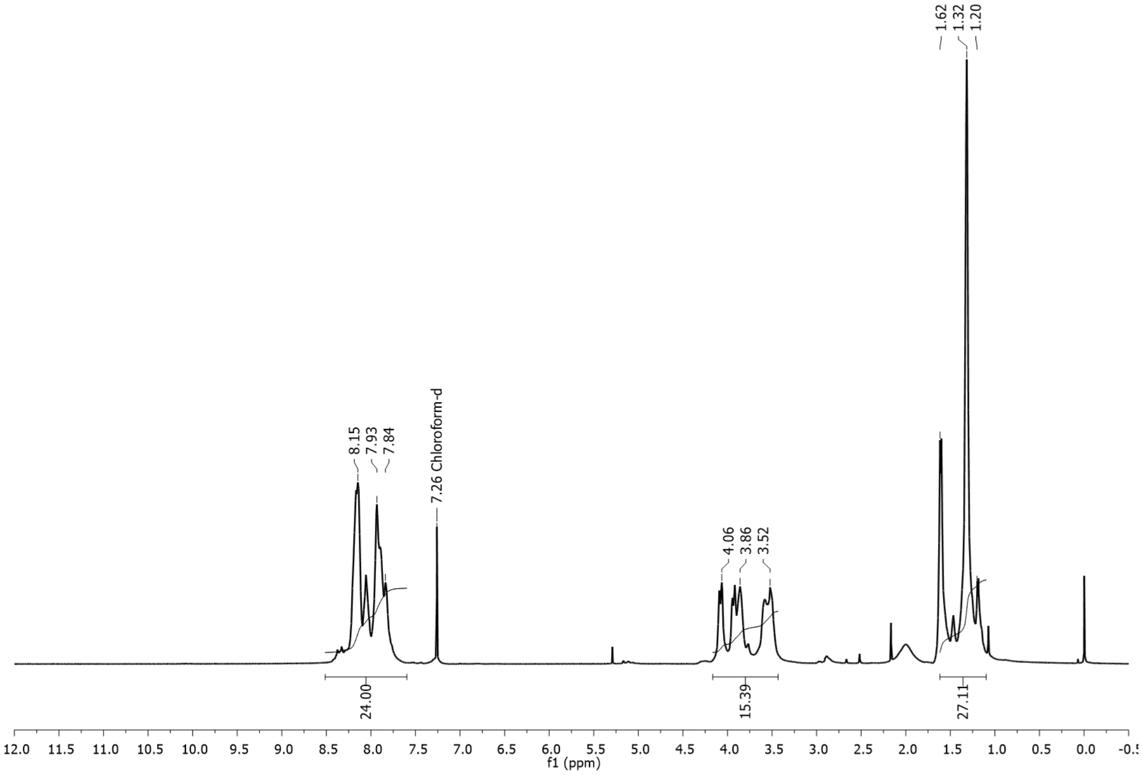

Fig. S52: ^{1}H NMR (CDCl$_3$) spectrum of scrambled **A^3:K^3** cage

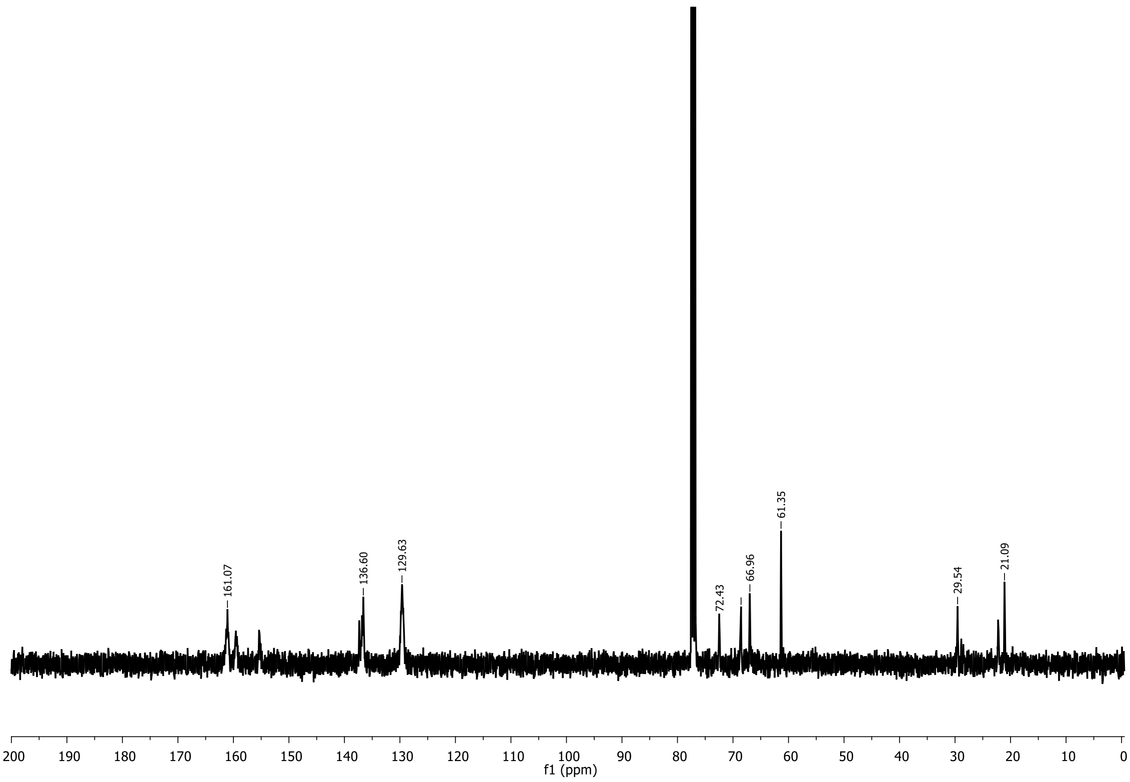

Fig. S53: ^{13}C NMR (CDCl$_3$) spectrum of scrambled **A^3:K^3** cage

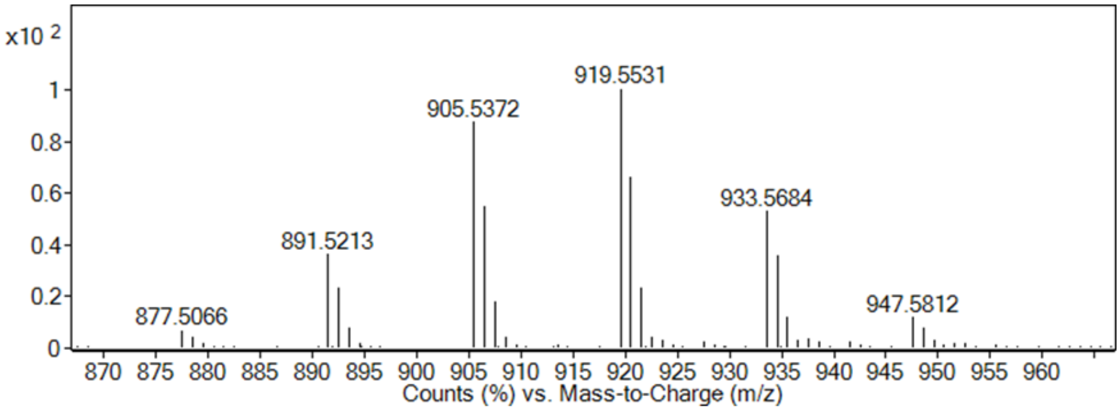

Fig. S54: HRMS spectra for the scrambled **A^3:K^3** cage

6.2. Purification of solvents

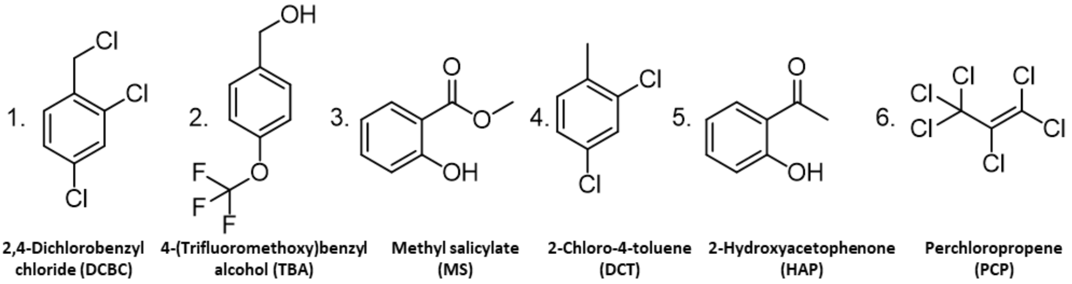

Fig. S55: Structures of the six size-excluded porous liquid solvents

One problem that can arise with Type 2 porous liquids is the solvent purity. Even trace impurities can result in a dramatic reduction in gas uptake as, if they are small enough, they can occupy the cage cavities and compete with other guests. This issue with the solvent was identified with the first reported scrambled cage porous liquid,[6] so it was important to ensure the new size-excluded solvents were pure enough that gas uptake was not affected, or this could incorrectly rule out potential porous liquids.

Various methods of purification were investigated for the different size-excluded solvents with xenon displacement experiments carried out to see if the gas uptake improved (Table S11). The same scrambled **3^3:13^3** (**A^3:E^3**) cage was used in each of the solvents as an expected porosity is already known in solvent 6 (PCP), allowing direct comparison between the different potential porous liquids. Additionally, for some of the solvents, there was not a clear reduction in the impurity peaks in the ^{1}H NMR spectra after purification, so gas evolution was determined to be the easiest method of determining if there was any improvement.

General procedure for xenon evolution measurements: Samples of the porous liquid were prepared by dissolving scrambled **3^3:13^3** cage (200 mg), desolvated in a vacuum oven at 90 °C overnight, in either the 'as bought' or purified solvent (1.0 mL) by sonication and stirring. Xenon was then added to the porous liquid by bubbling the gas through the sample at ~50-60 mL/min (60-66 on Gilmont flowmeter scale with a stainless steel float) for 10 mins per 1 mL of solvent used. Chloroform (16 µL, 1.0 eq. relative to cage) was then added to evolve the xenon and the displacement of water was measured in an inverted burette over 30 minutes (see Table S11 and Fig. S56) – a maximum of 4.6 mL of evolved xenon is expected based on 1:1 occupancy of the cages for a 200 mg sample.

General procedure for solvent purification by distillation: Each solvent was heated slowly in 10 °C increments in distillation apparatus under vacuum. Fractions were collected as they condensed with the first and last 10% discarded. The purified solvent was stored under N_2 in an oven-dried Schlenk tube over activated 4 Å sieves. If further purification was needed, the solvent was filtered 5 times through 5 separate activated basic alumina plugs (5 × 150 g aluminium oxide, activated, basic, Brockmann I, CAS 1344-28-1, Sigma-Aldrich).

2,4-Dichlorobenzyl chloride (DCBC, solvent 1) was collected after distillation as a colourless liquid. **^{1}H NMR** (400 MHz, $CDCl_3$): δ 7.32-7.29 (2H, m, , Ar**H**), 7.16 (1H, d, *J* = 8.0 Hz, Ar**H**), 4.58 (2H, s, C**H**$_2$); **^{13}C NMR** (101 MHz, $CDCl_3$): δ 135.02 (Ar**C**), 134.67 (Ar**C**), 133.62 (Ar**C**), 131.52 (Ar**C**), 129.55 (Ar**C**), 127.49 (Ar**C**), 42.46 (C**H**$_2$).

4-(Trifluoromethoxy)benzyl alcohol (TBA, solvent 2) was collected as a colourless liquid after distillation and passing over alumina. **^{1}H NMR** (400 MHz, $CDCl_3$): δ 7.29 (2H, d, *J* = 8.0 Hz, Ar**H**), 7.16 (2H, d, *J* = 8.0 Hz, Ar**H**), 4.56 (2H, d, *J* = 3.0 Hz, C**H**$_2$), 3.10 (1H, br s, O**H**); **^{13}C NMR** (101 MHz, $CDCl_3$): δ 148.74, (Ar**C**), 139.59 (Ar**C**), 128.36 (Ar**C**/**C**F$_3$), 121.14 (Ar**C**), 64.36 (**C**H$_2$) - CF_3 not observed- possibly due to overlap with ArC.

Methyl salicylate (MS, solvent 3) was collected after distillation as a colourless liquid. **^{1}H NMR** (400 MHz, $CDCl_3$): δ 10.76 (1H, s, O**H**), 7.82 (1H, d, *J*= 8.0 Hz, Ar**H**), 7.44 (1H, t, *J*= 16.0 Hz, Ar**H**), 6.97 (1H, d, *J*= 8.0 Hz, Ar**H**), 6.86 (1H, t, *J*= 16.0 Hz, Ar**H**), 3.92 (3H, s, C**H**$_3$); **^{13}C NMR** (101 MHz, $CDCl_3$): δ 170.43 (**C**O), 161.48 (Ar**C**OH), 135.53 (Ar**C**), 129.76 (Ar**C**), 119.00 (Ar**C**), 117.41 (Ar**C**), 112.24 (Ar**C**), 52.09 (**C**H$_3$).

2,4-Dichlorotoluene (DCT, solvent 4) was collected after distillation as a colourless liquid. **^{1}H NMR** (400 MHz, $CDCl_3$): δ 7.27 (1H, s, Ar**H**), 7.05 (2H, s, Ar**H**), 2.27 (3H, s, C**H**$_3$); **^{13}C NMR** (101 MHz, $CDCl_3$): δ 135.00 (Ar**C**), 134.54 (Ar**C**), 132.01 (Ar**C**), 131.60 (Ar**C**), 128.83 (Ar**C**), 126.80 (Ar**C**), 19.48 (**C**H$_3$).

2-Hydroxyacetophenone (HAP, solvent 5) was collected after distillation as a colourless liquid. **^{1}H NMR** (400 MHz, $CDCl_3$): δ 12.24 (1H, s, O**H**), 7.63–7.60 (1H, m, Ar**H**), 7.40–7.36 (1H, m, Ar**H**), 6.89–6.86 (1H, m, Ar**H**), 6.77-6.67 (1H, m, Ar**H**), 2.52–2.50 (3H, m, C**H**$_3$); **^{13}C NMR** (101 MHz, $CDCl_3$): δ 204.75 (**C**O), 162.48 (Ar**C**), 136.56 (Ar**C**), 130.95 (Ar**C**), 119.82 (Ar**C**), 119.08 (Ar**C**), 118.41 (Ar**C**), 26.65 (**C**H$_3$).

Table S11: Volume of xenon evolved from porous liquids made from scrambled **A^3:E^3** cage in the different size-excluded solvents (200 mg/mL) before and after purification

Solvent	Code	Purity (%)	Purification method	Xenon evolved (mL)	
				Measurement 1	Measurement 2
1	DCBC	97	As bought	0.6	0.8
		≥99	Distilled	1.7	1.0
2	TBA	97	As bought	1.5	1.8
		99	Distilled	2.2	1.9
		≥99	Distilled and alumina	2.8	2.8
3	MS	99	As bought	1.6	1.8
		≥99	Distilled	2.3	2.3
4	DCT	99	As bought	2.1	-
		≥99	Distilled	2.0	1.8
5	HAP	99	As bought	2.0	1.9
		≥99	Distilled	3.2	2.9
6	PCP	≥99	Alumina	4.3	4.5

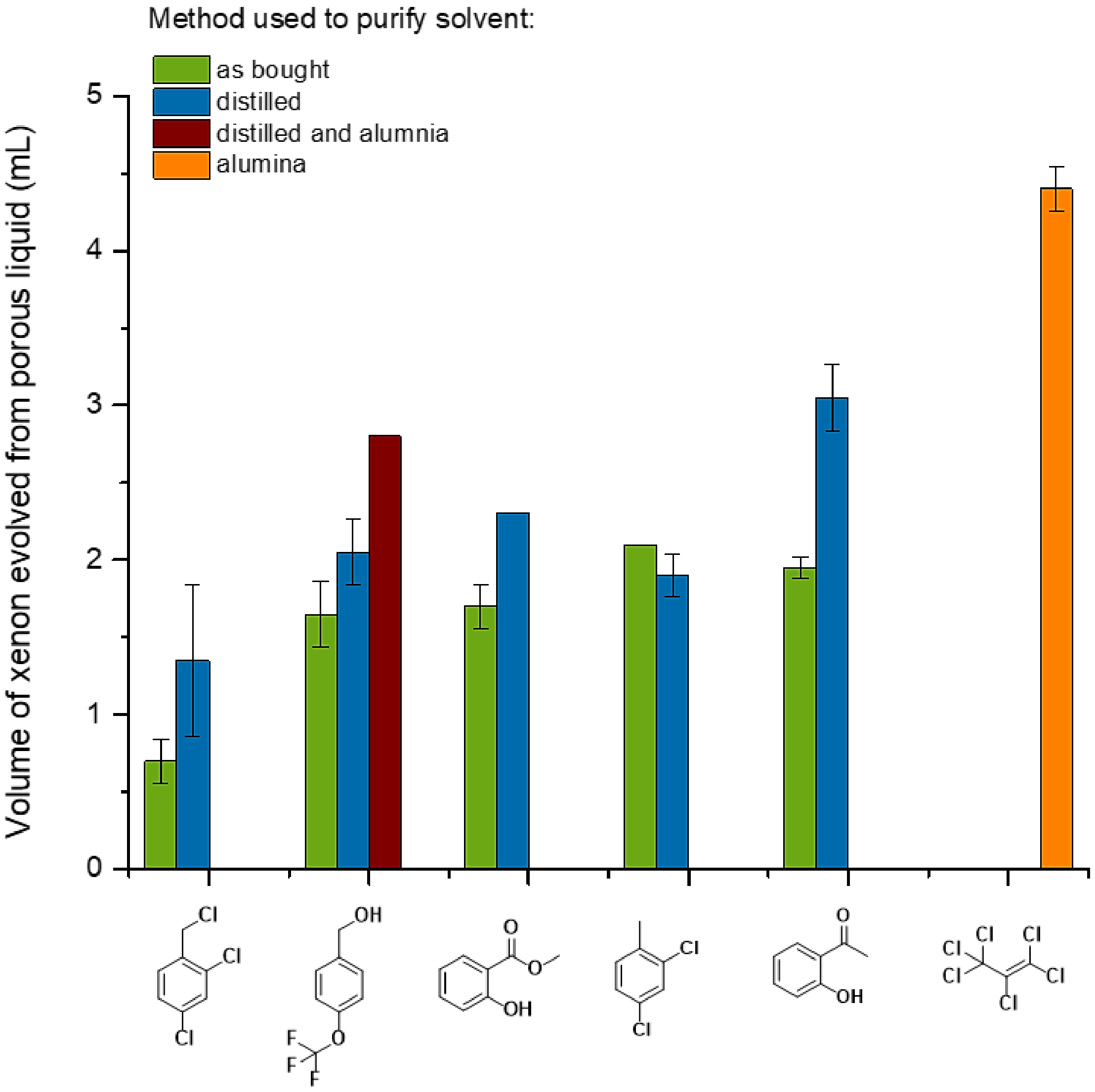

Fig. S56: Comparison of the volume of xenon released from porous liquids using scrambled **A^3:E^3** cage in the solvents used in the high-throughput solubility testing. Purifying the solvent before use is important as this can reduce the gas uptake in the resulting porous liquid.

2,4-Dichlorobenzyl chloride (solvent 1), methyl salicylate (solvent 3), and 2,4-dichlorotoluene (solvent 4), were purified by distillation but minimal improvement in gas evolution was observed – it is possible that solvent purity is not the only factor affecting gas uptake, for example, the viscosity could also reduce the gas uptake. 4-(Trifluoromethoxy)benzyl alcohol (solvent 2), and 2-hydroxyacetophenone (solvent 5), showed improved xenon evolution after purification that was of the same order of magnitude in comparison to perchloropropene (solvent 6).

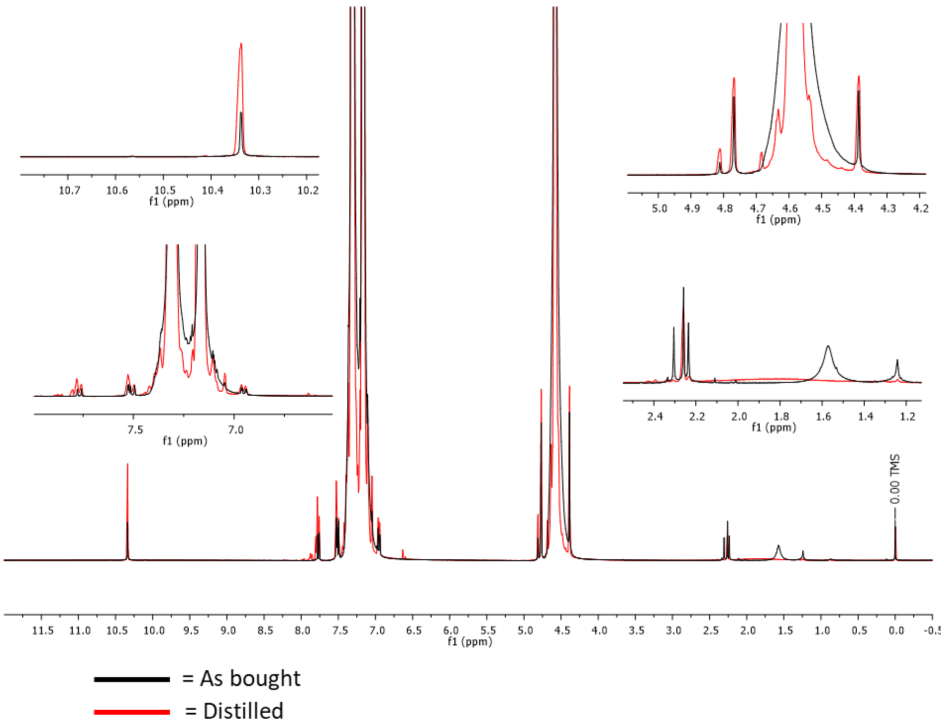

Fig. S57: ^{1}H NMR ($CDCl_3$) spectra of 2,4-dichlorobenzyl chloride (solvent 1), as bought (black) and after distillation (red), expansions showing a reduction in impurities.

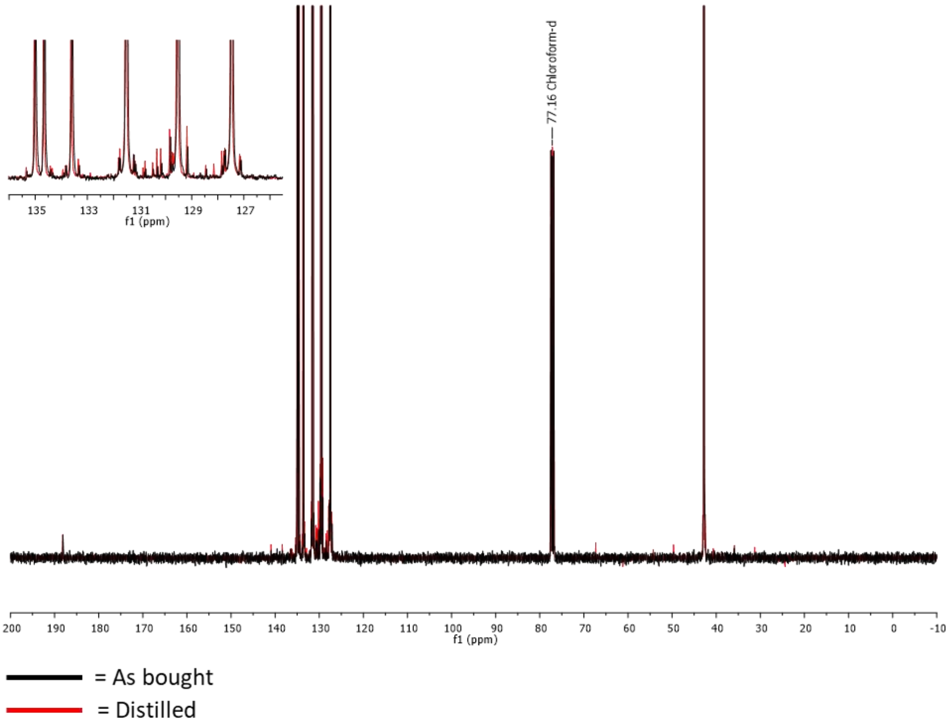

Fig. S58: ^{13}C NMR ($CDCl_3$) spectra of 2,4-dichlorobenzyl chloride (solvent 1), as bought (black) and after distillation (red).

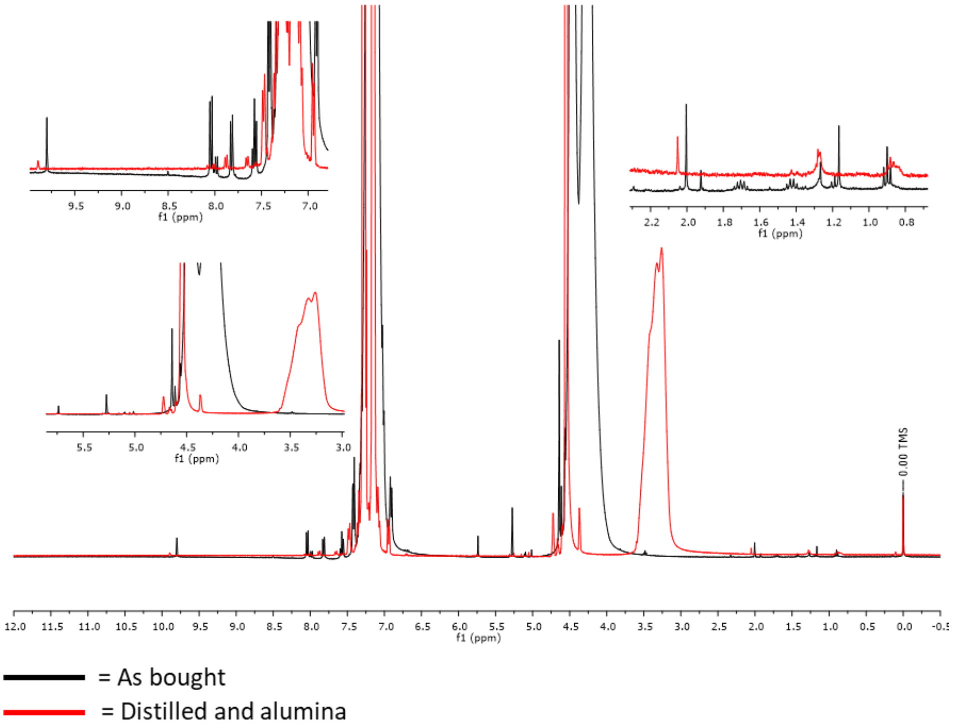

Fig. S59: ^{1}H NMR (CDCl$_3$) spectra of 4-(trifluoromethoxy) benzyl alcohol (solvent 2), as bought (black) and after distillation and passing through alumina (red), with expansions showing a reduction in impurities.

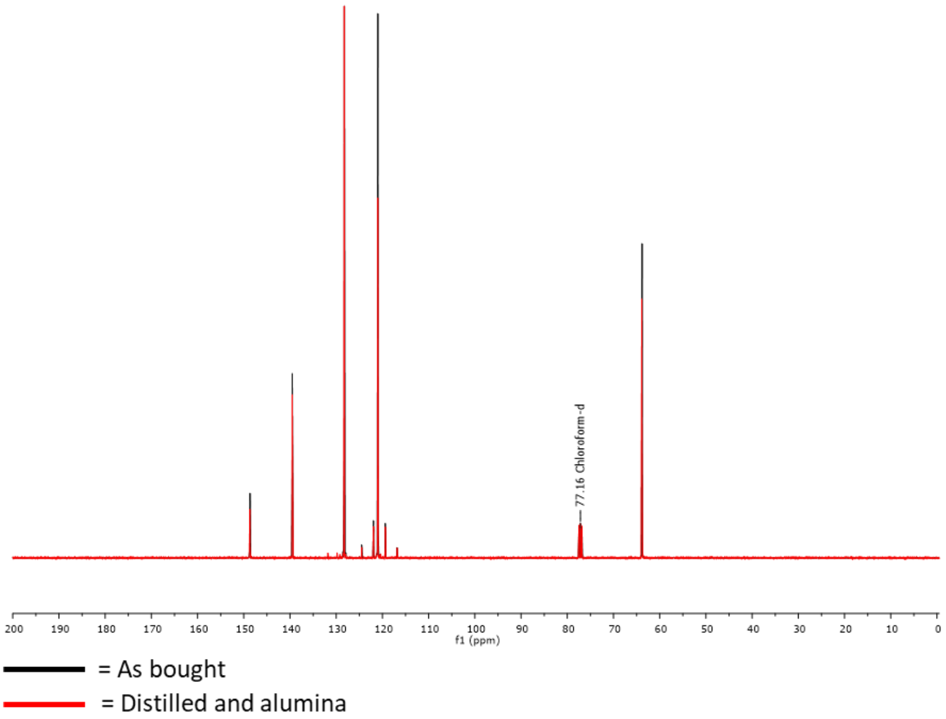

Fig. S60: ^{13}C NMR (CDCl$_3$) spectra of 4-(trifluoromethoxy)benzyl alcohol (solvent 2), as bought (black), and after distillation and passing through alumina (red).

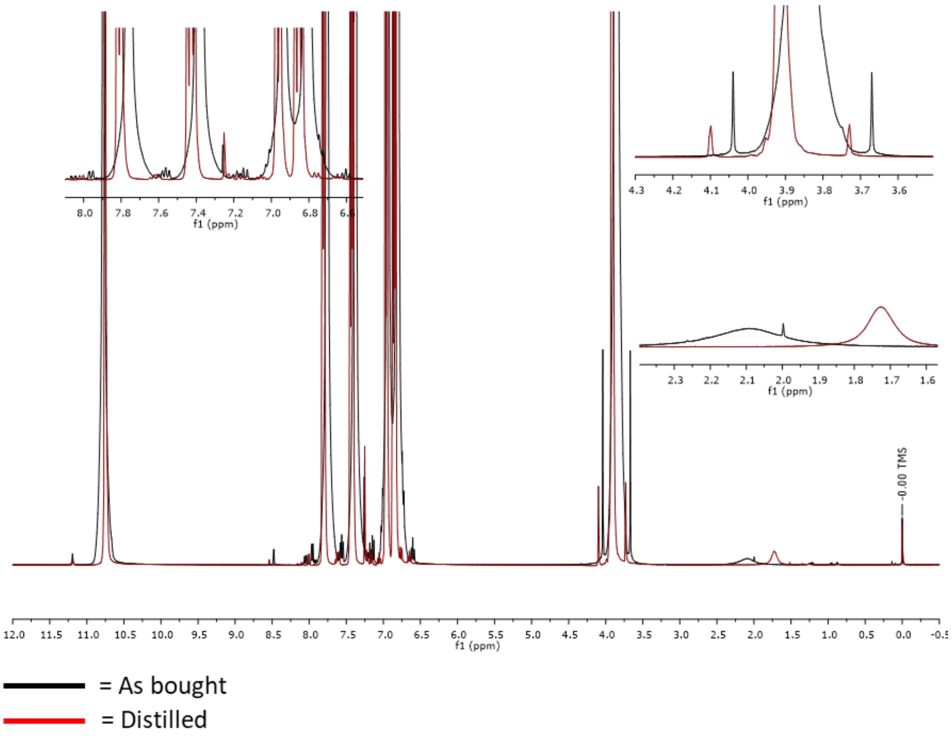

Fig. S61: ^{1}H NMR ($CDCl_3$) spectra of methyl salicylate (solvent 3), as bought (black), and after distillation (red).

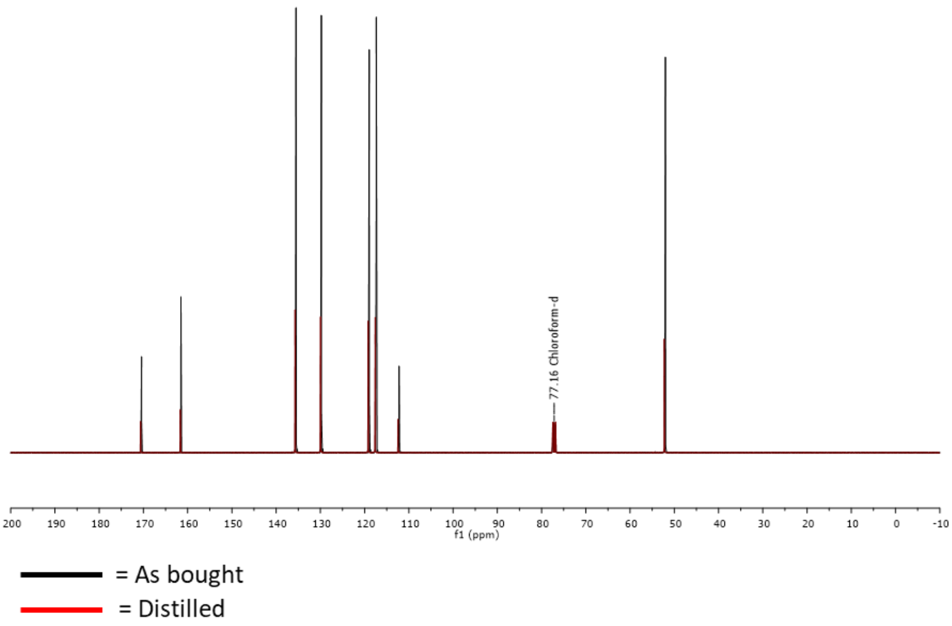

Fig. S62: ^{13}C NMR ($CDCl_3$) spectra of methyl salicylate (solvent 3), as bought (black), and after distillation (red).

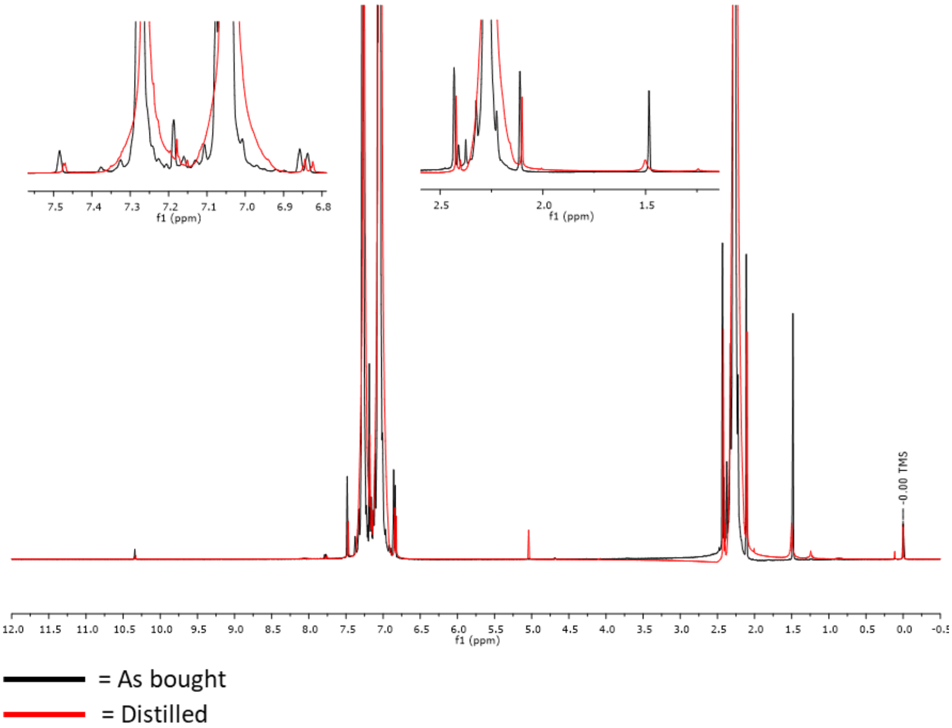

Fig. S63: ^{1}H NMR ($CDCl_3$) spectra of 2,4-dichlorotoluene (solvent 4), as bought (black), and after distillation (red).

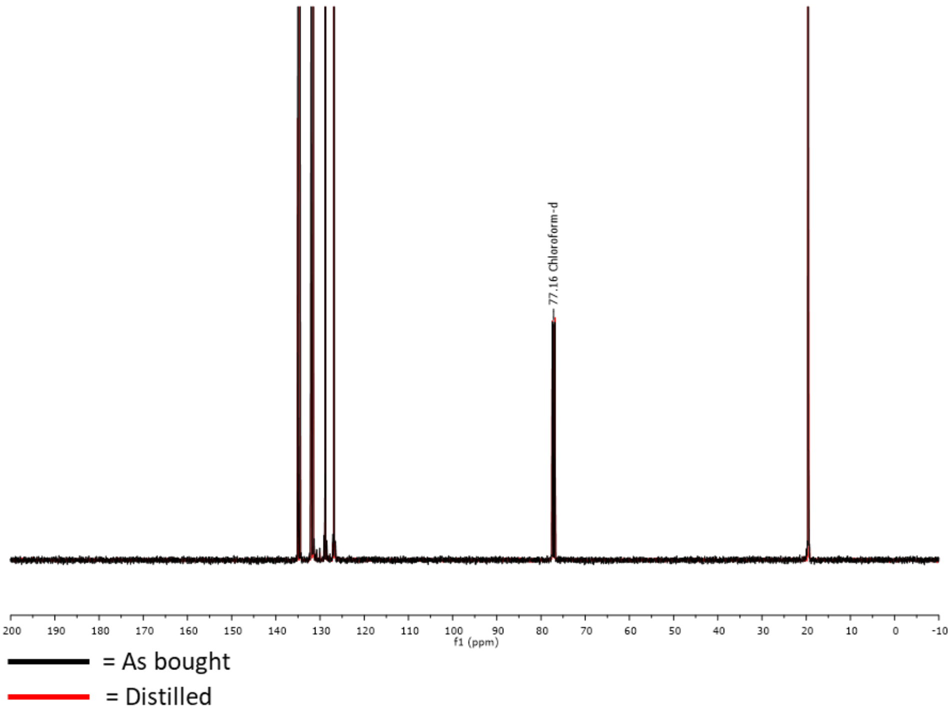

Fig. S64: ^{13}C NMR ($CDCl_3$) spectra of 2,4-dichlorotoluene (solvent 4), as bought (black), and after distillation (red).

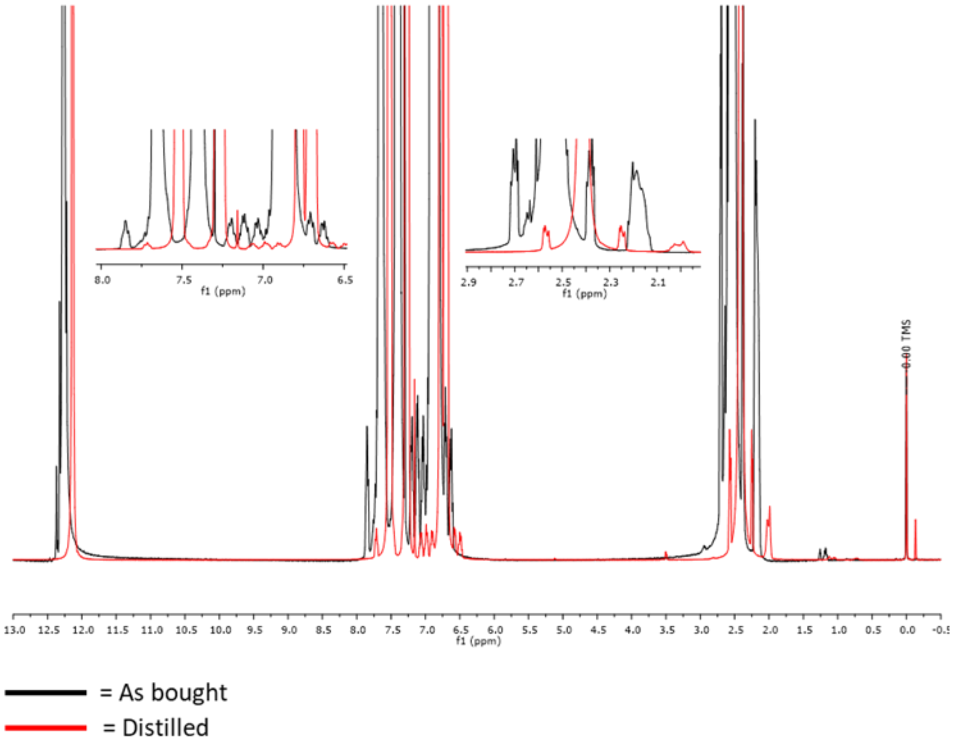

Fig. S65: ^{1}H NMR ($CDCl_3$) spectra of 2-hydroxyacetophenone (solvent 5), as bought (black), and after distillation (red).

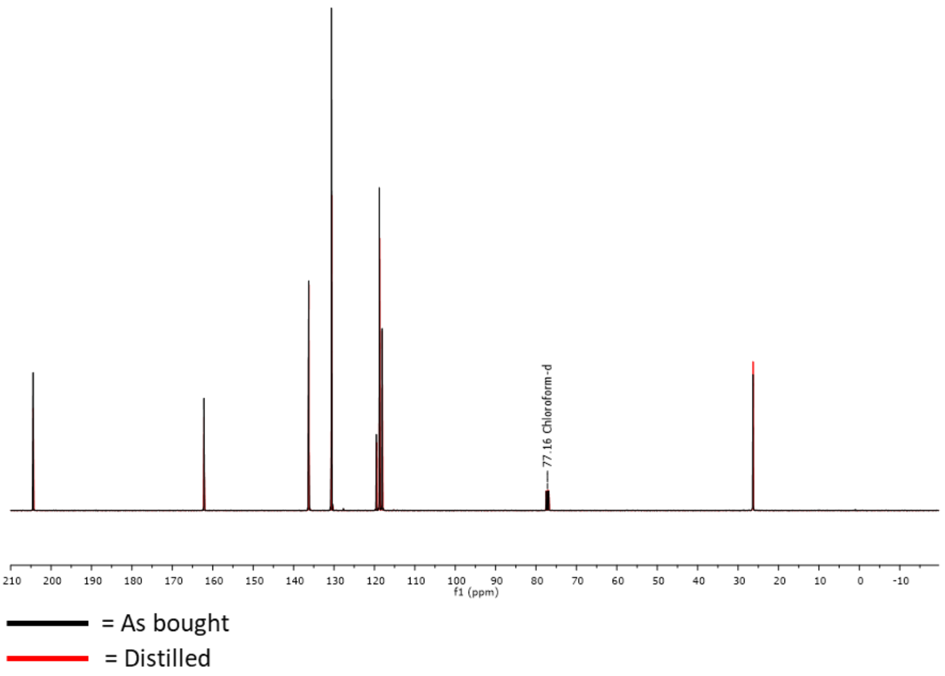

Fig. S66: ^{13}C NMR ($CDCl_3$) spectra of 2-hydroxyacetophenone (solvent 5), as bought (black), and after distillation (red).

6.3. Solubility and porosity screen

General procedure for porosity screen: The selected solvent (1 mL) was added to a scrambled cage (200 mg) and stirred until dissolved. Any cages which did not dissolve, or formed a gel at this concentration at the higher volume, were discounted. Xenon was added to the porous liquid at ~50-60 mL min^{-1} for 10 mins per 1 mL of solvent. Chloroform (1.0 eq. relative to cage) was then added to evolve the xenon and the displacement of water was measured in an inverted burette over 30 minutes. This screen of the potential new porous liquids was carried out to narrow down the hits further, and the systems with the highest volume evolved were investigated further at higher concentrations.

Table S12: Summary of porosity testing carried out using chemical displacement of xenon to determine which of the new cage/solvent combinations were porous.

Porous liquid code	Scrambled cage	Solvent	Dissolved at 200 mg mL^{-1}	Xenon evolved at 200 mg mL^{-1}
E3	**A^3:E^3**	1	✓	1.4
E9	**A^3:E^3**	2	✓	2.8
E15	**A^3:E^3**	3	✓	2.3
E21	**A^3:E^3**	4	✓	1.9
E27	**A^3:E^3**	5	✓	3.1
G3	**A^3:G^3**	1	✓	1.4
G4	**A^2:G^4**	1	✓	0.8
G5	**A^1:G^5**	1	✓	1.0
G8	**A^4:G^2**	2	✓	0.5
G9	**A^3:G^3**	2	✓	0.8
G10	**A^2:G^4**	2	✓	1.2
G11	**A^1:G^5**	2	✓	1.0
G15	**A^3:G^3**	3	✓	1.2
G16	**A^2:G^4**	3	✓	2.8*
G17	**A^1:G^5**	3	✓	1.9
G21	**A^3:G^3**	4	✓	1.1
G22	**A^2:G^4**	4	✓	0.9
G23	**A^1:G^5**	4	✓	1.6
G27	**A^3:G^3**	5	✓	0.4
G28	**A^2:G^4**	5	✓	0.6
G29	**A^1:G^5**	5	✓	1.2
H25	**A^5:H^1**	5	✓	2.1
I4	**A^2:I^4**	1	✓	1.1
I10	**A^2:I^4**	2	✓	1.0
I16	**A^2:I^4**	3	✓	0.4
I22	**A^2:I^4**	4	✓	2.0
I26	**A^4:I^2**	5	✓	2.2
I27	**A^3:I^3**	5	✓	2.0*
I28	**A^2:I^4**	5	✓	1.7
K9	**A^3:K^3**	2	Gel formed	n/a

***carried out at 100 mg in 0.5 mL due to low yield**

NB. **G16** appeared to have a reasonable xenon uptake when tested in the initial porosity screen (Table S12), but when gas evolution was attempted at a higher volume (>1 mL), the porous liquid suffered from gelation, so was not investigated further.

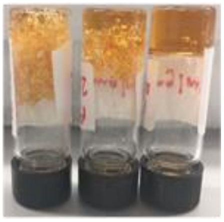

Fig. S67: On scale-up, some of the initial porous liquid hits were found to form gels instead of liquids, including **K9** as shown.

6.4. Effect of changing the porous liquid solvent

NB: The naming of the porous liquids that are studied further have been changed from this point (see main text and Table S13).

Table S13: New naming system for the porous liquids found in the high-throughput screen and investigated further to study the effect of changing the porous liquid solvent

High-throughput code	Porous liquid name
E3	**3^3:13^3_{DCBC}**
E9	**3^3:13^3_{TBA}**
E15	**3^3:13^3_{MS}**
E21	**3^3:13^3_{DCT}**
E27	**3^3:13^3_{HAP}**
E33	**3^3:13^3_{PCP}**

6.4.1. Porous Liquid Properties

Viscosity measurements: Scrambled $\mathbf{3^3{:}13^3}$ cage (200 mg) was dissolved in one of the bulky solvents (1 mL), and the viscosity of the sample measured using a RheoSense µVISC viscometer (using either a 0.01–100 or 10-2000 cP microfluidic chip) with the temperature set at 25 °C. The procedure was repeated three times to calculate the average viscosity and standard deviation.

Table S14: Average viscosities calculated for the $\mathbf{3^3{:}13^3}$ porous liquid family at 20% w/v

Porous liquid	Measurement 1 (cP)	Measurement 2 (cP)	Measurement 3 (cP)	Average ± SD (cP)	Average Temperature (°C)
$\mathbf{3^3{:}13^3_{DCBC}}$	14.91	14.90	14.97	14.93 ± 0.038	25.01
$\mathbf{3^3{:}13^3_{TBA}}$	31.93	32.48	32.98	32.46 ± 0.53	25.02
$\mathbf{3^3{:}13^3_{MS}}$	9.841	9.841	9.840	$9.84 \pm 5.7\text{x}10^{-4}$	25.03
$\mathbf{3^3{:}13^3_{DCT}}$	3.694	3.698	3.700	3.70 ± 0.0031	25.03
$\mathbf{3^3{:}13^3_{HAP}}$	9.800	9.825	9.826	9.82 ± 0.015	24.97

Table S15: Average viscosities measured for the neat parent solvents after purification

Solvent	Measurement 1 (cP)	Measurement 2 (cP)	Measurement 3 (cP)	Average ± SD (cP)	Average Temperature (°C)
DCBC	3.291	3.281	3.291	3.29 ± 0.0058	24.99
TBA	7.924	7.920	7.930	7.92 ± 0.0050	25.01
MS	2.961	2.964	2.964	2.96 ± 0.0017	24.99
DCT	1.330	1.331	1.334	1.33 ± 0.0021	25.01
HAP	2.919	2.926	2.917	2.92 ± 0.0047	25.03

Density measurements: Scrambled $\mathbf{3^3:13^3}$ cage (200 mg) was dissolved in one of the bulky solvents (1 mL), before a sample of each porous liquid was added to a pre-weighed 1 mL volumetric flask. The volumetric flask was then re-weighed and the density of the porous liquid (20% w/v) calculated. The procedure was repeated three times to calculate the average density and standard deviation.

Table S16: Average densities calculated for the $\mathbf{3^3:13^3}$ porous liquid family at 20% w/v

Porous liquid	Sample 1	Sample 2	Sample 3	Average density (g mL^{-1})	Standard deviation (± g mL^{-1})
	Mass (g)	Mass (g)	Mass (g)		
$\mathbf{3^3:13^3_{DCBC}}$	1.3073	1.3088	1.3135	1.3099	0.0032
$\mathbf{3^3:13^3_{TBA}}$	1.2656	1.2675	1.2612	1.2648	0.0032
$\mathbf{3^3:13^3_{MS}}$	1.1244	1.1236	1.1233	1.1238	0.0006
$\mathbf{3^3:13^3_{DCT}}$	1.1883	1.1931	1.1803	1.1872	0.0065
$\mathbf{3^3:13^3_{HAP}}$	1.0294	1.0226	1.0201	1.0240	0.0048

Table S17: Average densities measured for the neat parent solvents after purification

Solvent	Reported density (g mL^{-1})*	Sample 1	Sample 2	Sample 3	Average density (g mL^{-1})	Standard deviation (± g mL^{-1})
		Mass (g)	Mass (g)	Mass (g)		
DCBC	1.407	1.3218	1.3693	1.3403	1.3438	0.0239
TBA	1.326	1.2417	1.2362	1.2592	1.2457	0.0120
MS	1.174	1.1606	1.1441	1.1609	1.1552	0.0096
DCT	1.246	1.1524	1.1639	1.1913	1.1692	0.0200
HAP	1.131	1.0868	1.0844	1.0857	1.0856	0.0012

*Reported from Sigma Aldrich

Table S18: Calculation of the scrambled cage to solvent ratio in each of the porous liquids at 20% w/v

Porous liquid	Mmol cage in sample	Mmol solvent in sample	Cage: Solvent
3^3:$13^3$$_{DCBC}$	0.192	7.20	1:37
3^3:$13^3$$_{TBA}$	0.192	6.90	1:36
3^3:$13^3$$_{MS}$	0.192	7.72	1:40
3^3:$13^3$$_{DCT}$	0.192	7.74	1:40
3^3:$13^3$$_{HAP}$	0.192	8.31	1:40
3^3:$13^3$$_{PCP}$	0.192	6.89	1:37

Calculating total pore volume: using the previously reported method, the total pore volume for the scrambled **3^3:13^3** porous liquid family can be calculated and compared for 200 mg of scrambled **3^3:13^3** cage dissolved in 1 mL of each solvent (**Tables S19-S21**).[7]

Table S18: Properties of the **3^3:13^3** scrambled cage used to calculated total pore volumes in the porous liquid family.

Scrambled Cage	Mass(g)	MW (g mol^{-1})	Moles of cage (mol)	Molecules of cage using Avogadro's constant	Pore volume of single cage (mL)
3^3:13^3	0.2	1039.43	$1.92X10^{-4}$	$1.159x10^{20}$	$6.545x10^{-23}$

Table S19: Total pore volumes calculated for the scrambled **3^3:13^3** cage porous liquid family at 20% w/v (200 mg in 1 mL).

Porous liquid	Measured density of solvent (g mL^{-1})	Mass of PL sample (g)	Measured density of PL (g mL^{-1})	Overall PL volume (mL)	Pore volume (%)
3^3:$13^3$$_{DCBC}$	1.3438	1.5438	1.3099	1.18	**0.64**
3^3:$13^3$$_{TBA}$	1.2457	1.4457	1.2648	1.14	**0.66**
3^3:$13^3$$_{MS}$	1.1552	1.3552	1.1238	1.21	**0.63**
3^3:$13^3$$_{DCT}$	1.1692	1.3692	1.1872	1.15	**0.66**
3^3:$13^3$$_{HAP}$	1.0856	1.2856	1.0240	1.17	**0.65**

6.4.2. Xenon uptake studies by gas displacement

General Procedure: Samples of each porous liquid were prepared by dissolving scrambled **3^3:13^3** cage (200 mg, 0.192 mmol), desolvated in a vacuum oven at 90 °C overnight, in each of the purified solvents (1.0 mL) by sonication and stirring. Xenon was then added to each porous liquid by bubbling the gas through the sample at ~50-60 mL min^{-1} (60-66 on Gilmont flowmeter scale with a stainless steel float) for 10 mins per 1 mL of solvent used. Chloroform (16 µL, 0.192 mmol, 1.0 eq. relative to cage) was then added to evolve the xenon and the displacement of water was measured in an inverted burette over 30 minutes. The theoretical maximum volume of xenon that can be evolved based on a 1:1 cage:Xe ratio is 4.6 cm^3 (calculated in Section 4.3).

Table S20: Summary of **3^3:13^3** porous liquid properties used in subsequent calculations

Porous liquid	Mass of cage (g)	Mass of solvent (g)	Mass of PL (g)	Density of PL (g mL^{-1})
3^3:13^3_{DCBC}	0.2	1.3438	1.5438	1.3099
3^3:13^3_{TBA}	0.2	1.2457	1.4457	1.2648
3^3:13^3_{MS}	0.2	1.1552	1.3552	1.1238
3^3:13^3_{DCT}	0.2	1.1692	1.3692	1.1872
3^3:13^3_{HAP}	0.2	1.0856	1.2856	1.0240
3^3:13^3_{PCP}	0.2	1.7112	1.9112	1.6193

Table S21: Volume of xenon evolved from the different scrambled **3^3:13^3** porous liquids at 20% w/v by chemical displacement with chloroform.

Porous liquid	Volume of xenon evolved (mL)		Average ± SD (mL)	% occupancy
	Measurement 1	Measurement 2		
3^3:13^3_{DCBC}	1.7	1.0	1.4 ± 0.5	30.4
3^3:13^3_{TBA}	2.8	3.0	3.0 ± 0.3	65.2
3^3:13^3_{MS}	2.2	2.3	2.3 ± 0.1	50.0
3^3:13^3_{DCT}	1.8	2.1	1.9 ± 0.1	41.3
3^3:13^3_{HAP}	3.2	2.9	3.1 ± 0.2	67.4
3^3:13^3_{PCP}	4.3	4.5	4.4 ± 0.1	95.7

Calculation of xenon uptake in µmol: To compare the xenon uptakes in the different scrambled **3^3:13^3** porous liquids at 20% w/v, the measurements were converted to moles using the ideal gas equation (Table S23).

$$n\ (mol) = \frac{pV}{RT}$$

P (Pa) = 101325
T (K) = 293
R (J K^{-1} mol^{-1}) = 8.314
V (m^3)

Example for 20% w/v 3^3:13^3_{HAP}: $n = \frac{101325 \times 0.0000029}{8.314 \times 293} = 0.126\ mmol$

Table S22: Volume of xenon evolved from **3^3:13^3** porous liquids at 20% w/v in µmol

Porous liquid	**Volume of xenon evolved (µmol)**		**Average ± SD (µmol)**
	Measurement 1	Measurement 2	
3^3:13^3_{DCBC}	70.7	41.6	56.2 ± 20.6
3^3:13^3_{TBA}	116.5	124.8	120.6 ± 5.9
3^3:13^3_{MS}	91.5	95.7	93.6 ± 2.9
3^3:13^3_{DCT}	74.9	87.3	81.1 ± 8.8
3^3:13^3_{HAP}	133.1	120.6	126.9 ± 8.8
3^3:13^3_{PCP}	178.9	187.2	183.0 ± 5.9

Calculation of xenon uptake in μmol g_{PL}^{-1}: To further compare the gas uptake in each scrambled **3^3:13^3** porous liquid at 20% w/v, the xenon uptake was also converted to μmol g_{PL}^{-1}:

Step 1:

$$Overall\ mass\ of\ porous\ liquid = M_{cage} + M_{solvent}$$

Step 2:

$$n\ (mol) = \frac{pV}{RT}$$

P (Pa) = 101325
T (K) = 293
R (J K^{-1} mol^{-1}) = 8.314
V (m^3)

Step 3:

$$\mu mol/g_{PL} = \frac{mmol\ uptake\ for\ whole\ sample}{mass\ of\ whole\ sample}$$

Example for 20% w/v 3^3:13^3_{DCBC}:

0.2 g + 1.3468 g = 1.5438 g

$$n = \frac{101325\ \times 0.0000017}{8.314\ \times 293} = 70.7\ \mu mol$$

$$\frac{70.7\ \mu mol}{1.5438\ g} = \ 45.8\ \mu mol/g_{PL}$$

Table S23: Calculated xenon uptake (μmol g_{PL}^{-1}) from gas evolution measurements for scrambled **3^3:13^3** porous liquid family at 20% w/v

Porous liquid	**Volume of xenon evolved (μmol g_{PL}^{-1})**		**Average ±SD (μmol g_{PL}^{-1})**
	Measurement 1	Measurement 2	
3^3:13^3_{DCBC}	45.8	26.9	36.4 ± 13.4
3^3:13^3_{TBA}	80.6	86.3	83.5 ± 4.0
3^3:13^3_{MS}	67.5	70.6	69.1 ± 2.2
3^3:13^3_{DCT}	54.7	63.8	59.3 ± 6.4
3^3:13^3_{HAP}	103.5	93.8	98.7 ± 6.9
3^3:13^3_{PCP}	93.6	97.9	95.6 ± 3.0

Calculation of xenon uptake in µmol mL_{PL}^{-1}: In order to compare xenon and subsequent methane uptakes, the gas uptake was converted to µmol mL_{PL}^{-1}:

$$\mu mol\ mL^{-1} = \mu mol\ g^{-1} \times \rho\ (g\ mL^{-1})$$

Table S24: Calculated xenon uptake (µmol mL_{PL}^{-1}) from gas evolution measurements for scrambled **3^3:13^3** porous liquid family at 20% w/v

Porous liquid	**Measured Density of PL**	**Volume of xenon evolved (µmol mL_{PL}^{-1})**		**Average ±SD (µmol mL_{PL}^{-1})**
		Measurement 1	Measurement 2	
3^3:13^3_{DCBC}	1.3099	60.0	35.3	47.6 ± 17.5
3^3:13^3_{TBA}	1.2648	101.9	109.2	105.5 ± 5.1
3^3:13^3_{MS}	1.1238	75.9	79.3	77.6 ± 2.4
3^3:13^3_{DCT}	1.1883	65.0	75.8	70.4 ± 7.7
3^3:13^3_{HAP}	1.024	106.0	96.1	101.0 ± 7.0
3^3:13^3_{PCP}	1.6193	151.5	158.6	155.1 ± 5.0

Xenon uptake in parent solvents:

Table S25: Calculated xenon uptakes from gas evolution measurements for parent solvents

Solvent	**Volume of xenon evolved (mL)**	**Mass of solvent used (g)**	**Density of solvent (g mL^{-1})**	**Xenon uptake (µmol)**	**Xenon uptake (µmol g_{sol}^{-1})**	**Xenon uptake (µmol mL_{sol}^{-1})**
DCBC	0.4	1.3438	1.3438	16.6	12.4	16.7
TBA	0.3	1.2457	1.2457	12.5	10.0	12.5
MS	0.3	1.1552	1.1552	12.5	10.8	12.5
DCT	0.6	1.1692	1.1692	25.0	21.3	24.9
HAP	0.2	1.0856	1.0856	8.3	7.7	8.4
PCP	0.2	1.7112	1.7650	8.3	4.9	8.4

6.4.3. Methane uptake studies by ^{1}H NMR spectroscopy

The porous liquids that were based on the scrambled **A^3:E^3** (**3^3:13^3**) cage gave the highest xenon evolution measurements, but that does not necessarily indicate that the gas is located within the cage cavities. ^{1}H NMR spectroscopy can be used to demonstrate the liquids have permanent porosity. Methane uptake can be quantitatively measured using ^{1}H NMR and a calibrated capillary, and it has previously been reported that the methane peak shifts when shielded by the cage. A shift in the methane peak was observed for all porous liquids in this family but by varying amounts, showing that there is a solvent effect as the cage species remained the same. Solvent 5 was found to dissolve more methane than the other solvents, and **3^3:13^3**$_{PCP}$ had the largest peak shift. This porous liquid also had the highest methane concentration, indicating there is a correlation between the solubility of the guest in the solvent and in the resulting porous liquid.

General procedure for measuring methane uptake: Scrambled **3^3:13^3** cage (200 mg), desolvated in vacuum oven at 90 °C before use in a porous liquid, was dissolved in each solvent (1 mL) by vortexing. Methane was added to the new porous liquids at ~50-60 mL min^{-1} for 10 mins per 1 mL of solvent used. ^{1}H NMR spectra were recorded of the porous liquids using a calibrated TMS/CD_2Cl_2 capillary. The integration of the methane peak was compared to that of the NC*H* stretch for the scrambled cage, and the overall cage concentration was determined by comparing the integration to the TMS peak at 0.00 ppm.

Calibration of d_2-DCM/TMS sealed capillaries:

The same calibrated capillary (2) was used in this work as used previously by Greenaway *et al.* which was calibrated using **3^3:13^3** in perchloropropene (Fig. S68)[7]

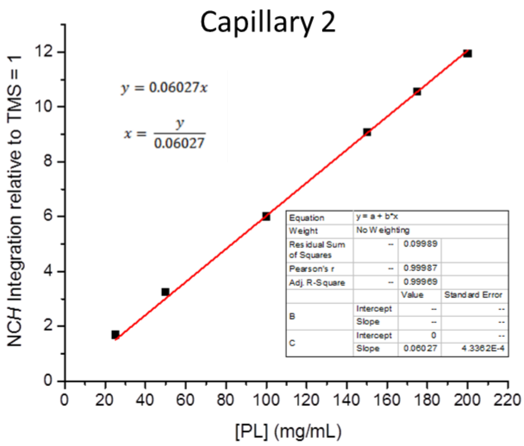

Equation	y = a + b*x		
Weight	No Weighting		
Residual Sum of Squares	--	0.09989	
Pearson's r	--	0.99987	
Adj. R-Square	--	0.99969	
		Value	Standard Error
B	Intercept	--	--
	Slope	--	--
C	Intercept	0	--
	Slope	0.06027	4.3362E-4

Porous Liquid Concentration (mg mL^{-1})	NCH Integration (12H, 3.819-2.682 ppm) relative to TMS = 1 (12H, 0.016 to -0.016 ppm)
25	1.69
50	3.24
100	6.01
150	9.08
175	10.56
200	11.94

Fig. S68: Calibration curve generated by Greenaway *et al.* for the sealed TMS/CD_2Cl_2 capillary by plotting the NC*H* integration, relative to TMS = 1, against the porous liquid concentration[7]

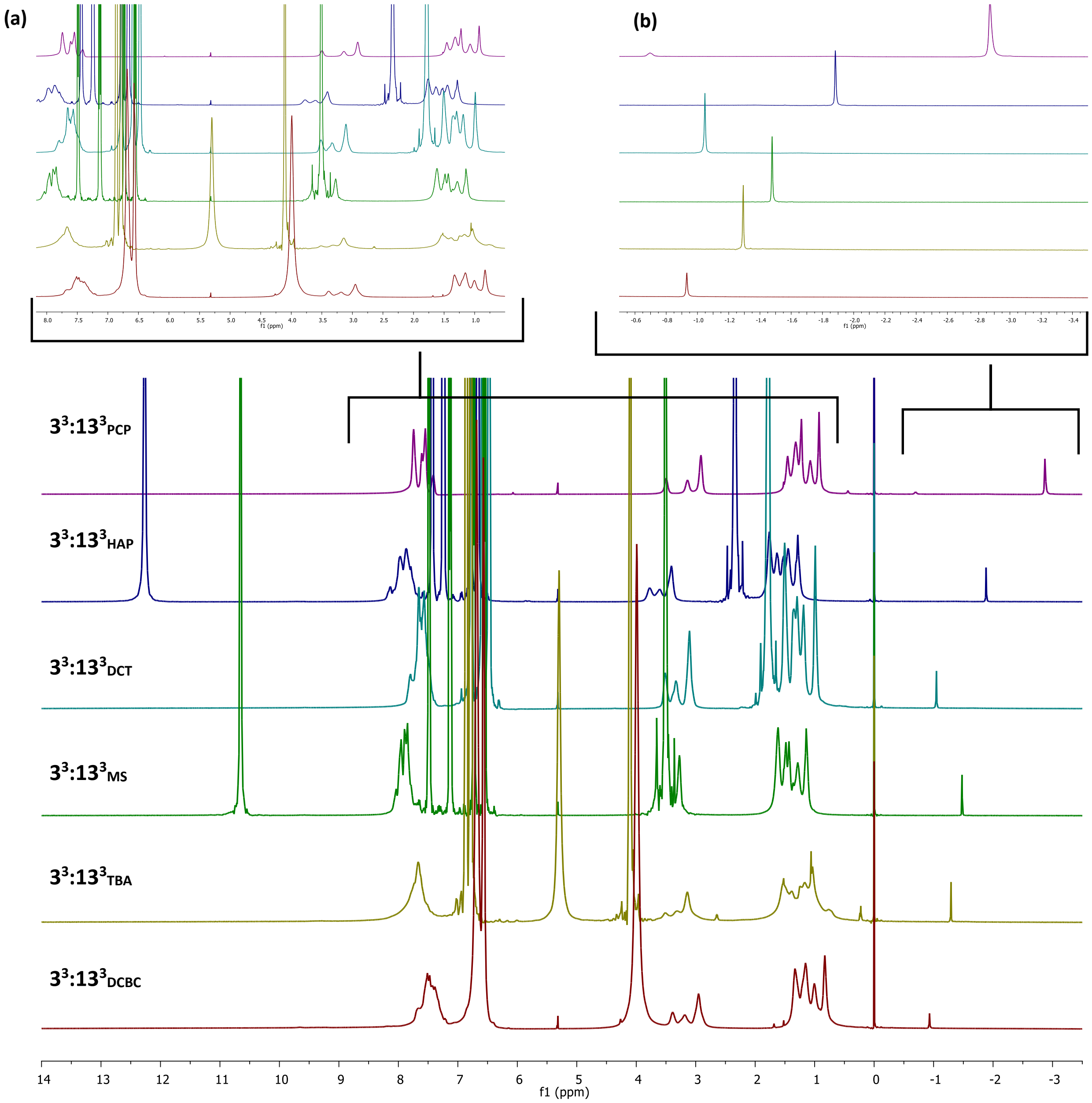

Fig. S69:^{1}H NMR spectra (CD_2Cl_2/TMS capillary) of **3^3:13^3**$_{PCP}$, **3^3:13^3**$_{HAP}$, **3^3:13^3**$_{DCT}$, **3^3:13^3**$_{MS}$, **3^3:13^3**$_{TBA}$, and **3^3:13^3**$_{DCBC}$ at 20% w/v (top to bottom), with an expansion of: (a) the peaks associated with the scrambled cage; (b) the methane chemical shift in each porous liquid.

Table S26: Methane uptake in scrambled **3^3:13^3** porous liquids at 20% w/v

Porous Liquid	NC*H* integration relative to TMS = 1	NC*H* integration range (ppm)	Calculated [PL] concentration from calibration curve (mg$_{cage}$ mL^{-1})	Calculated [PL] concentration (mmol$_{cage}$ mL^{-1}) using average MW = 1039.43	Value cage NC*H* integration set to:	CH$_4$ integration relative to cage (4H)	CH$_4$ shift (ppm)	CH$_4$ integration range (ppm)	Cage: CH$_4$ Ratio (based on integrations)	Calculated CH$_4$ uptake (µmol mL^{-1})
3^3:13^3_{DCBC}	11.90	3.50 to 2.60	197.4	0.190	12	0.30	-0.93	-0.90 to -0.96	1:0.075	14.2
3^3:13^3_{TBA}	8.59	3.61 to 2.80	142.5	0.137	12	0.55	-1.29	-1.27 to -1.31	1:0.138	18.9
3^3:13^3_{MS}[a]	9.87[a]	8.16 to 7.74	163.8	0.158	24[a]	0.52	-1.48	-1.46 to -1.50	1:0.130	20.5
3^3:13^3_{DCT}	10.73	3.64 to 2.94	178.0	0.171	12	0.41	-1.05	-1.02 to -1.07	1:0.103	17.6
3^3:13^3_{HAP}	9.13	3.92 to 3.28	151.5	0.146	12	0.70	-1.88	-1.86 to -1.91	1:0.175	25.5
3^3:13^3_{PCP}	10.45	3.67 to 2.70	173.4	0.167	12	1.96	-2.87	-2.83 to -2.96	1:0.490	81.7

[a] Typically, the cage concentration in the porous liquid is calculated using the calibration curve by comparing the NC*H* integration, equating to 12H, to TMS = 1. However, the solvent peaks overlapped with the NC*H* peaks in the **3^3:13^3_{MS}** porous liquid, which meant they could not be used to calculate the relative uptake in this system. In this case, the aromatic and imine protons in the cage were used which have an integration of 24. Therefore, the integration (Ar*H* + N=C*H* = 19.74, relative to TMS = 1) was halved to account for this before the concentration of the porous liquid was calculated. TMS was integrated between 0.01 to -0.01 for all spectra.

The methane uptake in the parent solvent can then be calculated by using the same calibrated capillary (Table S28).

Table S27: Calculation of the CH$_4$ uptake in each parent solvent

	Cage: CH$_4$ ratio based on integrations		Conversion to mmol mL^{-1}		CH$_4$ integration range	Average CH$_4$ uptake from ^{1}H NMR (mmol mL^{-1})	Average CH$_4$ integration (4H) relative to TMS =1	Average calculated CH$_4$ uptake using integration ratios (mmol mL^{-1})	CH$_4$ uptake (µmol mL^{-1})
	Cage	CH$_4$	Cage	CH$_4$					
3^3:13^3_{DCBC}	1	0.075	0.190	0.0142	-0.90 to -0.96	0.0142	0.30	0.0142	14.2
DCBC	-	-	-	-	-0.34 to -0.35	-	0.06	0.00284	2.8
3^3:13^3_{TBA}	1	0.138	0.137	0.0189	-1.27 to -1.31	0.0189	0.55	0.0189	18.9
TBA	-	-	-	-	-0.12 to -0.13	-	0.12	0.00582	4.1
3^3:13^3_{MS}	1	0.130	0.158	0.0205	-1.46 to -1.50	0.0205	0.52	0.0205	20.5
MS	-	-	-	-	-0.02 to -0.02	-	0.19	0.00927	7.5
3^3:13^3_{DCT}	1	0.103	0.171	0.0176	-1.02 to -1.07	0.0176	0.41	0.0176	17.6
DCT	-	-	-	-	-1.02 to -1.07	-	0.13	0.00618	5.6
3^3:13^3_{HAP}	1	0.175	0.146	0.0255	-1.86 to -1.91	0.0255	0.70	0.0255	25.5
HAP	-	-	-	-	0.13 to 0.11	-	0.15	0.00736	5.5
3^3:13^3_{PCP}	1	0.490	0.167	0.0817	-2.83 to -2.96	0.0817	1.96	0.0817	81.7
PCP	-	-	-	-	-0.23 to -0.26	-	0.17	0.00817	7.1

Table S28: Comparison of the data for CH_4 uptake in the scrambled **3^3:13^3** family of porous liquids at 20% w/v

	3^3:13^3_{DCBC}	**3^3:13^3_{TBA}**	**3^3:13^3_{MS}**	**3^3:13^3_{DCT}**	**3^3:13^3_{HAP}**	**3^3:13^3_{PCP}**
CH_4 uptake in solvent (μmol mL^{-1})	2.8	4.1	7.5	5.6	5.5	7.1
CH_4 uptake in 20% w/v PL (μmol mL^{-1})	14.2	18.9	20.5	17.6	25.5	81.7
CH_4 peak in neat solvent (ppm)	-0.34	-0.12	-0.02	-0.15	0.12	-0.24
CH_4 peak in PL at 20% w/v (ppm)	-0.93	-1.29	-1.48	-1.05	-1.88	-2.87
Change in peak shift (ppm)	0.59	1.17	1.46	0.90	2.00	2.63

Conversion to μmol g_{PL}^{-1}: The methane uptakes calculated from the NMR studies can also be converted from μmol mL^{-1} to μmol g^{-1} (Table S30 and S31).

$$\frac{\mu mol}{g_{Pl}} = \frac{\mu mol/ml}{\rho\ (g/ml)}$$

Example for 20% w/v 3^3:13^3_{DCBC}:

$$\frac{14.2\ \mu mol/mol}{1.3099\ g/mL} = 10.9\ \mu mol/g_{Pl}$$

Table S29: Summary of the methane uptakes in the neat parent solvents (μmol mL_{sol}^{-1} and μmol g_{sol}^{-1})

Solvent	Density (g mL^{-1})	CH_4 uptake (μmol_{sol} mL^{-1})	CH_4 uptake (μmol g_{sol}^{-1})
DCBC	1.3438	2.8	2.1
TBA	1.2457	5.1	4.1
MS	1.1552	7.5	6.5
DCT	1.1692	5.6	4.8
HAP	1.0856	5.5	5.0
PCP	1.7650	7.1	4.0

Table S30: Summary of the methane uptakes for the scrambled **3^3:13^3** porous liquids at 20% w/v (μmol mL_{PL}^{-1} and μmol g_{PL}^{-1})

Porous liquid	Density (g mL^{-1})	CH_4 uptake (μmol mL_{PL}^{-1})	CH_4 uptake (μmol g_{PL}^{-1})
3^3:13^3_{DCBC}	1.3099	14.2	10.9
3^3:13^3_{TBA}	1.2648	18.9	14.9
3^3:13^3_{MS}	1.1238	20.5	18.2
3^3:13^3_{DCT}	1.1872	17.6	14.8
3^3:13^3_{HAP}	1.0240	25.5	24.9
3^3:13^3_{PCP}	1.6073[6]	81.7	50.9

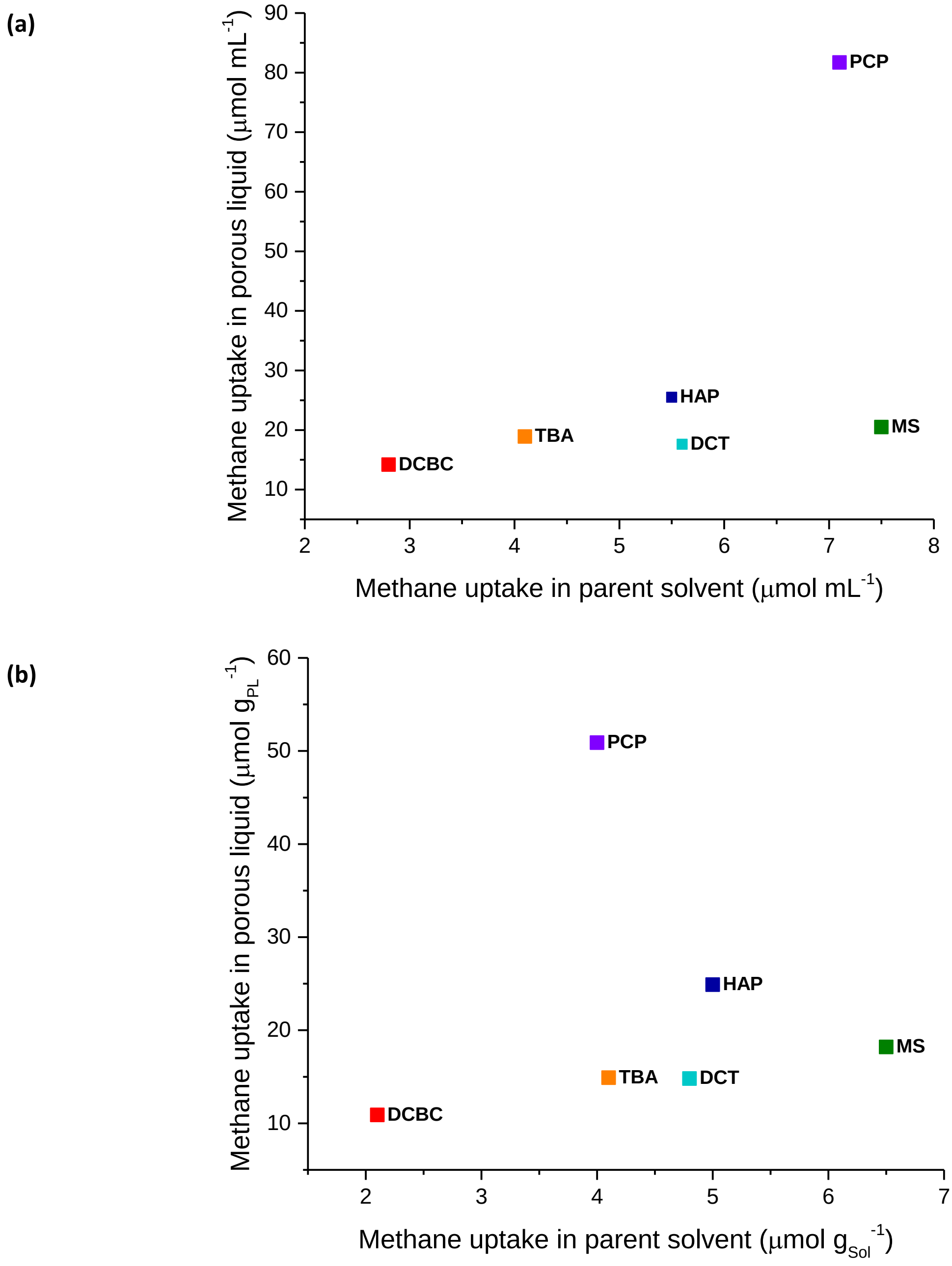

Fig. S70: Graphical representation of the relationship between (a) the methane uptake (μmol mL^{-1}) in the neat solvent and the corresponding porous liquid at 20% w/v, and (b) the methane uptake (μmol g^{-1}) in the neat solvent and the corresponding porous liquid at 20% w/v.

6.4.4. Summary of gas uptakes for 3^3:13^3 porous liquid family at 20% w/v using a range of size-excluded solvents

Table S31: Summary of the measured methane and xenon uptakes (µmol mL^{-1}) for the solvents used in the high-throughput screen, and the corresponding porous liquids using the scrambled **3^3:13^3** cage at 20% w/v (200 mg of cage in 1 mL of solvent)

Porous liquid	**Methane uptake (µmol mL^{-1})**		**Xenon uptake (µmol mL^{-1})**	
	Porous liquid	**Solvent**	**Porous liquid**	**Solvent**
3^3:13^3_{DCBC}	14.1	2.8	47.6	16.7
3^3:13^3_{TBA}	18.9	5.1	105.5	12.5
3^3:13^3_{MS}	20.5	7.5	77.6	12.5
3^3:13^3_{DCT}	17.6	5.6	70.4	24.9
3^3:13^3_{HAP}	25.5	5.5	101.0	8.4
3^3:13^3_{PCP}	81.7	7.1	155.0	8.4

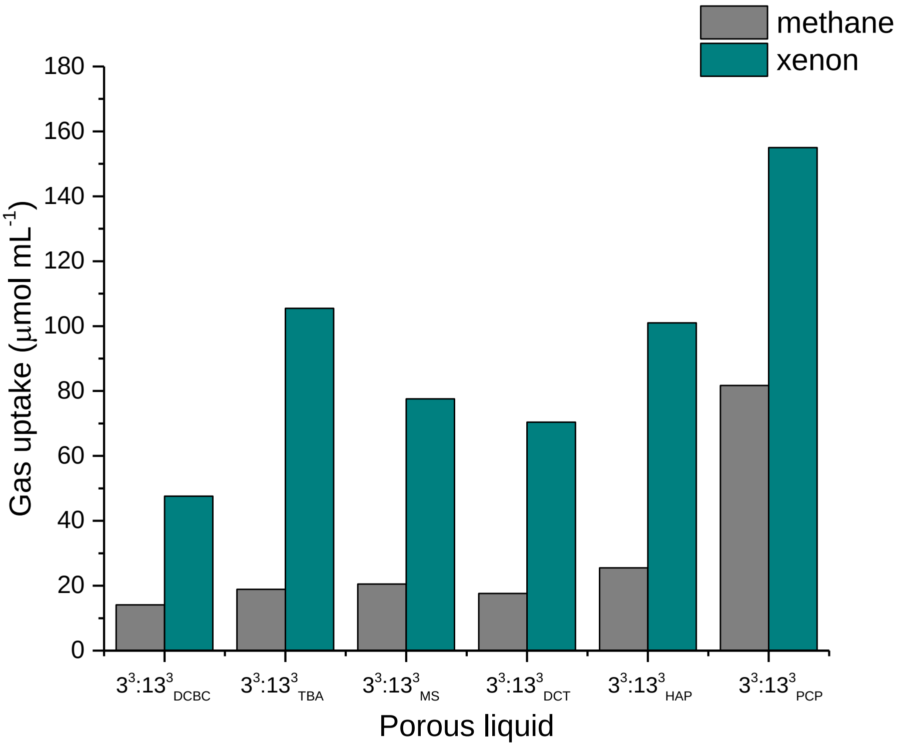

Fig. S71: Comparison of the methane and xenon uptakes in the scrambled **3^3:13^3** porous liquids at 20% w/v using the solvents from the high-throughput screen

6.5. Effect of changing the cage in the porous liquid

Table S32: New naming system for the porous liquids found in the high-throughput screen and investigated further to study the effect of changing the porous liquid cage component.

High-throughput Reference	Scrambled cage	Solvent	Porous liquid name	Xenon evolution (mL)
F15	$\mathbf{A^3:G^3}$	3	$\mathbf{A^3:G^3_{MS}}$	1.2
F16	$\mathbf{A^2:G^4}$	3	$\mathbf{A^2:G^4_{MS}}$	2.8
F17	$\mathbf{A^1:G^5}$	3	$\mathbf{A^1:G^5_{MS}}$	1.9
G25	$\mathbf{A^5:H^1}$	5	$\mathbf{A^5:H^1_{HAP}}$	2.1
H26	$\mathbf{A^4:I^2}$	5	$\mathbf{A^4:I^2_{HAP}}$	2.2

6.5.1. Porous Liquid Properties

Calculation of the cage to solvent ratio and wt% ratio in the different porous liquids: using the measured density of each purified solvent, the cage to solvent ratio and the wt% ratio for the corresponding porous liquids at 20% w/v (200 mg of cage in 1 mL of solvent), can be calculated and compared.

$$wt\ \% = \frac{M_{cage}}{(M_{cage} + M_{solvent})} \times 100$$

Table S34: Summary of properties for scrambled porous liquids containing cages with varying diamine ratios or chain lengths

Porous liquid	Mass of cage (g)	Mass of solvent (g)	Mmol cage	Mmol solvent	Cage: solvent	Wt%
$\mathbf{A^{3}{:}G^{3}_{MS}}$	0.2	1.1238	0.177	7.716	1:44	15
$\mathbf{A^{2}{:}G^{4}_{MS}}$	0.2	1.1238	0.169	7.716	1:46	15
$\mathbf{A^{1}{:}G^{5}_{MS}}$	0.2	1.1238	0.161	7.716	1:48	15
$\mathbf{A^{5}{:}H^{1}_{HAP}}$	0.2	1.0240	0.197	8.307	1:42	16
$\mathbf{A^{4}{:}I^{2}_{HAP}}$	0.2	1.0240	0.169	8.307	1:49	16

6.5.2. Xenon uptake studies by gas displacement

Table S35: Volume of xenon evolved from the different scrambled porous liquids containing different cage components at 20% w/v by chemical displacement with chloroform.

Porous liquid	Xenon evolution (mL)	Xenon evolution (µmol)
$\mathbf{3^{3}{:}13^{3}_{MS}}$	2.3	95.7
$\mathbf{3^{3}{:}13^{3}_{HAP}}$	3.1	129.0
$\mathbf{3^{3}{:}13^{3}_{PCP}}$	4.4	183.0
$\mathbf{A^{3}{:}G^{3}_{MS}}$	1.2	50.0
$\mathbf{A^{2}{:}G^{4}_{MS}}$	2.8	116.5
$\mathbf{A^{1}{:}G^{5}_{MS}}$	1.9	79.0
$\mathbf{A^{5}{:}H^{1}_{HAP}}$	2.1	87.3
$\mathbf{A^{4}{:}I^{2}_{HAP}}$	2.2	91.5

6.5.3. Methane uptake studies by ^{1}H NMR spectroscopy

Table S33: Methane uptake (µmol mL^{-1}) for scrambled porous liquids containing different scrambled cages at 20% w/v

Porous Liquid	NC*H* integration relative to TMS = 1	NC*H* integration range (ppm)	Calculated [PL] concentration from calibration curve (mg$_{cage}$ mL^{-1})	Calculated [PL] concentration (mmol$_{cage}$ mL^{-1}) using average MW	Value cage NC*H* integration set to	CH_4 integration relative to cage (4H)	CH_4 shift (ppm)	CH_4 integration range (ppm)	Cage: CH_4 Ratio (based on integrations)	Calculated CH_4 uptake (µmol mL^{-1})
A^3:G$^3_{MS}$[a]	8.46	8.33 to 7.59	140.4	0.249	24[a]	0.60	-0.91	-0.90 to -0.95	1:0.15	20.6
A^2:G$^4_{MS}$[a]	7.77	8.22 to 7.58	128.8	0.217	24[a]	0.76	-0.84	-0.80 to-0.90	1:0.19	18.6
A^1:G$^5_{MS}$[a]	6.74	8.19 to 7.58	111.7	0.179	24[a]	0.84	-1.54	-1.51 to -1.58	1:0.21	18.9
A^5:H$^1_{HAP}$	10.01	4.10 to 3.28	166.1	0.163	12	0.57	-1.10	-1.06 to -1.14	1:0.14	23.3
A^4:I$^2_{HAP}$	6.09	4.10 to 3.20	101.0	0.085	12	0.89	-1.17	-1.107 to -1.123	1:0.22	19.0

[a] Typically, the cage concentration in the porous liquid is calculated using the calibration curve by comparing the NC*H* integration, equating to 12H, to TMS = 1. However, the solvent peaks overlapped with the NC*H* peaks in the **MS** based porous liquids, which meant they could not be used to calculate the relative uptake in this system. In this case, the aromatic and imine protons in the cage were used which have an integration of 24. Therefore, the integration (Ar*H* + N=C*H* = 19.74, relative to TMS = 1) was halved to account for this before the concentration of the porous liquid was calculated. TMS was integrated between 0.01 to -0.01 for all spectra.

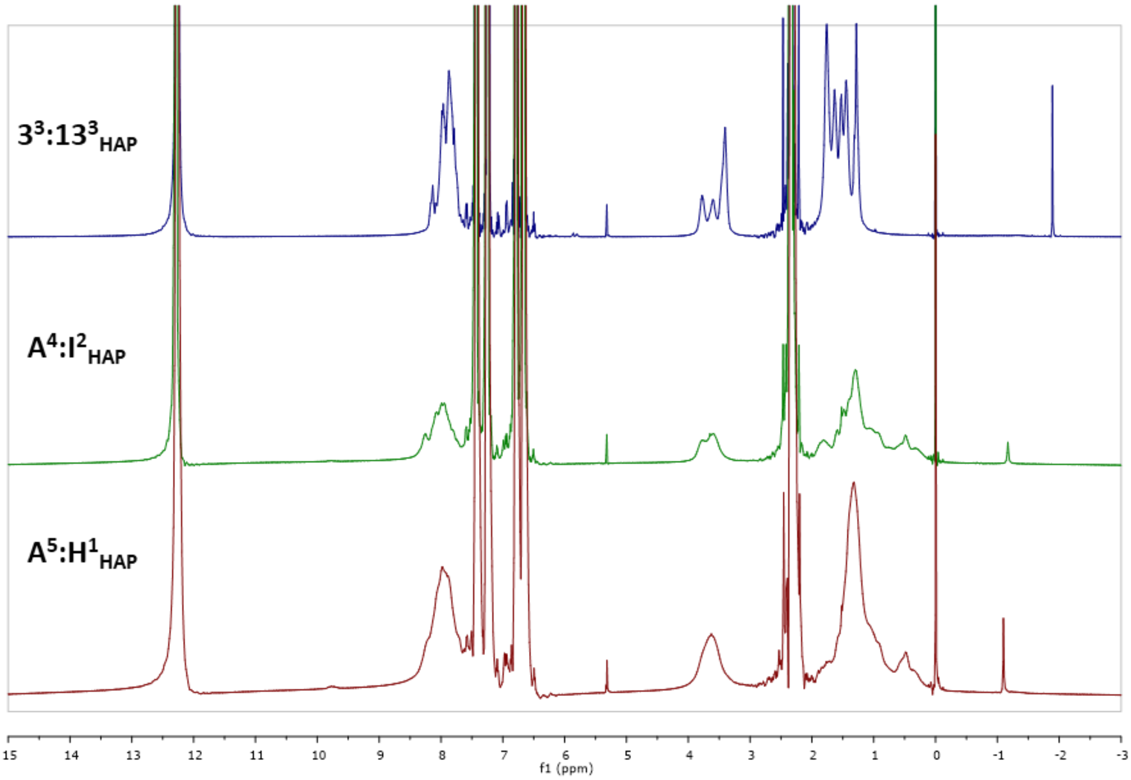

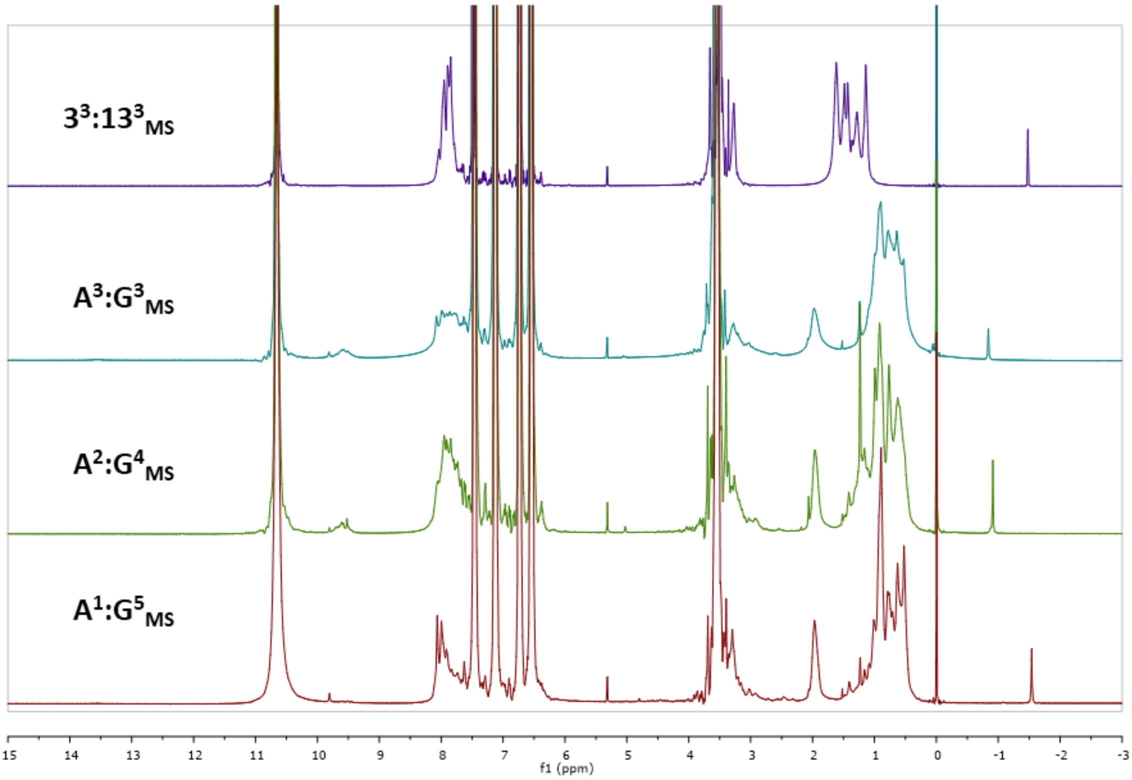

Fig. S72: Stacked ^{1}H NMR spectra (CD_2Cl_2/TMS capillary) for porous liquids with the same solvent, HAP (upper) and MS (lower), but scrambled cages with varying diamine chain length (upper) or diamine feed ratio (lower) .

6.5.4. Summary of gas uptakes for porous liquids containing different scrambled cages

Table S34: Comparison of the data for methane uptake in the scrambled porous liquids containing different scrambled cages at 20% w/v

	A^3:G^3_{MS}	A^2:G^4_{MS}	A^1:G^5_{MS}	A^5:H^1_{HAP}	A^4:I^2_{HAP}
CH_4 uptake in solvent (μmol mL^{-1})	7.5	7.5	7.5	5.1	5.1
CH_4 uptake in 20% w/v PL (μmol mL^{-1})	20.6	18.6	18.9	23.3	19.0
CH_4 peak in neat solvent (ppm)	-0.02	-0.02	-0.02	0.12	0.12
CH_4 peak in PL at 20% w/v (ppm)	-0.91	-0.84	-1.54	-1.10	-1.17
Change in peak shift (ppm)	0.89	0.82	1.52	1.22	1.29

6.6. Effect of changing the porous liquid concentration

6.6.1. Porous liquid properties

The $\mathbf{3^3{:}13^3_{HAP}}$ and $\mathbf{3^3{:}13^3_{TBA}}$ porous liquid families were studied at different concentrations to determine the effect on gas uptake and other scrambled porous liquid properties.

Porous liquid sample preparation: Scrambled $\mathbf{3^3{:}13^3}$ cage (200 to 600 mg) was dried in a vacuum oven overnight at 90 °C before being dissolved in purified 2-hydroxyacetophenone or 4-(trifluoromethoxy)benzyl alcohol (1 mL) using prolonged stirring and sonication.

Density measurements of $\mathbf{3^3{:}13^3_{HAP}}$ and $\mathbf{3^3{:}13^3_{TBA}}$ at varying concentrations: Scrambled $\mathbf{3^3{:}13^3}$ cage (200 to 600 mg) was dissolved in each solvent (1 mL), before a sample of each porous liquid was added to a pre-weighed 1 mL volumetric flask. The volumetric flask was then re-weighed and the density of the porous liquid calculated. The procedure was repeated three times to calculate the average density and standard deviation.

Table S35: Average densities calculated for the $\mathbf{3^3{:}13^3_{HAP}}$ porous liquid family at different concentrations

Concentration (% w/v)	Sample 1	Sample 2	Sample 3	Average density (g mL^{-1})	Standard deviation (± g mL^{-1})
	Mass (g)	Mass (g)	Mass (g)		
20	1.0294	1.0226	1.0201	1.0240	0.0048
30	1.0826	1.0851	1.0846	1.0841	0.0013
40	1.0915	1.0986	1.0954	1.0952	0.0036
60	1.1007	1.1052	1.1036	1.1032	0.0023

Table S36: Average densities calculated for the $\mathbf{3^3{:}13^3_{TBA}}$ porous liquid family at different concentrations

Concentration (% w/v)	Sample 1	Sample 2	Sample 3	Average density (g mL^{-1})	Standard deviation (± g mL^{-1})
	Mass (g)	Mass (g)	Mass (g)		
20	1.2656	1.2675	1.2612	1.2648	0.00323
40	1.2585	-	-	1.2585	-

Calculating wt% and cage:solvent ratios:

Table S37: The range of concentrations of scrambled **3^3:13^3_{HAP}** porous liquids studied

Concentration (% w/v)	Mass of cage (g)	Mass of solvent (g)	wt%
20	0.2	1.0240	16
30	0.3	1.0841	22
40	0.4	1.0952	27
60	0.6	1.1032	35

Table S41: Summary of component amounts in **3^3:13^3_{HAP}** at various concentrations and the calculated cage to solvent ratio

Concentration (wt %)	Mmol solvent	Mmol cage	Cage: Solvent
8	0.0962	8.307	1:86
16	0.192	8.307	1:43
22	0.289	8.307	1:29
27	0.385	8.307	1:22

Table S42: The range of concentrations of scrambled **3^3:13^3_{TBA}** porous liquids studied

Concentration (% w/v)	Mass of cage (g)	Mass of solvent (g)	wt%
20	0.2	1.2648	14
40	0.4	1.2585	24

Viscosity measurements of 3^3:13^3_{HAP} and 3^3:13^3_{TBA} at varying concentrations: Scrambled cage (200 to 600 mg) was dissolved in bulky solvent (1 mL) and the viscosity of the sample measured using RheoSense µVISC viscometer (using either 0.01–100 or 10-2000 cP chip) with the temperature set at 25 °C. The procedure was repeated three times to calculate the average viscosity and standard deviation.

Table S43: Average viscosity for scrambled **3^3:13^3** porous liquids in HAP and TBA at various concentrations

Sample	Measurement 1 (cP)	Measurement 2 (cP)	Measurement 3 (cP)	Average (cP)	Average temperature (°C)
3^3:13^3_{HAP} @8 wt %	4.772	4.771	4.761	4.77 ± 0.0061	25.01
3^3:13^3_{HAP} @16 wt %	9.800	9.825	9.826	9.82 ± 0.015	25.03
3^3:13^3_{HAP} @22 wt %	26.88	26.81	26.88	26.86 ± 0.040	25.01
3^3:13^3_{HAP} @27 wt %	62.54	62.73	62.65	62.64 ± 0.095	24.97
3^3:13^3_{TBA} @14 wt %	31.93	32.48	32.98	32.46 ± 0.53	25.02
3^3:13^3_{TBA} @24 wt %	296.2	298.2	299.8	298.07 ± 1.8	25.07

6.6.2. Xenon uptake studies by gas displacement

The porous liquids with the highest xenon evolution from the high-throughput porosity screen were also tested at higher concentrations to see if increasing concentration also increased gas uptake. Samples of $\mathbf{3^3{:}13^3_{HAP}}$ at 16, 22, 27 and 35 wt%, and $\mathbf{3^3{:}13^3_{TBA}}$ at 14 and 24 wt%, were prepared and xenon gas was then added to each porous liquid by bubbling the gas through the sample at ~50-60 mL min^{-1} (60-66 on Gilmont flowmeter scale with a stainless steel float) for 10 mins per 1 mL of solvent used. Chloroform (1.0 eq. relative to cage) was then added to evolve the xenon and the displacement of water was measured in an inverted burette over 30 minutes. $\mathbf{3^3{:}13^{13}_{HAP}}$ was found to evolve double the volume of gas after doubling the concentration, but this was not the case for $\mathbf{3^3{:}13^3_{TBA}}$

Table S44: Volume of chloroform required to displace xenon from $\mathbf{3^3{:}13^3_{HAP}}$ at different concentrations (1.0 equiv. relative to cage)

Cage Present (mg)	Volume of chloroform (µg)
200	16
300	23
400	32
600	46

Table S45: Xenon uptake (mL and µmol) for scrambled $\mathbf{3^3{:}13^3_{HAP}}$ and $\mathbf{3^3{:}13^3_{TBA}}$ porous liquids at various concentrations

Porous Liquid	Conc. (wt%)	Expected volume (mL)	Volume of Xenon (mL)		Average ± SD (mL)	Volume of Xenon (µmol)		Average ± SD (µmol)
			Sample 1	Sample 2		Sample 1	Sample 2	
$\mathbf{3^3{:}13^3_{HAP}}$	16	4.6	3.2	2.9	3.1 ± 0.2	133.1	120.6	126.9 ± 8.8
$\mathbf{3^3{:}13^3_{HAP}}$	22	6.9	4.9	4.7	4.8 ± 0.1	203.8	195.5	199.7 ± 5.9
$\mathbf{3^3{:}13^3_{HAP}}$	27	9.2	6.6	6.1	6.4 ± 0.4	274.5	253.7	264.1 ± 14.7
$\mathbf{3^3{:}13^3_{HAP}}$	35	13.9	4.0	4.0	4.0	166.4	166.4	166.4
$\mathbf{3^3{:}13^3_{TBA}}$	14	4.6	2.8	3.0	2.9 ± 0.1	116.5	124.8	120.6 ± 5.9
$\mathbf{3^3{:}13^3_{TBA}}$	24	9.2	2.9	2.9	2.9	120.6	120.6	120.6

Table S46: Xenon uptake (µmol g_{PL}^{-1}) for scrambled $\mathbf{3^3{:}13^3_{HAP}}$ and $\mathbf{3^3{:}13^3_{TBA}}$ porous liquid at various concentrations

Porous Liquid	Concentration (wt%)	Mass of cage (g)	Mass of solvent (g)	Mass of PL (g)	Volume of Xenon (µmol g_{PL}^{-1})		Average ± SD (µmol g_{PL}^{-1})
					Sample 1	Sample 2	
$\mathbf{3^3{:}13^3_{HAP}}$	16	0.2	1.0856	1.2856	103.5	93.8	98.7 ± 6.9
$\mathbf{3^3{:}13^3_{HAP}}$	22	0.3	1.0856	1.3856	147.1	141.1	144.1 ± 4.2
$\mathbf{3^3{:}13^3_{HAP}}$	27	0.4	1.0856	1.4856	184.8	170.8	177.8 ± 9.9
$\mathbf{3^3{:}13^3_{HAP}}$	35	0.6	1.0856	1.6856	98.7	98.7	98.7
$\mathbf{3^3{:}13^3_{TBA}}$	14	0.2	1.2457	1.4457	80.6	86.3	83.4 ± 4.1
$\mathbf{3^3{:}13^3_{TBA}}$	24	0.4	1.2457	1.6457	73.3	73.3	73.3

Table S47: Xenon uptake (μmol mL_{PL}^{-1}) for scrambled **3^3:13^3_{HAP}** and **3^3:13^3_{TBA}** porous liquid at various concentrations

Porous Liquid	Concentration (wt%)	Mass of cage (g)	Density of PL (g mL^{-1})	Volume of Xenon (μmol mL_{PL}^{-1})		Average ± SD (μmol mL_{PL}^{-1})
				Sample 1	Sample 2	
3^3:13^3_{HAP}	16	0.2	1.0240	106.0	96.1	101.0 ± 7.0
3^3:13^3_{HAP}	22	0.3	1.0841	159.5	153.0	156.2 ± 4.6
3^3:13^3_{HAP}	27	0.4	1.0952	202.4	187.1	194.7 ± 10.8
3^3:13^3_{HAP}	35	0.6	1.1032	108.9	108.9	108.9
3^3:13^3_{TBA}	14	0.2	1.2648	101.9	109.2	105.5 ± 5.1
3^3:13^3_{TBA}	24	0.4	1.2585	92.2	92.2	92.2

6.6.3. Methane uptake studies by ^{1}H NMR spectroscopy

Methane saturation studies: 3^3:13^3_{HAP} was then investigated further as the xenon uptake varied with concentration. Saturation studies were carried out with methane and investigated using ^{1}H NMR spectroscopy. Methane was added to different **3^3:13^3_{HAP}** samples at different concentrations (8, 15, 21 and 26 wt%) over five minute intervals. Each porous liquid seemed to reach full saturation within five minutes, with only small fluctuations after this time (Fig. S73). For all subsequent experiments, porous liquid samples were purged with a gas for 10 min per 1 mL of solvent used to ensure saturation.

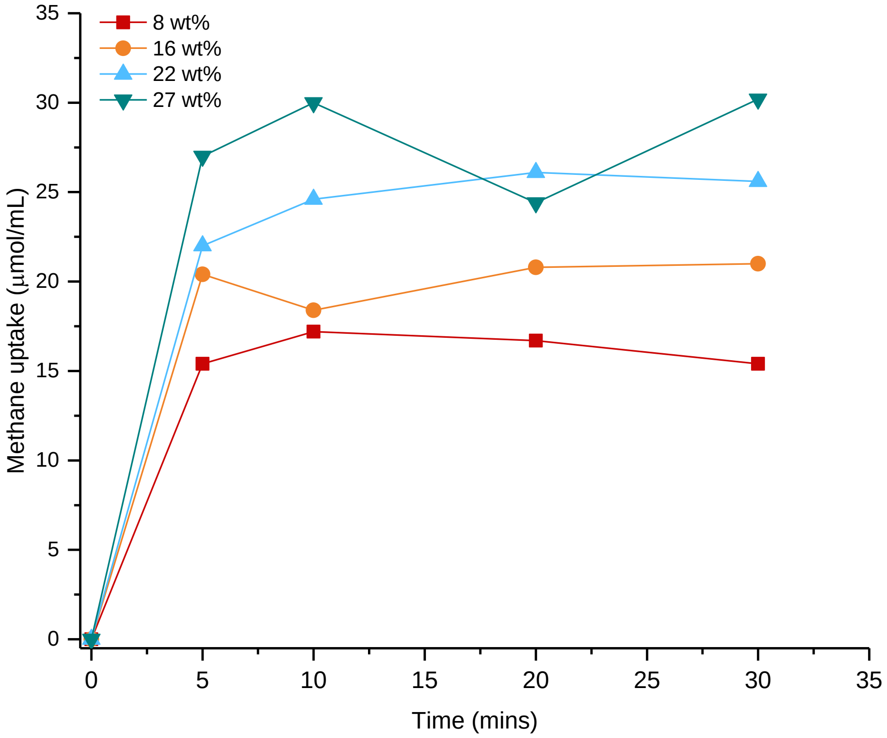

Fig. S73: The methane concentration in **3^3:13^3_{HAP}** at 8, 16, 22 and 27 wt% calculated from the ^{1}H NMR spectra after being purged at five minute intervals – all of the samples were saturated after 5 minutes.

Table S38: Methane uptake (µmol mL^{-1}) for scrambled **3^3:13^3_{HAP}** porous liquid at **8 wt%**

TMS integration: 0.10 to -0.10 ppm
NCH integration: 3.90 to 3.30 ppm

Total Methane Addition Time (min)	**NC*H* integration relative to TMS = 1**	**Calculated [PL] concentration from calibration curve (mg$_{cage}$ mL^{-1})**	**Calculated [PL] concentration (mmol$_{cage}$ mL^{-1}) using average MW = 1039.43**	**Value cage NC*H* integration set to**	**CH$_4$ integration relative to cage (4H)**	**CH$_4$ shift (ppm)**	**CH$_4$ integration range (ppm)**	**Cage: CH$_4$ Ratio (based on integrations)**	**Calculated CH$_4$ uptake (µmol mL^{-1})**
5	4.23	70.18	0.0675	12	0.91	-1.05	-1.04 to -1.07	1:0.228	15.4
10	4.90	81.30	0.0782	12	0.88	-1.09	-1.07 to -1.11	1:0.220	17.2
20	4.87	80.80	0.0777	12	0.86	-1.14	-1.12 to -1.16	1:0.215	16.7
30	4.25	70.52	0.0678	12	0.91	-1.18	-1.17 to -1.20	1:0.228	15.4

Table S39: Methane uptake (µmol mL^{-1}) for scrambled **3^3:13^3_{HAP}** porous liquid at **16 wt%**

TMS integration: 0.10 to -0.10 ppm
NCH integration: 3.90 to 3.25 ppm

Total Methane Addition Time (min)	**NC*H* integration relative to TMS = 1**	**Calculated [PL] concentration from calibration curve (mg$_{cage}$ mL^{-1})**	**Calculated [PL] concentration (mmol$_{cage}$ mL^{-1}) using average MW = 1039.43**	**Value cage NC*H* integration set to**	**CH$_4$ integration relative to cage (4H)**	**CH$_4$ shift (ppm)**	**CH$_4$ integration range (ppm)**	**Cage: CH$_4$ Ratio (based on integrations)**	**Calculated CH$_4$ uptake (µmol mL^{-1})**
5	8.36	138.71	0.133	12	0.61	-1.34	-1.32 to -1.37	1:0.153	20.4
10	8.53	141.53	0.136	12	0.54	-1.39	-1.38 to -1.42	1:0.135	18.4
20	8.54	141.70	0.136	12	0.61	-1.45	-1.43 to 1.48	1:0.153	20.8
30	8.33	138.21	0.133	12	0.63	-1.49	-1.47 to -1.52	0.158	21.0

Table S40: Methane uptake (µmol mL^{-1}) for scrambled **3^3:13^3_{HAP}** porous liquid at **22 wt%**

TMS integration: 0.10 to -0.10 ppm
NCH integration: 4.10 to 3.10 ppm

Total Methane Addition Time (min)	**NC*H* integration relative to TMS = 1**	**Calculated [PL] concentration from calibration curve (mg$_{cage}$ mL^{-1})**	**Calculated [PL] concentration (mmol$_{cage}$ mL^{-1}) using average MW = 1039.43**	**Value cage NC*H* integration set to**	**CH$_4$ integration relative to cage (4H)**	**CH$_4$ shift (ppm)**	**CH$_4$ integration range (ppm)**	**Cage: CH$_4$ Ratio (based on integrations)**	**Calculated CH$_4$ uptake (µmol mL^{-1})**
5	11.27	187.00	0.180	12	0.49	-1.62	-1.58 to -1.66	1:0.123	22.0
10	11.61	192.63	0.185	12	0.53	-1.66	-1.62 to -1.71	1:0.185	24.6
20	12.11	201.00	0.193	12	0.54	-1.71	-1.64 to -1.76	1:0.193	26.1
30	11.04	183.18	0.176	12	0.58	-1.74	-1.70 to -1.78	1:0.176	25.6

Table S41: Methane uptake (µmol mL^{-1}) for scrambled **3^3:13^3_{HAP}** porous liquid at **27 wt%**

TMS integration: 0.10 to -0.10 ppm
NCH integration: 4.12 to 3.10 ppm

Total Methane Addition Time (min)	**NC*H* integration relative to TMS = 1**	**Calculated [PL] concentration from calibration curve (mg$_{cage}$ mL^{-1})**	**Calculated [PL] concentration (mmol$_{cage}$ mL^{-1}) using average MW = 1039.43**	**Value cage NC*H* integration set to**	**CH_4 integration relative to cage (4H)**	**CH_4 shift (ppm)**	**CH_4 integration range (ppm)**	**Cage: CH_4 Ratio (based on integrations)**	**Calculated CH_4 uptake (µmol mL^{-1})**
5	13.02	216.03	0.208	12	0.52	-1.76	-1.70 to -1.83	1:0.130	27.0
10	13.56	225.0	0.216	12	0.55	-1.80	-1.75 to -1.87	1:0.138	30.0
20	11.97	198.61	0.191	12	0.51	-1.85	-1.76 to -1.95-	1:0.128	24.4
30	13.29	220.51	0.212	12	0.57	-1.88	-1.82 to -1.96	1:0.143	30.2

Methane uptake measurements for 3^3:13^3_{HAP} at different concentrations: Using the findings from the saturation study, a sample of **3^3:13^3_{HAP}** at 8, 16, 22, and 27 wt% was loaded with methane gas for 10 min per 1 mL of solvent used, and the uptake calculated using ^{1}H NMR analysis. Overall, the methane uptake increases with increasing concentration, as well as the methane peak shifting more downfield, indicating a preference for the cage cavity.

Table S42: Methane uptake (µmol mL^{-1}) for scrambled **3^3:13^3_{HAP}** porous liquid samples at increasing concentrations

TMS integration range: 0.10 to -0.10 ppm

(wt%)	**NC*H* integration relative to TMS = 1**	**Calculated [PL] concentration from calibration curve (mg$_{cage}$ mL^{-1})**	**Calculated [PL] concentration (mmol$_{cage}$ mL^{-1}) using average MW = 1039.43**	**Value cage NC*H* integration set to**	**CH_4 integration relative to cage (4H)**	**CH_4 shift (ppm)**	**CH_4 integration range (ppm)**	**Cage: CH_4 Ratio (based on integrations)**	**Calculated CH_4 uptake (µmol mL^{-1})**	**CH_4 uptake (µmol^{-1})**
8	4.96	3.90 to 3.30	82.30	0.0792	0.82	-1.46	-1.44 to -1.48	1:0.205	0.0162	16.2
16	9.12	3.90 to 3.25	151.32	0.1456	0.70	-1.88	-1.86 to -1.91	1:0.175	0.0255	25.5
22	12.33	4.10 to 3.10	204.58	0.1968	0.70	-2.10	-2.06 to -2.16	1:0.175	0.0344	34.4
27	18.15	4.12 to 3.10	301.14	0.290	0.57	-2.21	-2.18 to -2.24	1:0.143	0.0413	41.3

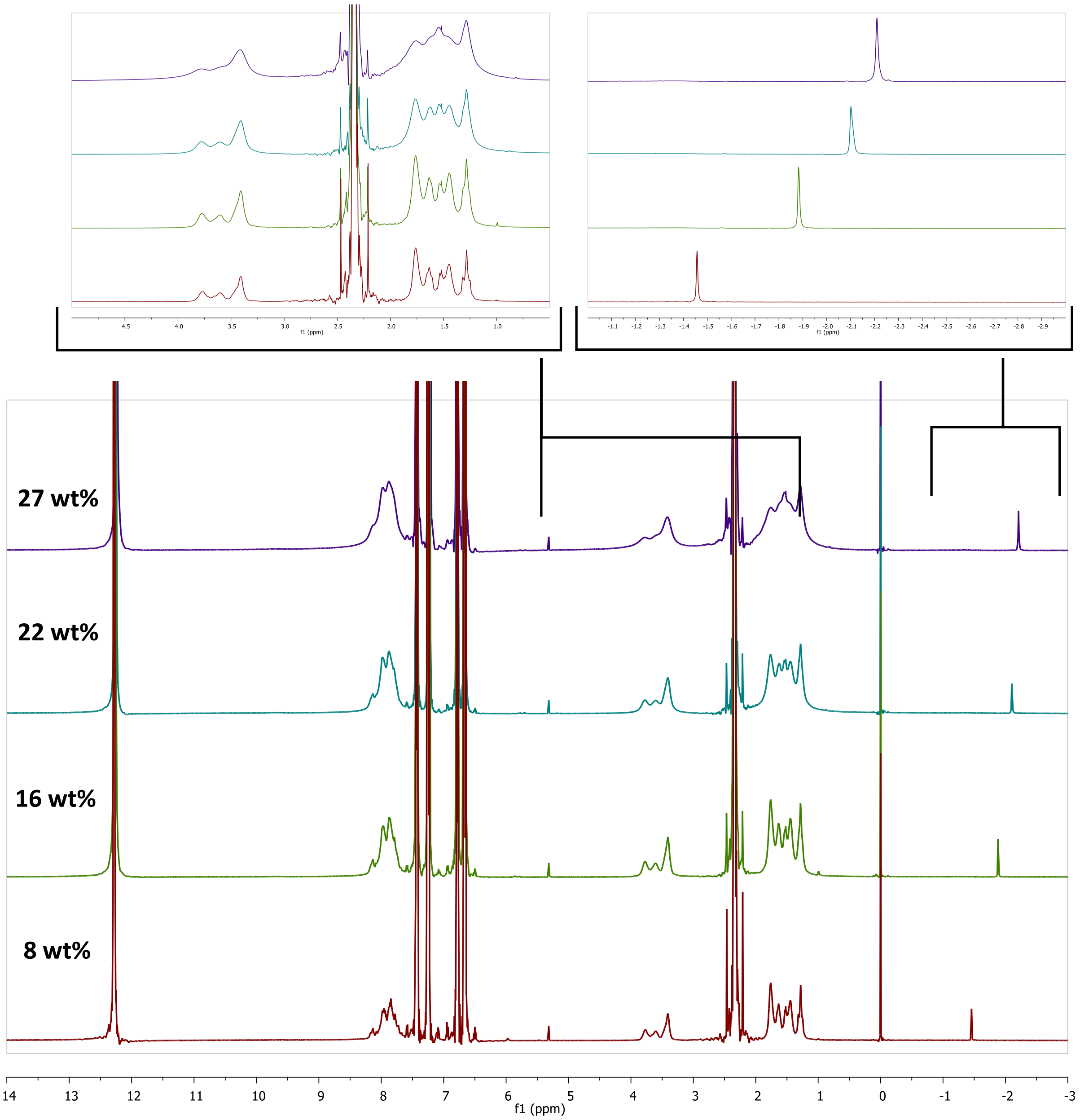

Fig. S74: Stacked ^{1}H NMR spectra for $\mathbf{3^3{:}13^3_{HAP}}$ (CD_2Cl_2/TMS capillary) at different concentrations with expansions showing the cage imine peaks (top left) used to determine the porous liquid concentration, showing broadening, and the methane chemical shifts (top right).

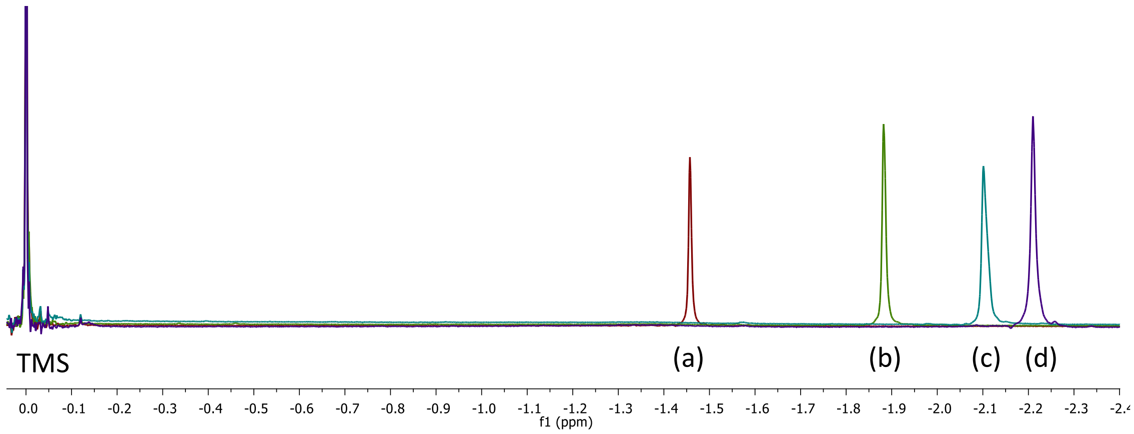

Fig. S75: Overlaid ^{1}H NMR spectra (CD_2Cl_2/TMS capillary) for different concentrations of **3^3:$13^3$$_{\mathbf{HAP}}$** loaded with methane at 8 (a), 16 (b), 22 (c) and 27 (d) wt%, showing the shift corresponding to methane relative to TMS.

Table S43: Summary of properties for **3^3:$13^3$$_{\mathbf{HAP}}$** at different concentrations

Concentration (wt %)	Methane uptake (µmol mL_{PL}^{-1})	Chemical shift (ppm)	Viscosity (cP)
8	16.2	-1.46	4.77
16	25.5	-1.88	9.82
22	34.4	-2.10	26.86
27	41.3	-2.21	62.64

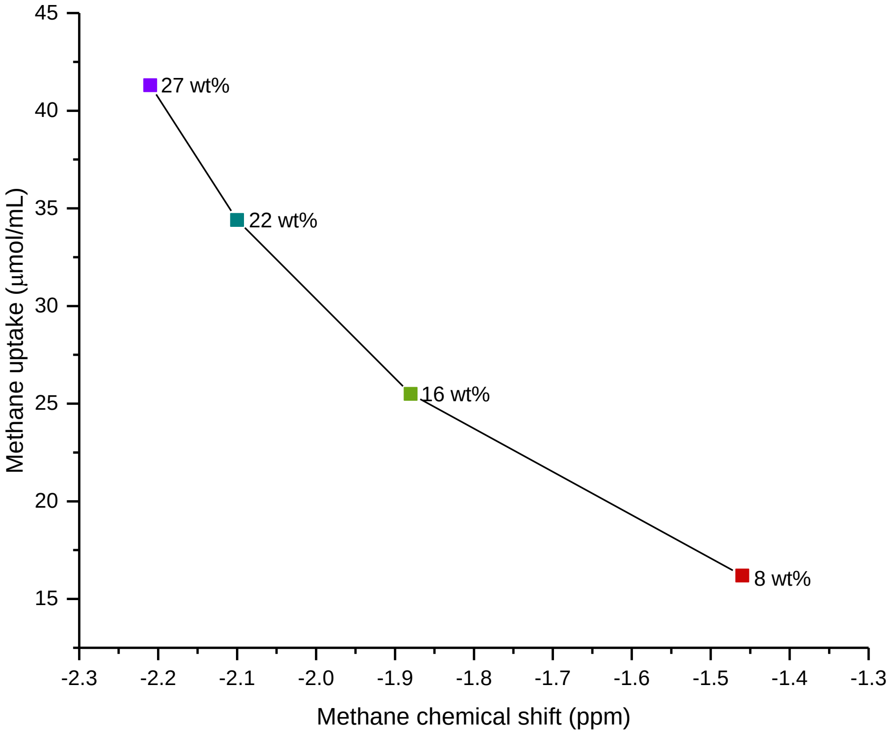

Fig. S76: Graphical representation of the relationship between the methane chemical shift in **3^3:$13^3$$_{\mathbf{HAP}}$** at various concentrations and the calculated methane uptake in the porous liquid.

6.7. Temperature release experiments

Chemical displacement of loaded gases in a porous liquid using chloroform is not a commercially practical method for gas release, and therefore other methods were investigated. Pressure swings are one method used to desorb gas from liquids, but is unsuitable for the current porous liquids due to their inherent vapour pressure. Therefore, temperature release studies were carried out on **$3^3{:}13^3_{\mathrm{HAP}}$** at various concentrations.

Table S54: Summary of the volume of chloroform or temperature needed to displace xenon in **$3^3{:}13^3_{\mathrm{HAP}}$** porous liquid at various concentrations

Concentration (wt %)	Mass of cage (mg)	Maximum volume of Xe that can be evolved* (mL)	Volume of $CHCl_3$ needed to displace Xe* (µL)	Temperature required to release Xe (°C)
16	200	4.6	16	60-70
22	300	6.9	23	60-80
27	400	9.2	32	60-80
35	600	13.9	46	80-120

*Based on a maximum 1:1 Xe: cage ratio

General procedure: Scrambled **$3^3{:}13^3$** cage (200 to 600 mg) was dissolved in 2-hydroxyacetophenone (1 mL) and purged with xenon at ~50-60 mL/min for 10 min per mL of solvent. The porous liquid was then heated slowly to the required temperature and the water displacement measured by collecting the gas released in an inverted burette.

Table S55: Summary of the xenon evolution experiments for temperature release from **$3^3{:}13^3_{\mathrm{HAP}}$** in mL

Concentration (wt%)	Mass of cage (mg)	Expected volume (mL)	Volume of xenon released (mL)			Average ± SD (mL)
			Sample 1	Sample 2	Sample 3	
16	200	4.6	2.9	3.0	-	3.0 ± 0.07
22	300	6.9	3.5	3.9	-	3.7 ± 0.28
27	400	9.2	6.0	6.0	6.4	6.1 ± 0.23
35	600	13.9	8.2	7.5	7.8	7.8 ± 0.35

Table S56: Summary of the xenon evolution experiments for temperature release from **$3^3{:}13^3_{\mathrm{HAP}}$** in µmol

Concentration (wt%)	Mass of cage (mg)	Expected volume (mL)	Volume of xenon released (µmol)			Average ± SD (µmol)
			Sample 1	Sample 2	Sample 3	
16	200	4.6	120.6	124.8	-	122.7 ± 3.00
22	300	6.9	145.6	162.2	-	153.9 ± 11.7
27	400	9.2	250.0	250.0	266.2	225.4 ± 9.35
35	600	13.9	341.1	312.0	324.4	325.8 ± 14.6

Table S57: Summary of the xenon evolution experiments for temperature release from $\mathbf{3^3{:}13^3_{HAP}}$ in µmol g_{PL}^{-1}

Concentration (wt%)	**Mass of cage (mg)**	**Expected volume (mL)**	**Volume of xenon released (µmol g_{PL}^{-1})**			**Average ± SD (µmol g_{PL}^{-1})**
			Sample 1	Sample 2	Sample 3	
16	200	4.6	93.8	97.1	-	95.5 ± 2.33
22	300	6.9	105.1	117.1	-	111.1 ± 8.49
27	400	9.2	168.0	168.0	179.2	171.7 ± 6.45
35	600	13.9	202.3	185.1	192.5	193.3 ± 8.63

Table S58*:* Summary of the xenon evolution experiments for temperature release from $\mathbf{3^3{:}13^3_{HAP}}$ in µmol mL_{PL}^{-1}

Concentration (wt%)	**Mass of cage (mg)**	**Expected volume (mL)**	**Volume of xenon released (µmol mL_{PL}^{-1})**			**Average ± SD (µmol mL_{PL}^{-1})**
			Sample 1	Sample 2	Sample 3	
16	200	4.6	96.1	99.4	-	97.8 ± 2.33
22	300	6.9	113.9	126.9	-	120.4 ± 9.19
27	400	9.2	184.0	184.0	196.3	188.1 ± 7.10
35	600	13.9	223.3	204.2	212.3	213.3 ± 9.59

With a 16 wt% (20% w/v) sample, xenon can be displaced by heating the porous liquid to 65 °C and this can be repeated on the same sample. However, after the second cycle, the porous liquid appears to decompose as there is an appearance of an aldehyde peak in the ^{1}H NMR spectra (Fig. S78).

Table S59: Volume of xenon released from the scrambled $\mathbf{3^3{:}13^3_{HAP}}$ porous liquid at a 16 wt% concentration after heating at 60-70 °C

Sample	**Xenon evolved**							
	(mL)		**(µmol)**		**(µmol g^{-1})**		**(µmol mL^{-1})**	
	Cycle 1	Cycle 2	Cycle 1	Cycle 2	Cycle 1	Cycle 2	Cycle 1	Cycle 2
1	3.0	2.6	124.8	108.1	97.1	84.1	99.4	86.1
2	2.9	2.1	120.6	87.3	93.8	67.9	96.1	70.0

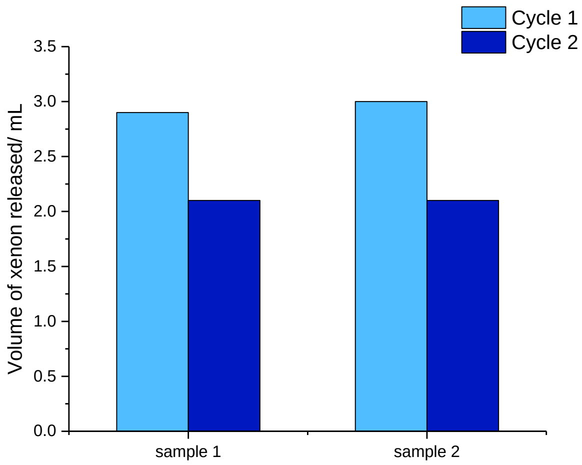

Fig. S77: Results of the temperature release experiments when heating xenon-loaded 16 wt% $\mathbf{3^3{:}13^3_{HAP}}$ porous liquid samples at 60-70 °C.

One important point of interest was the temperature required to liberate the gas from the porous liquid. Increasing the temperature increased the rate of release of xenon from the porous liquid. However, above 80 °C the liquid increased in viscosity and appeared to foam. So, although all the gas in the liquid appeared to be displaced, there was extra gas released after a certain point. This suggested that some decomposition of the porous liquid was occurring, with either the cage or solvent being affected. As identification of the gas is difficult with gas displacement experiments, the temperature was capped at 80 °C to prevent this from happening resulting in a slower rate of release.

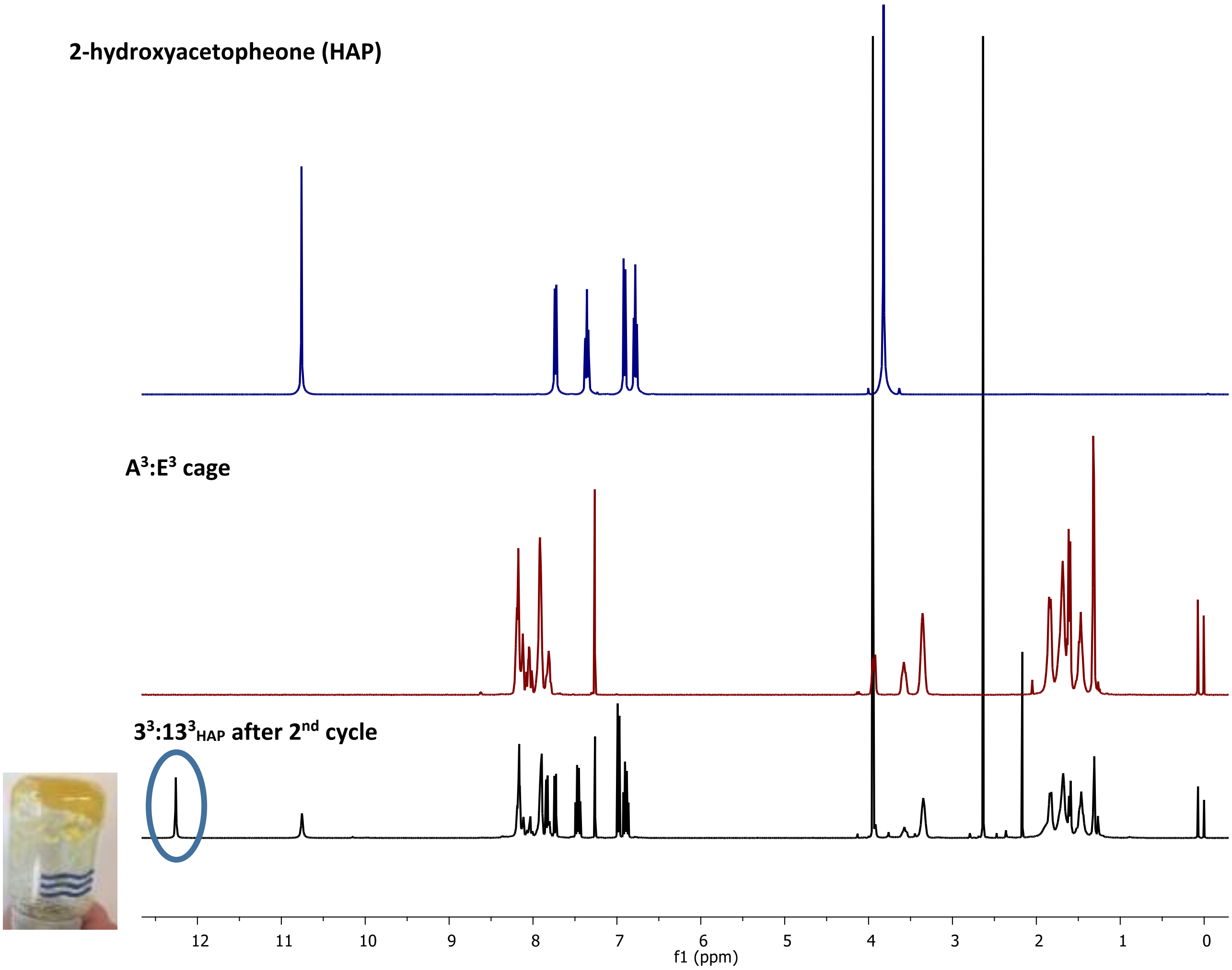

Fig. S78: Stacked ^1H NMR spectra ($CDCl_3$) of solvent 5 (top), **A^3:E^3** (middle), and 16 wt% **3^3:13^3_{HAP}** after 2 temperature release cycles, showing some decomposition (bottom)

The temperature release experiment was also repeated with xenon loaded scrambled **3^3:13^3_{HAP}** porous liquid samples at 27 wt% and 35 wt% concentrations.

General procedure: Scrambled **3^3:13^3** cage (400 mg or 600 mg) was dissolved in 2-hydroxyacetophenone (1 mL) and purged with xenon at ~50-60 mL/min for 10 min per mL of solvent. The porous liquid was then heated slowly to 60-80 °C and the water displacement measured by collecting the gas released in an inverted burette. The higher concentrations appeared to decompose after a single temperature release experiment so could not be cycled.

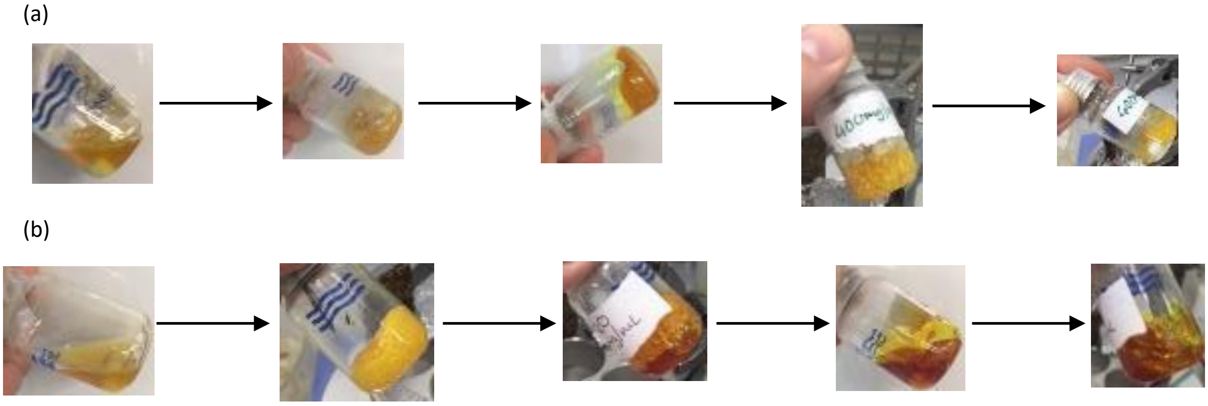

Fig. S79: The physical state of **3^3:13^3_{HAP}** at (a) 27 wt% and (b) 35 wt% when heated at 60-80 °C during guest release.

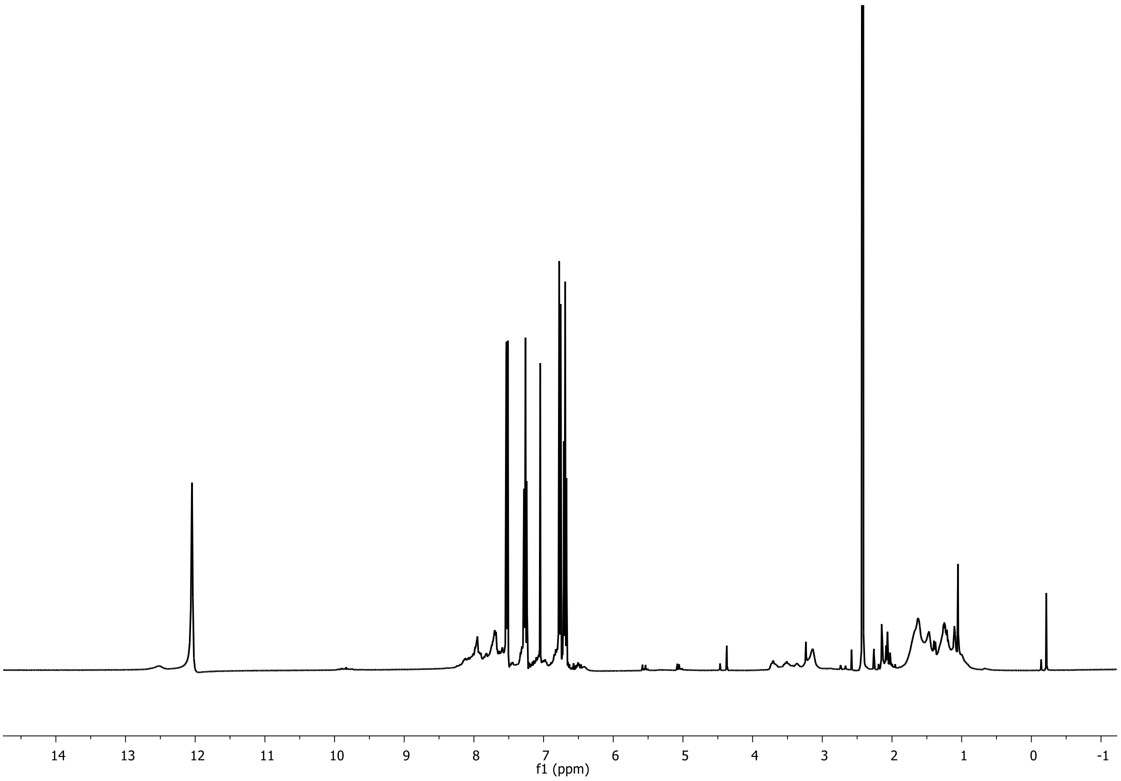

Fig. S80: ^{1}H NMR ($CDCl_3$) spectra of **3^3:13^3_{HAP}** at 35 wt% after temperature release of xenon

6.8. Sol-gel behaviour of porous liquid

General procedure: Scrambled $\mathbf{3^3{:}13^3}$ cage (400 or 600 mg) was dissolved in 2-hydroxyacetophenone (1mL) and saturated with xenon at ~50-60 mL min^{-1} for 10 min per mL of solvent. The xenon-loaded porous liquid was then cooled to between 0 and 6 °C until the solution underwent gelation. The gel was then heated at 60-85 °C for the 27 wt% sample, and 80-120 °C for the 35 wt% sample, to release the guest which was measured by water displacement in an inverted burette.

Table S60: The volume of xenon released from $\mathbf{3^3{:}13^3_{HAP}}$ at 26 and 35 wt% after setting as a gel

Concentration (wt %)	Sample 1	Sample 2	Sample 3	Sample 4	Average volume (mL)	Average volume (µmol)	Average volume (µmol g^{-1})	Average volume (µmol mL^{-1})
27	5.4	5.5	6.4	6.4	5.9 ± 0.55	245.4	165.2	180.9
35	9.2	8.8	8.7	8.3	8.8 ± 0.45	366.0	217.2	239.6

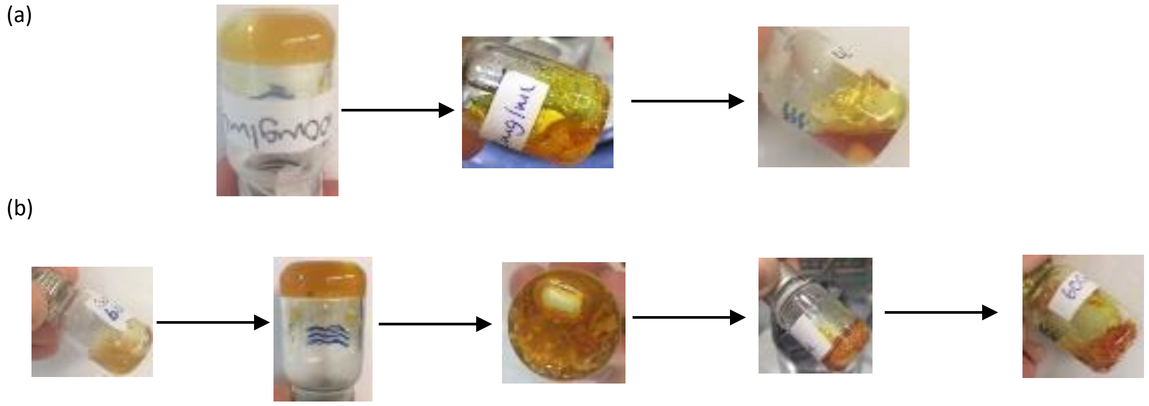

Fig. S81: The physical states of $\mathbf{3^3{:}13^3_{HAP}}$ at (a) 27 and (b) 35 wt % when the gel was heated to release the trapped guest

At 35 wt%, the gel releases trapped xenon after heating at 60-85 °C, and the liquid briefly reforms before solidifying again (Fig. S81). However, the ^{1}H NMR spectrum of the sample shows decomposition with the appearance of extra peaks between 1-5 ppm (Fig. S82).

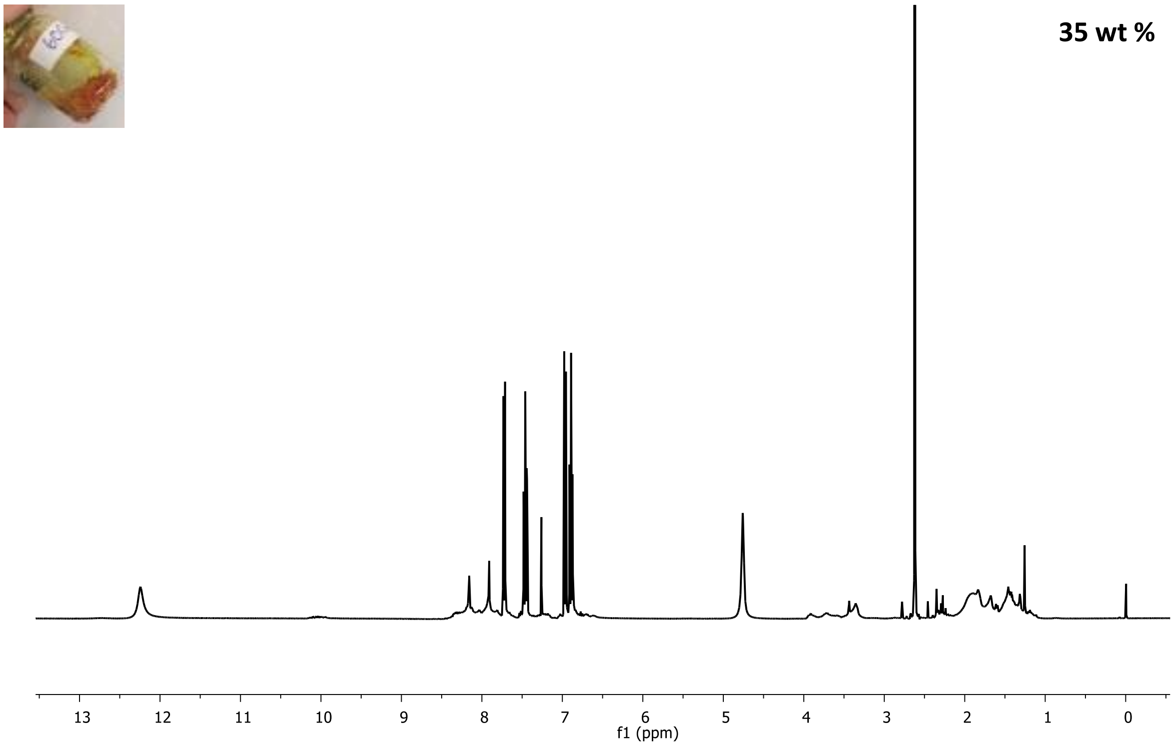

Fig. S82: ^{1}H NMR (CDCl$_3$) spectra of **3^3:13^3_{HAP}** at 35 wt % after sol-gel release

The physical properties of **3^3:13^3_{HAP}** at higher concentrations appear to change after a sol-gel cycle. The 27 wt% porous liquid, however, does not appear to decompose after a single temperature release experiment; with the ^{1}H NMR spectrum matching both the parent solvent and scrambled cage (Fig. S83). A second gas displacement with chloroform, to check porosity, was attempted on the same 27 wt% porous liquid but it seemed to no longer be porous, which could be due to the cages packing differently in the liquid state.

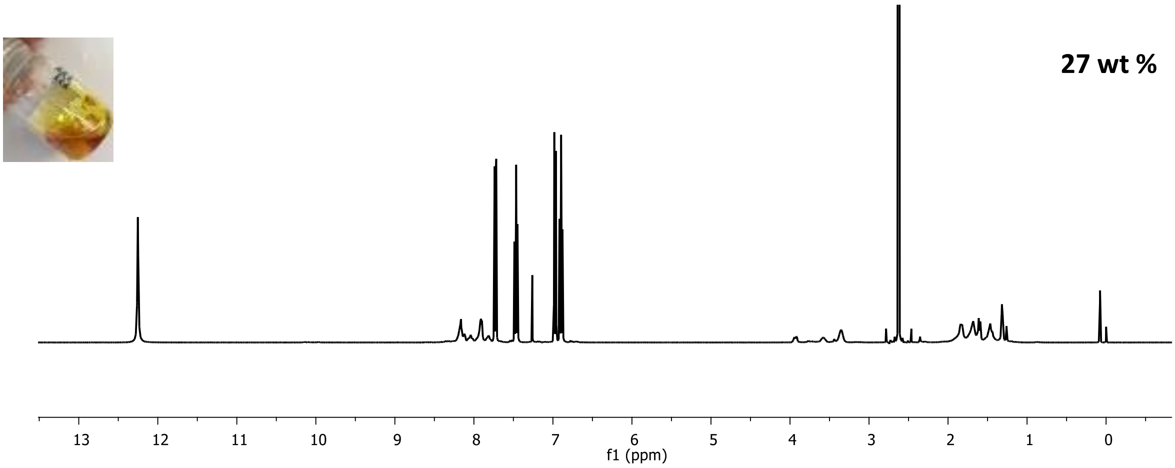

Fig. S83: ^{1}H NMR ($CDCl_3$) spectra of **3^3:13^3_{HAP}** at 27 wt% after a single temperature release cycle

Table S61: The volume of xenon evolved from **3^3:13^3_{HAP}** at 27 wt% when heated at 60-85 °C (cycle 1) followed by chemical displacement carried out on the same sample

Porous liquid	**Cycle 1**	**Cycle 2**
	Temperature release	**Chemical release**
3^3:13^3_{HAP} at 27 wt%	6.2 mL	0.2 mL

6.9. Retention of guest in $\mathbf{3^3{:}13^3_{HAP}}$

To determine if $\mathbf{3^3{:}13^3_{HAP}}$ could be used as a method of gas capture, the retention of xenon was studied in the system at several concentrations.

General procedure: The scrambled $\mathbf{3^3{:}13^3}$ cage (400 mg) was dissolved in 2-hydroxyacetophenone (1 mL) and purged with xenon at ~50-60 mL/min for 10 min per mL of solvent. The sample was sealed and left undisturbed. After 48 h, the sample was heated to release the trapped guest, which was collected in an inverted burette in water. The volume of water displaced equated to the volume of xenon in the porous liquid.

Table S62: Volume of xenon released and percentage retained by $\mathbf{3^3{:}13^3_{HAP}}$ liquid after immediate release and after 48 hrs.

Time (hrs)	Volume of xenon released (mL)	Volume of xenon released (μmol mL^{-1})	% Xe retained over time (%)
0	6.4	196.3	-
48	4.4	126.2	64

Loaded porous liquid samples were also left standing to gel over an extended period of time and the guest then released by heating. The aim was to observe the loss of guest from $\mathbf{3^3{:}13^3_{HAP}}$ over several weeks.

General procedure: The scrambled $\mathbf{3^3{:}13^3}$ cage (600 mg) was dissolved in 2-hydroxyacetophenone (1 mL) and purged with xenon at ~50-60 mL/min for 10 min per mL of solvent. Several samples were prepared in this manner and left standing at ambient temperature. Periodically, a sample was heated to release the trapped guest, which was collected in an inverted burette in water. The volume of water displaced equated to the volume of xenon retained in the porous liquid.

Table S63: Volume of xenon released from $\mathbf{3^3{:}13^3_{HAP}}$ gel after being left to stand for set amounts of time

Time after preparation (days)	Volume of xenon released (mL)	Volume of xenon released (μmol mL^{-1})	% Xe retained over time (%)
1	8.8	222.4	-
7	6.0	151.6	68
28	4.4	111.2	50

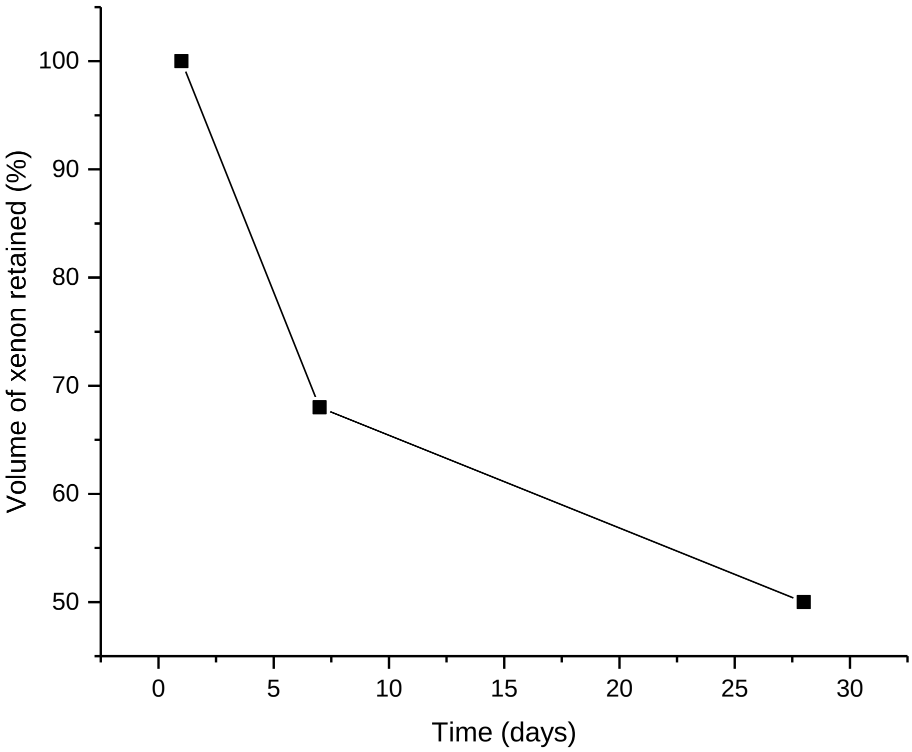

Fig. S84: Graphical representation for the retention of xenon by **3^3:13^3_{HAP}** gel over 28 days

6.10. Porous liquid stability

It is important to ensure the porous liquid is stable during use as imine chemistry is reversible in solution. If **3^3:$13^3$$_{HAP}$** is left standing, it appears to set as a gel but this is reversible if heated at 80 °C to reform the liquid. The gelation can be avoided if the porous liquid is stirred continuously.

Leaving standing:

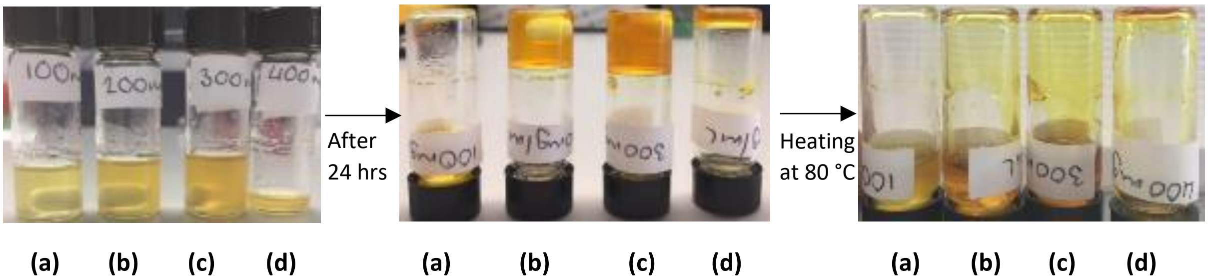

Fig. S85: Stability of **3^3:$13^3$$_{HAP}$** at several concentrations (a) 8, (b) 16, (c) 22 and (d) 27 wt%. Gelation occurs after 24 h but this can be reversed by heating to 80 °C

Stirring overnight:

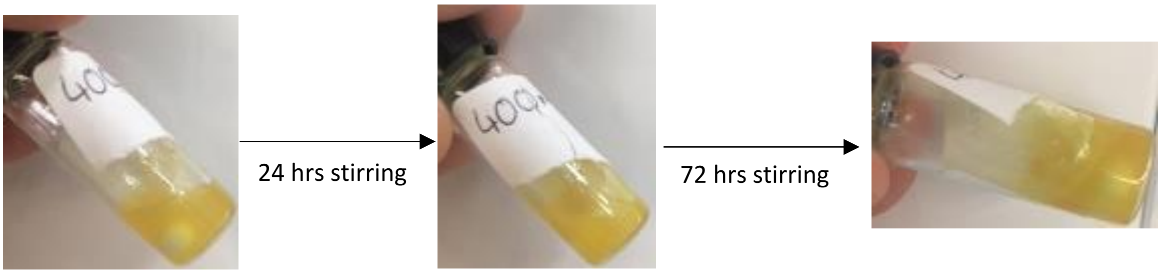

Fig. S86: Stability of **3^3:$13^3$$_{HAP}$** at 27 wt% showing continuous stirring maintains the liquid state

6.11. Recovery of scrambled cage

Although in some cases the porous liquid cannot be reused, the scrambled cage can be recovered and recycled into new porous liquids.

General procedure: Acetone was added to $\mathbf{3^3{:}13^3_{HAP}}$ until precipitation of the scrambled cage occurred. The solid was collected by filtration and dried at 70 °C in a vacuum oven. The scrambled cage was recovered as a white solid, and the ^{1}H NMR spectrum confirmed pure material had been recovered.

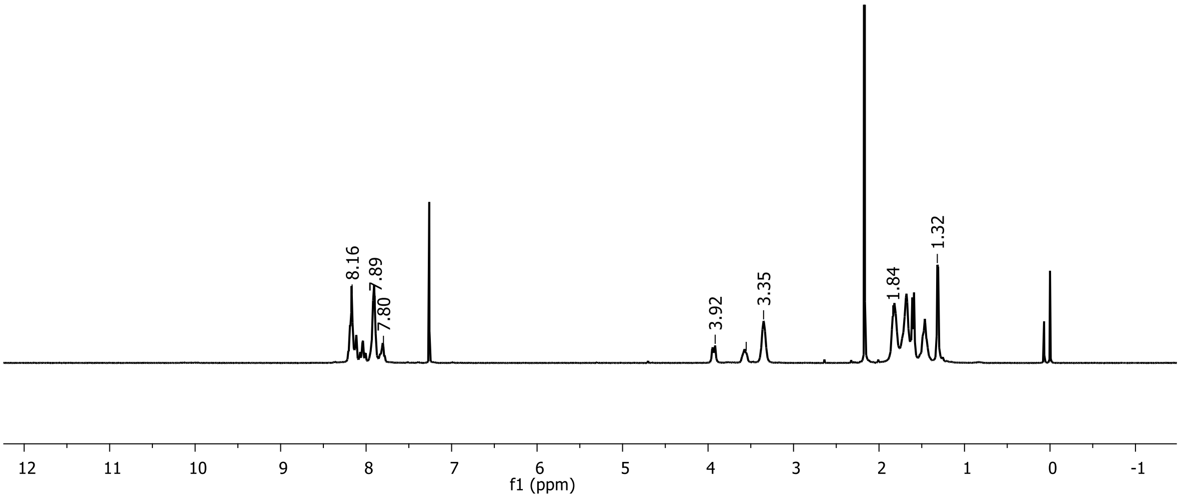

Fig. S87: ^{1}H NMR (CDCl$_3$) spectrum of $\mathbf{3^3{:}13^3}$ after recovery from a porous liquid by precipitation with acetone

Table S64: Volume of xenon released from 20% w/v porous liquids formed using recycled scrambled cage

Porous liquid	Mass of cage (mg)	Volume of xenon evolved (mL)	Volume of xenon evolved (µmol mL_{PL}^{-1})
$\mathbf{3^3{:}13^3_{TBA}}$	200	2.3	83.3
$\mathbf{3^3{:}13^3_{HAP}}$	200	2.8	92.8

7. References

1 NIST Chemistry WebBook, https://webbook.nist.gov/chemistry/, (accessed 1 August 2018).

2 H. Kim, M. Staikova, A. J. Lough and J. Chin, Stereospecific synthesis of alkyl-substituted vicinal diamines from the mother diamine: Overcoming the 'intrinsic barrier' to the diaza-Cope rearrangement reaction, *Org. Lett.*, 2009, **11**, 157–160.

3 H. Kim, hydrogen bond-directed stereospecific interactions in (a) general synthesis of chiral vicinal diamines and (b) generation of helical chirality with amino acids by Hyunwoo Kim A thesis submitted in conformity with the requirements for the degree of Doc, *Phd Thesis*.

4 N. Giri, C. E. Davidson, G. Melaugh, M. G. Del Pópolo, J. T. A. Jones, T. Hasell, A. I. Cooper, P. N. Horton, M. B. Hursthouse and S. L. James, Alkylated organic cages: from porous crystals to neat liquids, *Chem. Sci.*, 2012, **3**, 2153.

5 G. Alvaro, F. Grepioni and D. Savoia, *Synthesis and X-ray Crystal Structure of*, 1997.

6 N. Giri, M. G. Del Pópolo, G. Melaugh, R. L. Greenaway, K. Rätzke, T. Koschine, L. Pison, M. F. C. Gomes, A. I. Cooper and S. L. James, Liquids with permanent porosity, *Nature*, 2015, **527**, 216–220.

7 R. L. Greenaway, D. Holden, E. G. B. Eden, A. Stephenson, C. W. Yong, M. J. Bennison, T. Hasell, M. E. Briggs, S. L. James and A. I. Cooper, Understanding gas capacity, guest selectivity, and diffusion in porous liquids, *Chem. Sci.*, 2017, **8**, 2640–2651.